Mitacs Accelerate Project
Final Report

Comparative assessment of NH_3 production and utilization in agriculture, energy and utilities, and transportation systems for Ontario

Period:
January-June 2016

Submission Date:
June 17, 2016

Supervisor:
Prof. Dr. Ibrahim Dincer

Intern:
Yusuf Bicer

Partner Organization:
Hydrofuel Inc.

TABLE OF CONTENTS

ACKNOWLEDGEMENT

The principal investigator and intern acknowledge the financial support provided by the Mitacs and Hydrofuel Inc.

Nomenclature

ATR	Auto-thermal Reforming
AP	Acidification Potential
BTX	Benzene-toluenexylene-ethylbenzene
CCS	Carbon Capture Storage
CF	Carbon Filaments
CML	Center of Environmental Science of Leiden University
CNG	Compressed Natural Gas
CV	Coefficient of Variance
CNT	Carbon Nanotubes
DBD	Dielectric Barrier Discharge
EV	Electric Vehicle
FCC	Federal Communications Commission
GHG	Greenhouse Gas
GREET	Greenhouse Gases, Regulated Emissions, and Energy Use in Transportation
GTA	Greater Toronto Area
HEV	Hybrid Electric Vehicle
HF	High Frequency
HRF	Heavy Residual Fractions
HRSG	Heat Recovery Steam Generator
ICE	Internal Combustion Engine
ISO	International Organization for Standards
LCA	Life Cycle Assessment
LHV	Lower Heating Value
LPG	Liquefied Petroleum Gas
MSWI	Municipal Waste Incineration Plant
ODP	Ozone Layer Depletion
PEC	Photoelectrochemical
POX	Partial Oxidation
PSA	Pressure Swing Absorption
PTW	Pump to Wheel
RCV	Refuse Collection Vehicles
RF	Radio Frequency
SAF	Super Abrasion Furnace
SD	Standard Deviation
SI	Sustainability Index
SMR	Steam Methane Reforming
TCD	Thermo-catalytic Decomposition
UCG	Underground Coal Gasification
UCTE	Union for the Co-ordination of Transmission of Electricity
UOP	Universal Oil Products
WGS	Water Gas Shift
WTP	Wheel to Pump
WTW	Well to Wheel

SUMMARY

In this first section of the final report, a comparative life cycle assessment of internal combustion engine (ICE) based vehicles fueled by various fuels, ranging from hydrogen to gasoline, is conducted in addition to electric and hybrid electric vehicles. Various types of vehicles are considered, such as ICE vehicles using gasoline, diesel, LPG, methanol, CNG, hydrogen and ammonia; hybrid electric vehicles using 50% gasoline and 50% electricity; and electric only vehicles for comprehensive comparison and environmental impact assessment. The processes are analyzed from raw material extraction to vehicle disposal using life cycle assessment methodology. In order to reflect the sustainability of the vehicles, seven different environmental impact categories are considered: abiotic depletion, acidification, eutrophication, global warming, human toxicity, ozone layer depletion and terrestrial ecotoxicity. The energy resources are chosen mainly conventional and currently utilized options to indicate the actual performances of the vehicles. The results show that electric and hybrid electric vehicles result in higher human toxicity, terrestrial ecotoxicity and acidification values because of manufacturing and maintenance phases. In contrast, hydrogen and ammonia vehicles yield the most environmentally benign options.

In the second section of this report, production of ammonia using conventional hydrocarbons is investigated by implying current technologies and developments. Hydrogen can be produced by dissociation of hydrocarbons which can be then converted to ammonia using a nitrogen supply. Decomposition of heavy fractions can bring some challenges because of various metal and sulfur contents, however, purification is possible and applicable. There are multiple pathways for decomposition namely; thermal, non-thermal, plasma, non-plasma techniques. An alternative method of hydrogen and ammonia production from hydrocarbons is their thermal decomposition which is accompanied by the formation of carbon deposits. Methane can be thermally or thermocatalytically decomposed (TCD) into carbon and hydrogen without CO or CO2 production. There are some research papers and patents in the literature regarding the application of microwave energy for hydrocarbons. They have shown that bitumen, which is the end product from oil sand, can be decomposed using microwave energy. Many of the inorganic particles in processed oil sands hold a charge, and could be influenced by electromagnetic radiation. They are excited at a different rate than the water and bitumen when irradiated, creating a temperature gradient between the different components of the oil sands.

In the third section, detailed cost and feasibility analyses of various key scenarios for production, storage and transportation of ammonia in Ontario, Newfoundland and Labrador, and Alberta are performed. Renewable resources based ammonia is quite attractive supplying similar costs in some cases compared to conventional steam methane reforming route. The high hydroelectric and wind energy source potential of Newfoundland and Labrador make the energy storage attractive using ammonia. Ontario, with decreasing electricity prices, has potentials for hydropower especially in Northwestern region for on-site ammonia production. The hydrocarbon decomposition option is also considered for Alberta province and it is observed that the cost of ammonia can be lower than conventional steam methane reforming. Storage and transportation of ammonia brings additional costs after production which is a significant disadvantage for long distance transportation. The results imply that using appropriate renewable resources and cleaner hydrocarbon utilization paths, ammonia production can be cost-effective and environmentally friendly.

CHAPTER 1. COMPARATIVE ASSESSMENT OF ALTERNATIVE FUELED VEHICLES INCLUDING AMMONIA

1. Introduction

The transportation sector is one of the fundamental sectors contributing the GHG emissions worldwide. In a current report by International Energy Agency (IEA), it can be seen that the transportation sector consumed 61.2% of the world's oil, subsidizing 28% of the total final energy supply [1] and 23% of the world's CO_2 emissions [2]. Because of these reasons, a further investigation for sustainable transport systems is considered to diminish the utilization of fossil fuels, by implementing alternative fuels such as biofuels, electricity and ammonia. Globally, generation of electricity and heat relies greatly on coal which is in fact the most carbon intensive fossil fuel. The usage of fossil fuel based electricity decreases the attractiveness of electric (EV) and hybrid electric (HEV) vehicles. Henceforth, noteworthy attention should be paid to the power generation technologies and their CO_2 intensity, used to supply electricity to EVs or HEVs.

As an alternative energy carrier and transportation fuel, ammonia (NH_3), is a deviation of hydrogen fuel. It is a molecule which composes of three atoms of hydrogen and one atom of nitrogen. Note that the physical characteristics of ammonia are similar to propane. The capability to convert a liquid at adequate pressure permits ammonia to store more hydrogen per unit volume than compressed hydrogen/cryogenic liquid hydrogen. Besides having a significant advantages in storing and transporting hydrogen, ammonia may also be burned directly in ICE. Compared to gasoline vehicles, ammonia-fueled vehicles do not produce direct CO_2 emission during operation. . Furthermore, ammonia can be produced at locations where oil and natural gas extraction wells are located. In this way, generated CO_2 can be reinjected into the ground for sequestration. Ammonia can then be easily transferred through pipelines, railway cars, and ships by delivering to consumption area where it may be utilized as a source of hydrogen, chemical substance, fertilizer for agriculture, fuel for transportation, power generation sector, and working fluid or refrigerant. Ammonia as a hydrogen carrier seems to be more attractive than methane in numerous features such as storing more hydrogen energy per volumetric tank, having three times less energy cost, having fewer danger because of non-flammability and being non-explosive in spite of its toxicity.

One of the key factors in decision of alternative fueled vehicles is to conduct life cycle assessment from cradle to grave. In this progress report, a comprehensive environmental impact analyses of fuel and vehicle cycle of various fueled passenger cars are investigated using life cycle assessment tool. The environmental impact categories taken into account in this study are human toxicity, global warming, acidification potential, eutrophication, depletion of abiotic resources, stratospheric ozone depletion and terrestrial ecotoxicity. The considered vehicle options for analyses and assessments are listed as follows:

- Gasoline fueled ICE vehicle
- Diesel fueled ICE vehicle
- Methanol (90%) & gasoline (10%) fueled ICE vehicle
- Electric vehicle (EV) using lithium ion battery
- Hybrid electric vehicle (HEV) using lithium ion battery and ICE
- Ammonia fueled ICE
- Hydrogen fueled ICE
- Liquefied petroleum gas (LPG) fueled vehicle
- Compressed natural gas (CNG) fueled vehicle.

2. Methodology

A characteristic life cycle of a vehicle technology can be categorized into two main steps, namely fuel cycle and vehicle cycle. In the fuel cycle, the processes beginning from the feedstock production to fuel utilization in the vehicle are considered. At this phase of CNG production, the related input of energy to extract natural gas and the emissions linked to the extraction are taken into account. Similarly, the extraction of crude petroleum is accounted for diesel. Transformation of crude oil feedstock into useful fuels is a too energy intensive stage of the fuel cycle, producing substantial amounts of GHG. Nevertheless, purification of natural gas results in considerably fewer energy usage and GHG. The fuel needs to be transported to be available for vehicle usage. Hence, emissions and energy usages associated with fueling trucks/pipelines are thus accounted for in the fuel delivery step [3]. The boundaries of the current analyses are illustrated in Fig. 1 including fuel and vehicle cycles.

A noteworthy part of any life cycle analysis involves gathering of reliable data. The excellence of data has a deep influence on the quality of the results predicted or estimated by an LCA tool. National Laboratory has developed a full life cycle model called GREET (Greenhouse gases, Regulated Emissions, and Energy use in Transportation), sponsored by the U.S. Department of Energy, Office of Energy Efficiency and Renewable Energy, which allows to evaluate various vehicle and fuel combinations on a full fuel cycle or vehicle cycle basis.

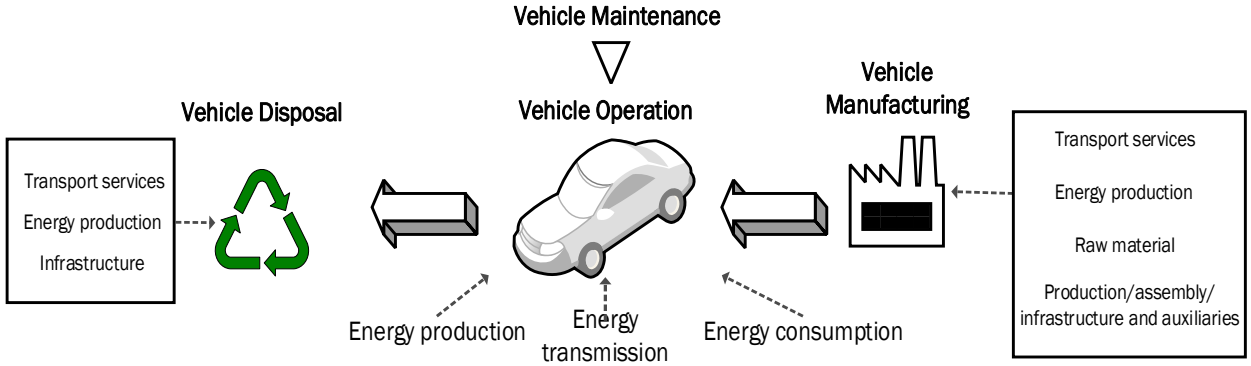

Fig.1. Boundaries of conducted LCA analyses including fuel/vehicle cycle.

It is a strong software with a substantial amount of alternative vehicles. It takes into account the well to pump (WTP) and well to wheel (WTW) processes. WTW phases for each fuel starts with the extraction of the primary energy and ends with the consumption in vehicles. WTP consists of the feedstock and fuel phases, counting fuel feedstock extraction, transmission, distribution and storage. Pump to wheel (PTW) represents the energy use and emissions during vehicle operation. The functional unit is the distance travelled by the vehicle. The results of the primary energy demand and the GHG emissions for each vehicle type are expressed as MJ/km and g CO_2 eq/km respectively [4].

In this study, GREET 2015 software is utilized to simulate the life cycle GHG emissions for the selected vehicles only for the operation process. After the required operation data is obtained from GREET software, they are used in SimaPro LCA tool for complete LCA analyses. The scope of the analyses represent a complete LCA since they include the well to wheel (WTW) stages as well as the equipment life cycle. The equipment life cycle includes production, manufacturing, maintenance and end-of-life of vehicle infrastructure. GREET software can calculate energy use with high accuracy. In this study, the vehicle operation emissions belonging

to different types of vehicles and transportation fuels are based on GREET 2015 calculations [5]. A part of GREET model characterizes the life cycle of vehicles, including production, maintenance, operation and disposal [6]. For this study, we have utilized only the operation parameters of all selected vehicles. Besides, electric and hybrid electric vehicle data are utilized from production until disposal and then adapted in SimaPro LCA software. The LCA database ecoinvent, v2.2 was used as source of background LCI data. Life cycle impact assessment (LCIA), quantification of life-cycle environmental weights and potential impacts was carried out using the LCA software SimaPro [7].

2.1 Uncertainty analyses

In the absence of an uncertainty analysis in LCA, the assessment results is questionable and non-satisfactory for interpretation phase. In order to capture the characteristic variability of data in the process or production systems, Monte Carlo analysis can be used embedded in SimaPro software. This tool simulates a probable range of outcomes given a set of variable conditions and can be applied within life cycle inventory framework to capture parameter variability. Hence, Monte Carlo is a method engaged to quantify variability and uncertainty using probability distributions. In quantifying the effect of the uncertainty in diverse data inputs on your LCA results, it shows whether the inventoried data is of appropriate quality and the whether the uncertainty in LCA results is tolerable.

3. Systems Description

On average, lifetime performance of a passenger car is assumed to be 239,000 person km. Generally, the average utilization factor is expected to be 1.59-1.6 passengers per car. Henceforth, the lifetime of the selected vehicles is approximately 150,000 km. Here, the assessment comprises the following life cycle phases, as illustrated in Fig. 1:

- manufacturing of the vehicle,
- operation of the vehicle,
- maintenance of the vehicle,
- disposal of the vehicle.

3.1 Passenger car manufacturing

The inventory contains processes of energy, water and material usage in passenger car manufacturing. Rail and road transport of materials is accounted for. The groundwork of plant is involved together with the issues such as land use, building, road and parking structure. The material consumption reflect a modern vehicle. The data for vehicle production are representative for manufacturing sites with an environmental management system. Thus, the resulting data may be an underestimation of environmental impacts of an average vehicle fleet.

The electricity comes from a mixture of UCTE (Union for the Co-ordination of Transmission of Electricity) countries. The UCTE is the association of transmission system operators in which about 450 million people are supplied electricity. In the electricity usage process, electricity production in UCTE, the transmission network and direct SF6-emissions to air are included. Electricity losses during medium-voltage transmission and transformation from high-voltage are also accounted for. The conversion of high-medium voltage as well as the transmission of electricity at medium voltage are taken into account. Besides, the required high temperature is assumed to be from methane burned in industrial furnace higher than 100kW which in turn

contains fuel feed from high pressure gas network, infrastructure (boiler), emissions, and required electricity of operation.

In an electric vehicle, motion is attained from an electric motor and whole energy used for traction is kept in a battery system. The car can travel if sufficient energy is available in the battery. When the battery energy is consumed, the battery needs recharging by electricity grid or exchanging. The operation of EV varies from the conventional vehicles in some characteristics as the first difference is the energy source for operation where electricity is utilized despite of petrol or diesel. Henceforth, there are no tail-pipe emissions. It is therefore assumed that emissions are restricted to tire and brake wear and abrasion from the surface of road. Conceptually, a HEV is very parallel to EV with the exception that it involves a fuel tank and an ICE. Whenever the battery energy is consumed, the ICE can be used to recharge the battery or for traction power. In the current study, HEV is assumed to be 50% electric and 50% gasoline. For electric vehicles, the required amount of steel is lower compared to conventional cars since there is no ICE in the car. However, for EVs and HEVs, production of electric motor and lithium ion batteries are included. The battery is the on board energy storage system of the car. It contains an array of connected cells, the packaging, and the battery management system. If a car is intended to have a range of 100 km with a regular consumption of about 0.2 kWh per km, a minimum of 20 kWh of energy needs to be stored on-board. When energy density of 0.1 kWh/kg is assumed for the battery, the total battery weight would be about 250 kg. Currently, commercially available car batteries range between 100 kg and 400 kg, depending on automobile size and preferred range [8]. The average masses of electric motor for and lithium ion battery are assumed to be 104 kg and 312 kg, respectively for this study [9]. The inventory data for battery production and disposal is utilized from GREET model and Ref. [10].

3.2 Maintenance

The inventory of maintenance of vehicles contains resources used for alteration parts and energy consumption of garages. Rail and road transportation of supplies is accounted for. For EVs, during the lifetime of the car, one battery change is assumed. Henceforth, lithium ion battery replacement and disposal processes are also taken into account in the maintenance phase.

3.3 Disposal of the vehicles

The inventory of vehicle disposal contains disposal processes for bulk materials. For the disposal of tires, a cut off allocation is applied. In addition, the transportation of tires to the cement works is taken into account. For the disposal of steel, aluminum, copper and tires, a cut off allocation is applied. Waste specific water together with air emissions from incineration and supplementary supply depletion for flue gas scrubbing are accounted for. Short term releases to river water and long term emissions to ground water from slag section and remaining material landfill are considered with process energy loads for municipal waste incineration plant (MSWI). The following processes are applied for the disposal of a vehicle scenario:

- Disposal of plastics in mixture with 15.3% water to municipal incineration (65 kg)

Energy production net output. The waste yields 0.01693 kg of slag and 0.006594 kg of remains per kg of waste. They are landfilled. Supplementary solidifying with 0.002638 kg of cement is applied. MSWI: 3.48MJ/kg waste energy in electric form and 7.03MJ/kg waste energy in thermal form

- Disposal of glass to municipal incineration (30.1 kg)

Energy production in MSWI net output: 3.67MJ/kg waste electric energy and 7.39MJ/kg waste thermal energy. The waste yields 0.01704 kg of slag and 0.01217 kg of residues per kg of waste. They are landfilled. Supplementary solidifying with 0.004869 kg of cement is applied.

- Disposal of emulsion paint leftovers to HWI (100 kg)

Energy production in hazardous waste incineration (HWI) plant, net output: 17.11MJ/kg electric energy and 1.27MJ/kg thermal energy. The waste yields 0.707 kg of remains per kg of waste. They are landfilled. Supplementary solidifying with 0.2828 kg of cement is applied.

- Disposal of zinc in car shredder remains to MSWI (5.89 kg)

One kg of this waste produces 0.6244 kg of slag and 0.6202 kg of residues. They are landfilled. Supplementary solidifying with 0.2481 kg of cement is applied.

Note that lithium ion batteries are recycled for numerous purposes. The most noticeable one is the retrieval of valued materials and to follow to ecological laws. Numerous methods are present for recycling lithium ion batteries with diverse environmental consequences. Usually, battery recycling procedures can be expressed in three main categories: mechanical, pyrometallurgical and hydrometallurgical processes. Hydrometallurgical processes are evaluated to require considerably less energy compared to pyrometallurgical processes. In this study, hydrometallurgical process for disposal of batteries are selected with an average efficiency of 57.5% and energy use of 140 kWh/tonne [8]. The inventory data for the disposal of batteries are taken from Ref. [8]. For ammonia and hydrogen fueled vehicles, required amount of steel and electrical energy is a little higher than other cars because of storage tank infrastructure.

3.4 Operation of vehicles

The operation process of the vehicles is one of the key sections of life cycle analyses. In this phase, fuel consumption is involved. Direct airborne emissions of gaseous materials, particulate matters and heavy metals are accounted for. Particulate emissions cover exhaust- and abrasions emissions. Hydrocarbon emissions include evaporation. Heavy metal emissions to soil and water produced by tire abrasion are accounted for. The values are based on operation of an average passenger car. The specific conditions for the selected vehicles are presented herein:

- Gasoline: All processes on the refinery site excluding the emissions from combustion facilities, including waste water treatment, process emissions and direct discharges to rivers are accounted for. The inventory data also includes the distribution of petroleum product to the final consumer including all necessary transports. Transportation of product from the refinery to the end user is considered together with operation of storage tanks and petrol stations. Emissions from evaporation and treatment of effluents are accounted for. Heavy metal emissions to soil and water caused by tire abrasion are accounted for.
- Diesel: Diesel is evaluated as low-Sulphur at regional storage with an estimation for the total conversion of refinery production to low-Sulphur diesel. An additional energy use (6% of energy use for diesel production in the refinery) has been estimated. The other processes are similar to gasoline. Heavy metal emissions to soil and water caused by tire abrasion are accounted for.
- CNG: Natural gas with a production mix at service station is taken into account. The inventory data contains electricity necessities of a natural gas service station together with emissions from losses. The data set represents service stations with high (92%), medium (6%) and low (2%) initial pressure. VOC emissions are obtained from gas losses and contents of natural gas. Heavy metal emissions to soil and water caused by tire abrasion are accounted for.

- Hydrogen: Hydrogen is produced during cracking of hydrocarbons. It includes combined data for all processes from raw material extraction until delivery at plant. The output fractions from an oil refinery are composite combinations of mainly unreactive saturated hydrocarbons. The first processing step in converting such elements into feedstock suitable for the petrochemical industries is cracking. Essentially a cracker achieves two tasks in (i) rising the complexity of the feed mixture into a smaller number of low molecular mass hydrocarbons and (ii) presenting unsaturation into the hydrocarbons to enable more reactivity. The raw hydrocarbon input from the refinery is fed to the heater unit where the temperature is increased. The forming reaction products vary based on the composition of the input, the temperature of the heater and the residence time. The cracker operator selects temperature and residence time to enhance product mix from a supplied input. Cracker feeds can be naphtha from oil refining or natural gas or a mixture of both. After exiting the heater, the hydrocarbon gas is cooled to prevent extra reactions. After that, it is sent to the separation phase where the individual hydrocarbons are separated from one another by fractional distillation. Heavy metal emissions to soil and water caused by tire abrasion are accounted for.
- Ammonia: Ammonia synthesis process is Haber-Bosch which is the most common method in the world. Ammonia production requires nitrogen and hydrogen. In this study, hydrogen is assumed to be from hydrocarbon cracking. Cryogenic air separation is mostly used method for massive amount of nitrogen production. In the life cycle assessment of nitrogen production, electricity for process, cooling water, waste heat and infrastructure for air separation plant are included. Haber-Bosch process is an exothermic method that combines hydrogen and nitrogen in 3:1 ratio to produce ammonia. The reaction is facilitated by catalyst (iron-oxide based) and the optimal temperature range is 450-600°C. Heavy metal emissions to soil and water caused by tire abrasion are accounted for.
- EV: Electricity consumption is included. Particulate emissions comprise exhaust and abrasions emissions. Heavy metal emissions to soil and water caused by tire abrasion are accounted for. In the electricity usage process, electricity production mix, the transmission network and direct SF6-emissions to air are included.
- HEV: Hybrid car is assumed to be 50% electric and 50% gasoline with ICE. Electricity and gasoline consumptions are included. Particulate emissions comprise exhaust and abrasions emissions. Heavy metal emissions to soil and water caused by tire abrasion are accounted for.
- Methanol: The selected fuel M90 consists of 90% methanol and 10% gasoline. The raw materials, processing energy, estimate on catalyst use, and emissions to air and water from process, plant infrastructure are included. The process describes the production of methanol from natural gas via steam reforming process to obtain syngas for the production of methanol. There is no CO_2 use and hydrogen is assumed as burned in the furnace. Raw materials, average transportation, emissions to air from tank storage, estimation for storage infrastructure are included for the distribution part where 40% of the methanol is assumed to be transported from overseas. Heavy metal emissions to soil and water caused by tire abrasion are accounted for.
- LPG: All processes on the refinery site excluding the emissions from combustion facilities, including waste water treatment, process emissions and direct discharges to rivers are considered. All flows of materials and energy due to the throughput of 1kg crude oil in the refinery is accounted for. Refinery data include desalting, distillation (vacuum and atmospheric), and hydro treating operations. Heavy metal emissions to soil and water caused by tire abrasion are accounted for.

The following fuel consumption rates are considered in the analyses as tabulated in Table 1.

Table 1. Energy consumptions per km for the selected vehicles

Fuel		Fuel/Energy Consumption		Fuel Cost (US$/kg or US$/kWh)	Driving Cost (US$/100 km)
Gasoline		0.0649108	kg/km	1.004	6.518
Diesel		0.0551536	kg/km	0.8534	4.707
M90	Methanol	0.1180535	kg/km	0.25	3.308
	Gasoline	0.0060664	kg/km		
Hydrogen		0.0195508	kg/km	2.3	4.497
Ammonia		0.0926600	kg/km	0.28	3.102
EV		0.2167432	kWh/km	0.15	3.251
HEV	Electric	0.1083716	kWh/km	0.4916	4.558
	Gasoline	0.0324554	kg/km		
CNG		0.0603914	kg/km	0.8	4.831
LPG		0.057629687	kg/km	0.8182	4.715

4. Results and Discussion

The selected vehicle types are environmentally assessed in SimaPro LCA software based on the energy consumption and GHG emissions of ICEV and EVs obtained from the wheel to wheel simulations using GREET 2015 model. The results presented here are given on per km basis. The energy use is based on units of MJ. The global warming potential is presented in kg per CO_2 equivalent.

The battery production and assembly requires high amounts of copper and aluminum. Henceforth, top two processes contributing issues related human toxicity are copper and aluminum production at plants. Operation of EVs causes only 1% of total human toxicity values as shown in Fig. 2. HEVs are quite similar to EVs in terms of battery manufacturing which yields second highest value.

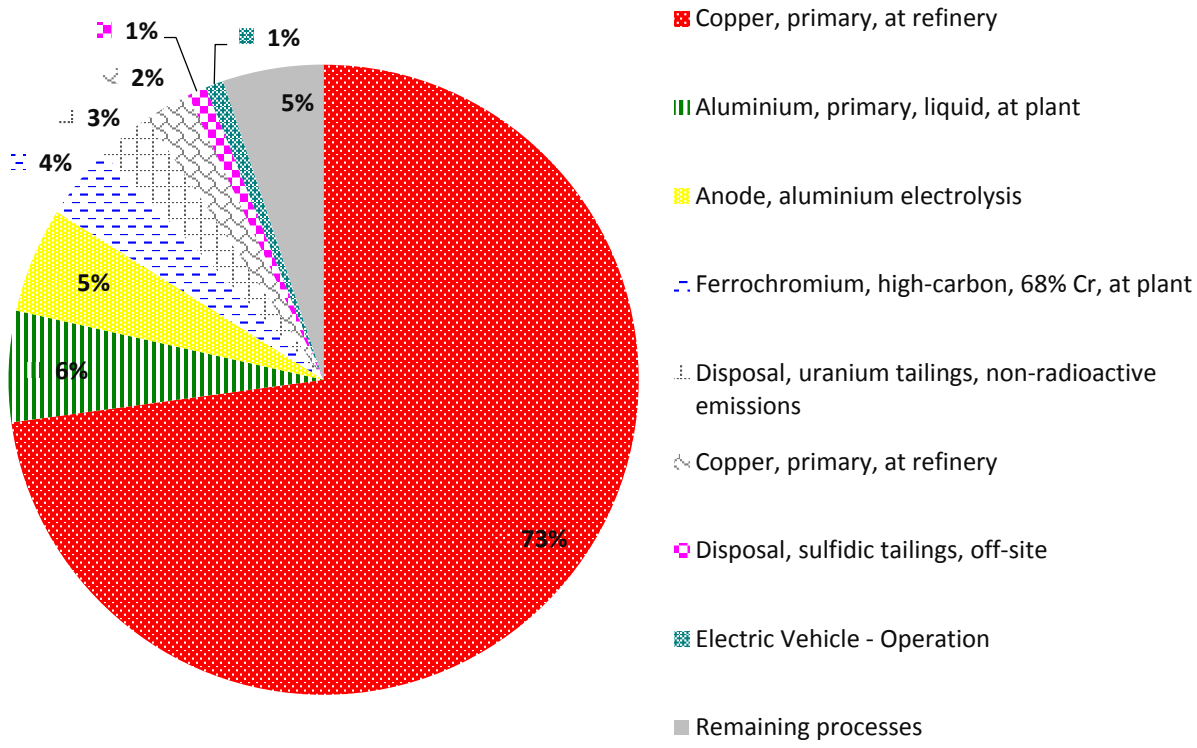

Fig. 2. Contribution of different processes to human toxicity values of electric vehicles

The depletion of ozone layer is one of the main reasons of environmental changes which is actually caused by carbon emissions to the atmosphere. Since diesel, gasoline, CNG and LPG fuels are fossil based and have huge amount of carbon substance, they have higher ozone layer depletion values. The highest is equal to 3.3×10^{-8} kg CFC-11 eq. per km for diesel vehicle as Fig. 3 represents. The lowest contributions are from ammonia vehicle corresponding to 7.19×10^{-9} kg CFC-11 eq/km. Because there is no direct CO_2 emission during operation of ammonia vehicle.

The eutrophication is the impact of excessive levels of macro-nutrients in the environment which is mainly caused by disposal processes. For EVs, HEVs and ammonia vehicles, the main reason of eutrophication is disposal of spoil from lignite mining in surface landfill in which it corresponds to about 66%, 49% and 47% for ammonia, EVs and HEVs respectively. There are also other spoils during disposals such as sulfidic tailings, oxygen furnace wastes, decarbonizing waste etc. which have minor impacts compared to coal mining processes. The lowest eutrophication value is observed in hydrogen vehicle with an amount of 7.29×10^{-5} kg PO_4 eq/km. Ammonia vehicles represent lower acidification values compared to EVs and HEVs as seen in Fig. 4.

Methanol is used on a limited basis to fuel internal combustion engines. Methanol is commonly produced via steam reforming of natural gas where natural gas is responsible about 90% of abiotic depletion. Therefore, the abiotic depletion values of methanol vehicle is more compared to CNG and gasoline vehicles. 0.0025 kg Sb eq/km is the maximum value for methanol vehicle while hydrogen and electric vehicles yield lower abiotic depletion.

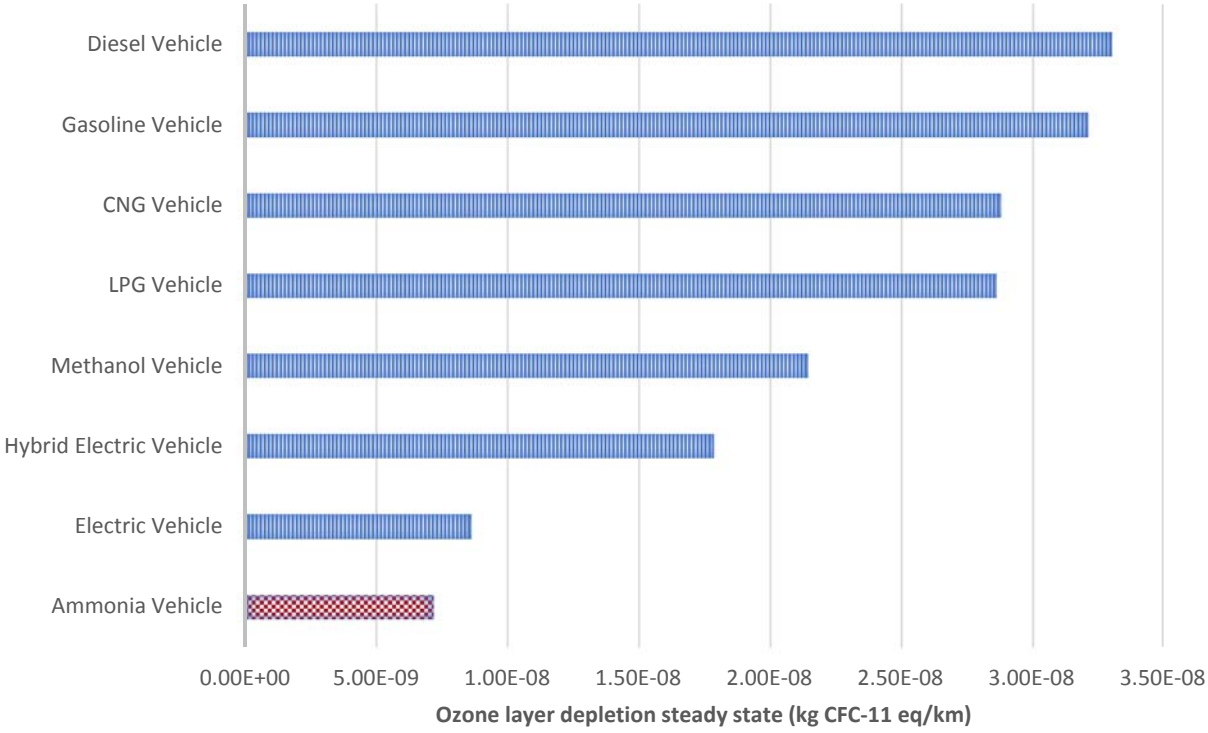

Fig. 3. Life cycle comparison of ozone layer depletion results for various vehicles

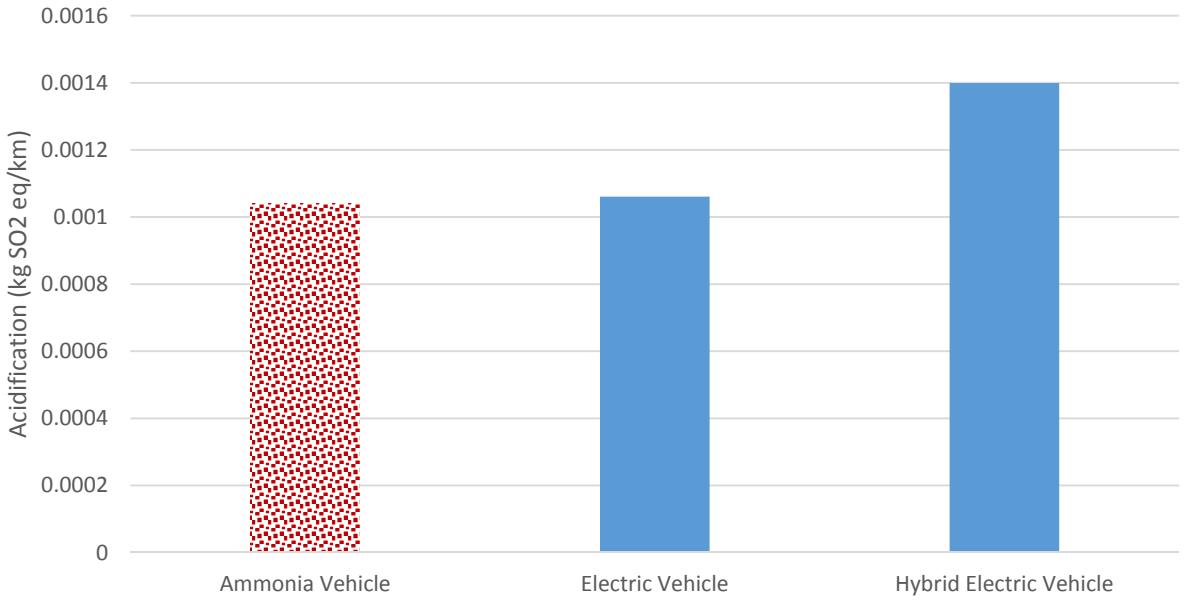

Fig. 4. Life cycle comparison of acidification results for various vehicles

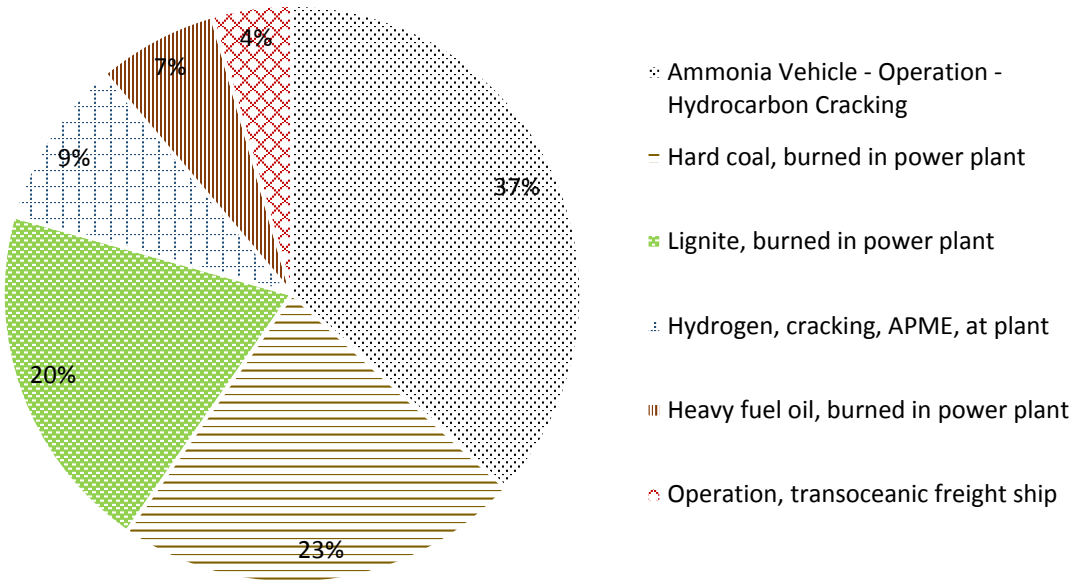

Fig. 5. Contribution of different processes to acidification values of ammonia vehicles

The acidification values of EVs and HEVs mainly cause by SO_2 emission which corresponds to 70% of overall acidification value. The source of SO_2 emission is predominantly the lignite and bituminous coal at mine that is used for electricity production mix and eventually consumed in the EVs and HEVs.

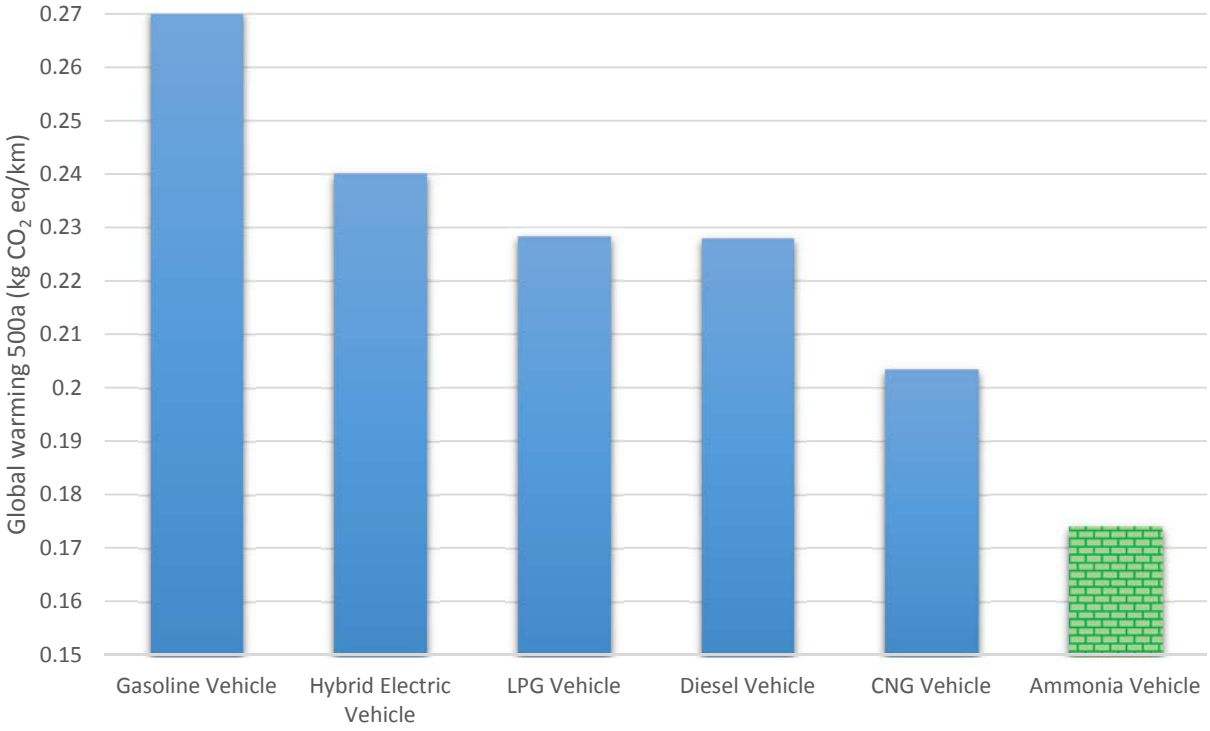

Fig. 6. Life cycle comparison of global warming results for various vehicles

Afterward, ammonia vehicle has an acidification value of 0.001 kg SO_2 eq/km as Fig. 4 specifies. 37% of this value is originated from ammonia vehicle operation and 9% comes from hydrogen production for ammonia synthesis as shown in Fig. 5. Hydrocarbon cracking for hydrogen production is fundamental contributor to hydrogen vehicle with 47%. Furthermore, platinum and nickel have about 21% share in which they are used for hydrogen vehicle manufacturing process.

The global warming potentials of assessed vehicles are comparatively shown in Fig. 6. The lowest GHG emissions are observed in hydrogen and ammonia vehicles where it corresponds to 0.17 kg CO_2 eq/km for ammonia vehicle. Ammonia driven vehicles represent a more environmentally friendly option among others.

Hydrogen production process contributes 32% of abiotic depletion for ammonia vehicle as seen in Fig. 7. It is followed by lignite, hard coal and natural gas where they are consumed mainly for electricity production.

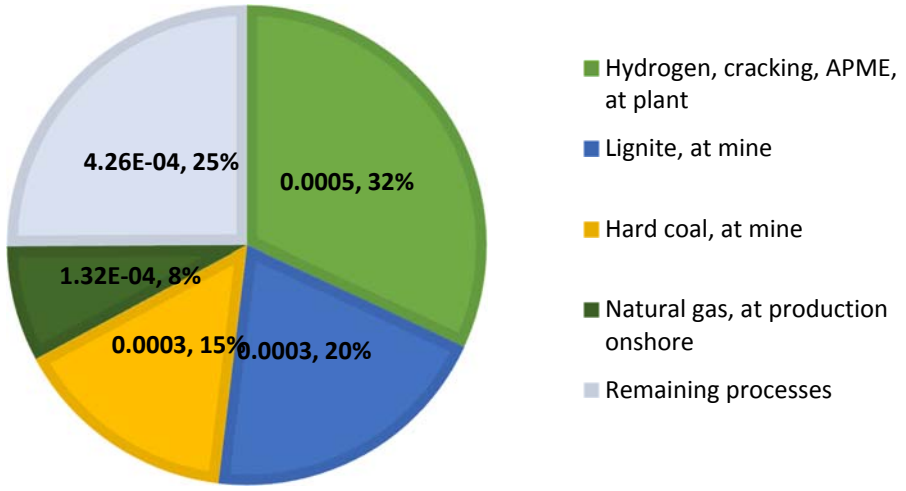

Fig. 7. Abiotic depletion values (kg Sb. Eq.) of various processes for ammonia vehicles

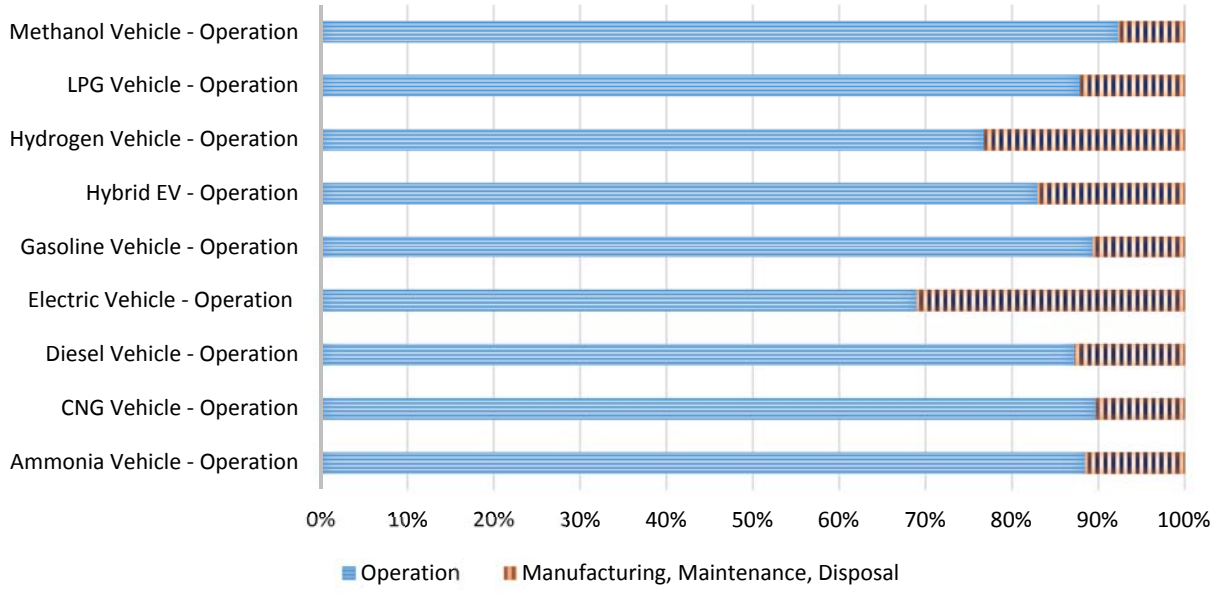

Fig. 8. Contribution of operation only process of the vehicles to abiotic depletion

As Fig. 8 shows, the abiotic depletion is mainly caused by the operation processes of vehicles. Highest percentage is observed in methanol vehicle operation since production of methanol is highly dependent on natural gas. Manufacturing, maintenance and disposal of EVs have higher shares during life cycle primarily initiated by production and disposal of lithium ion batteries.

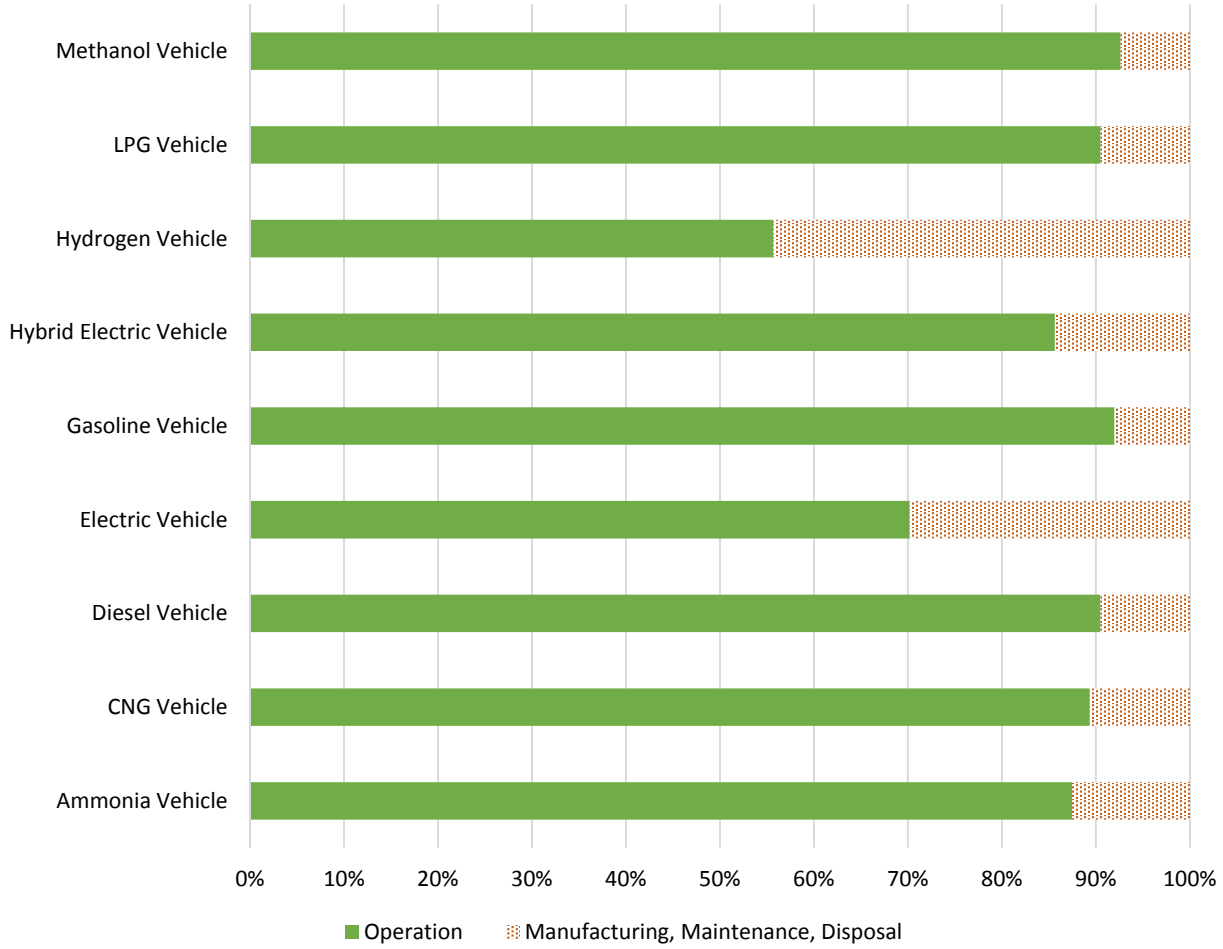

Fig. 9. Contribution of operation only process of the vehicles to global warming potential

On-board storage of hydrogen requires high resistant and strength tanks which leads to higher steel and process requirement. Henceforth, non-operation part of hydrogen vehicle constitute about 22% and 44% of overall hydrogen vehicle life cycle for abiotic depletion and global warming potential as illustrated in Figs. 8 and 9. Overall, operation of the vehicles are dominant contributors to complete life cycle.

Besides manufacturing and disposal of the vehicles, operation process is the fundamental part for the vehicle life cycle. As seen in Fig. 10, ammonia driven vehicles is the second environmentally benign option after electric vehicles during the operation.

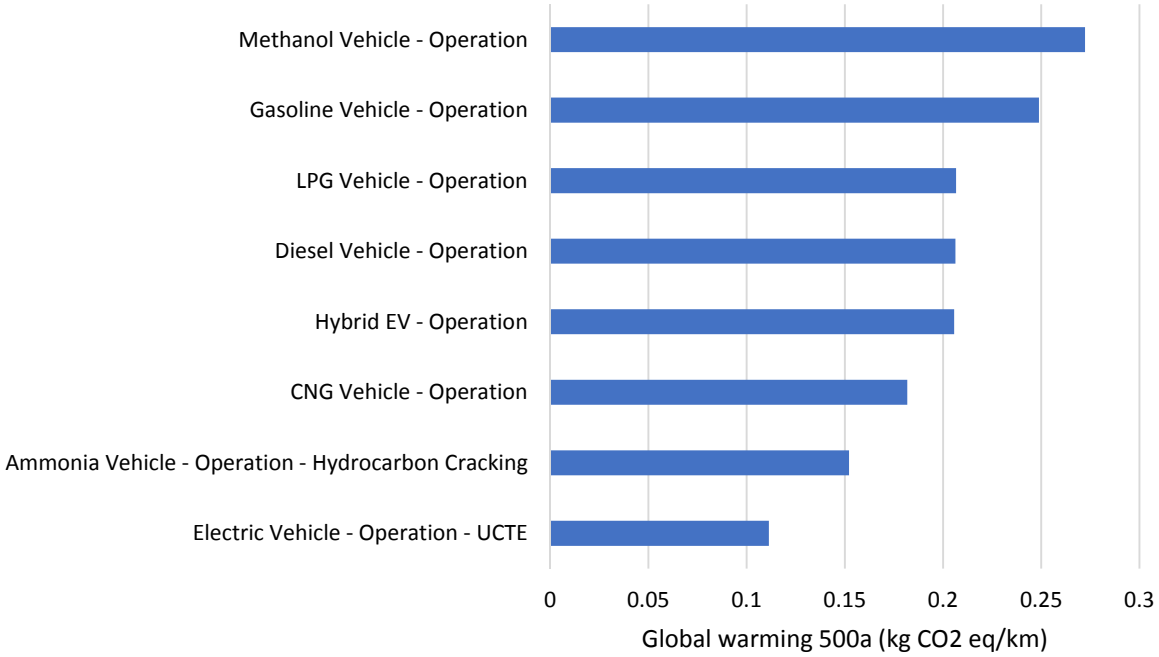

Fig. 10. Life cycle comparison of global warming results for operation only of various vehicles

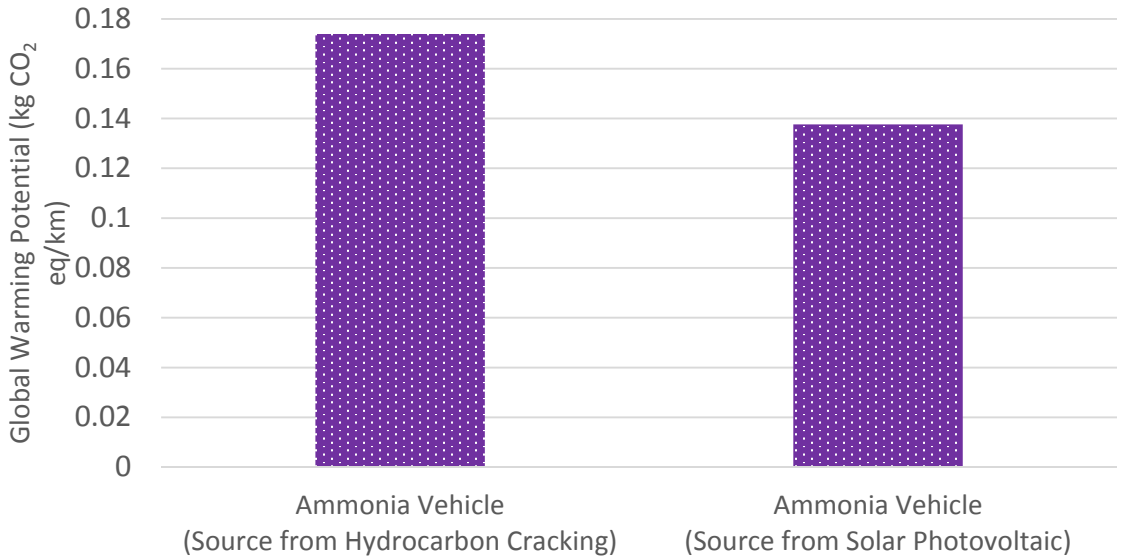

Fig. 11 Comparison of life cycle environmental impact of ammonia fueled vehicle from hydrocarbons and solar photovoltaics

Fig. 11 compares the global warming potential of ammonia driven vehicle where ammonia is either produced from solar energy or hydrocarbon cracking. Global warming potential of ammonia driven vehicle is similar for solar energy and fossil hydrocarbon based options. Hence, the utilization of ammonia in the transportation sector will certainly contribute to lessen global warming effect by using clean technologies even it is originated from fossil fuels.

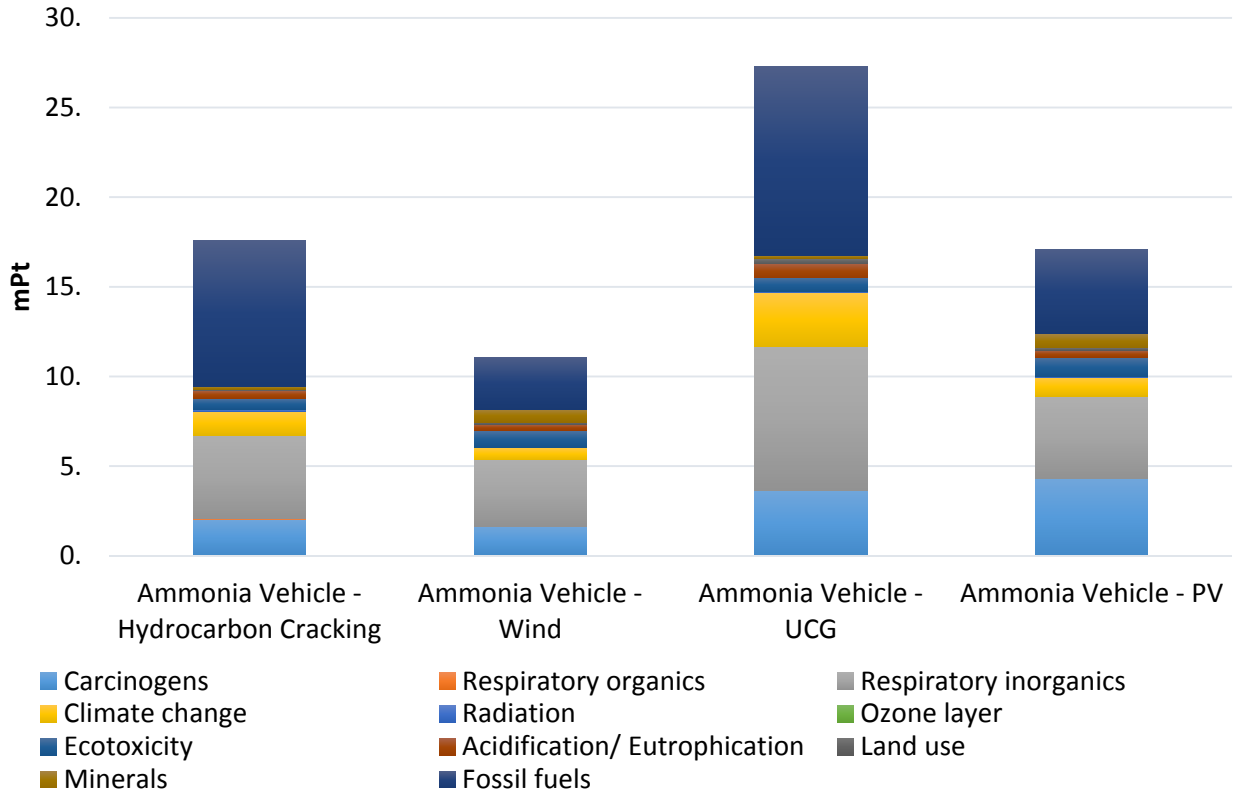

Fig. 12. Singe score comparison of various source ammonia vehicles according to Eco-Indicator 99

The single score serves as an easy starting point to get to know the product under consideration based on the environmental impact it creates. It relates the product's environmental impact to the overall environmental impacts in the country. A point (Pt) represents the annual environmental load (i.e. entire production/consumption activities in the economy) in the US divided up into the share of one American. It is important to understand that one point is not an individual's very own environmental impact. It represents the individual's annual share regardless of whether that individual participated in the economy's environmental impacts directly or indirectly. The single score indicator, the impact factor, is expressed in millipoints (mPts). One millipoint is 1/1000 th of a point. It enables the measurement of smaller systems since most products have a lower impact than one point. If we used points for most products, the results would be in small numbers with many zeros after the decimal point. Millipoint results are more practical for most expressing the environmental impacts of most products. Fig. 12 illustrates the single score results of ammonia driven vehicles from various resources. Overall wind energy based option yields lower environmental impact, however, hydrocarbon cracking and solar PV option have similar impact factors.

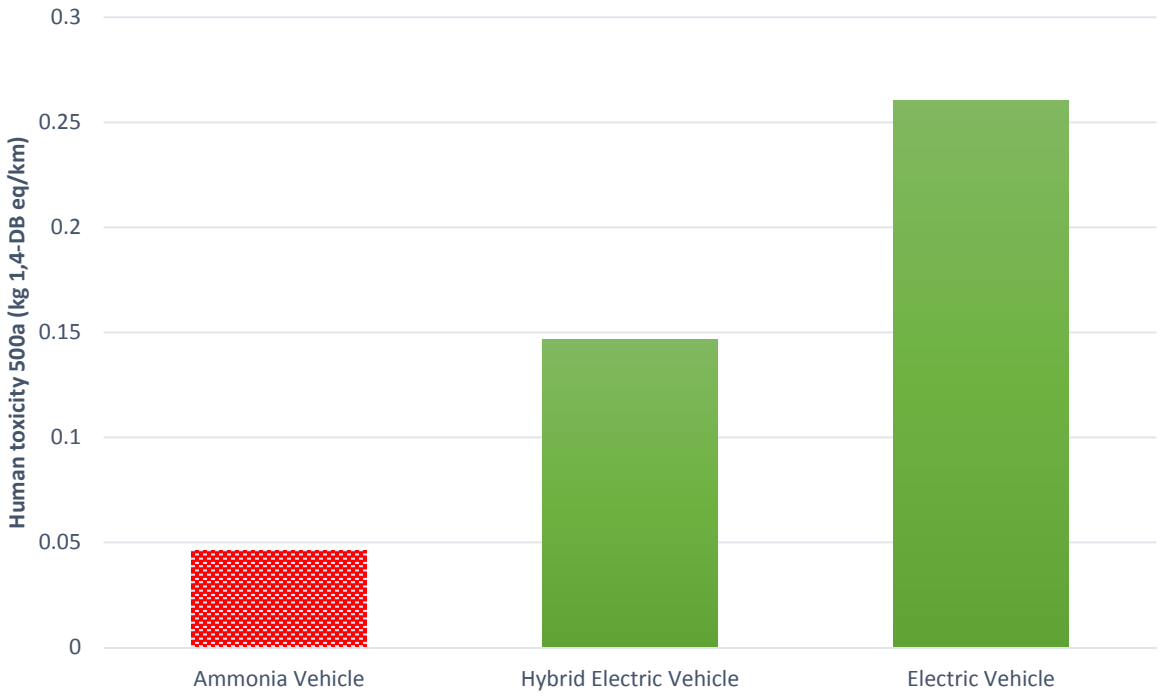

Fig. 13. Life cycle comparison of human toxicity results for various vehicles

The ammonia driven vehicles are significantly less human toxic compared to EVs and HEVs as seen in Fig. 13.

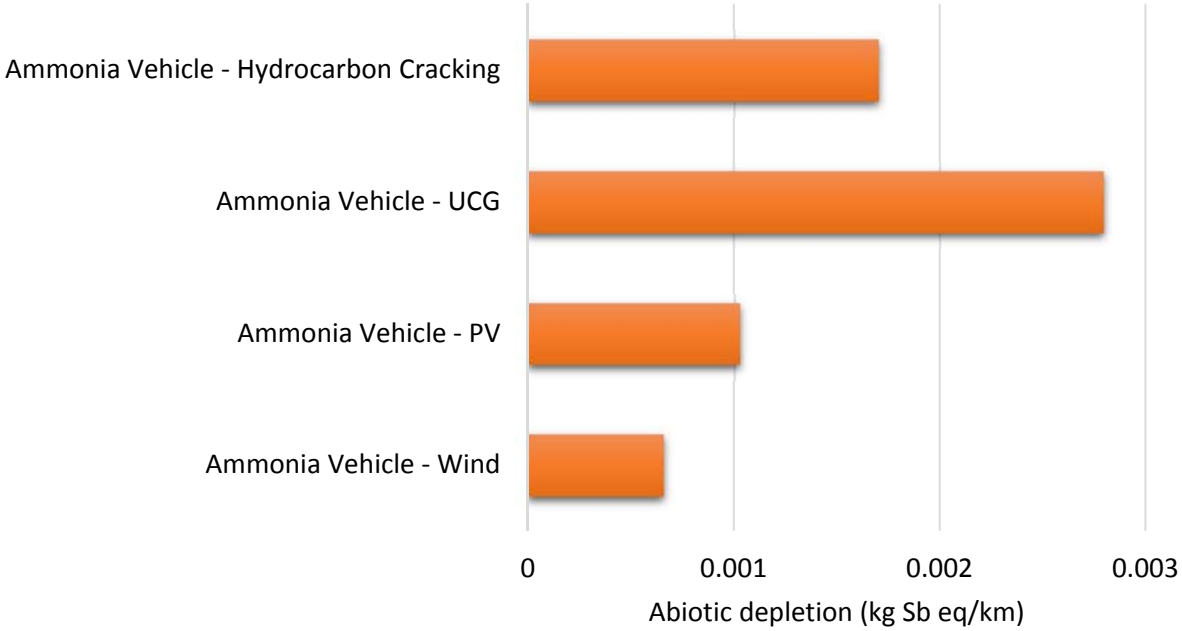

Fig. 14 Abiotic depletion comparison of various source ammonia vehicles according to CML 2001

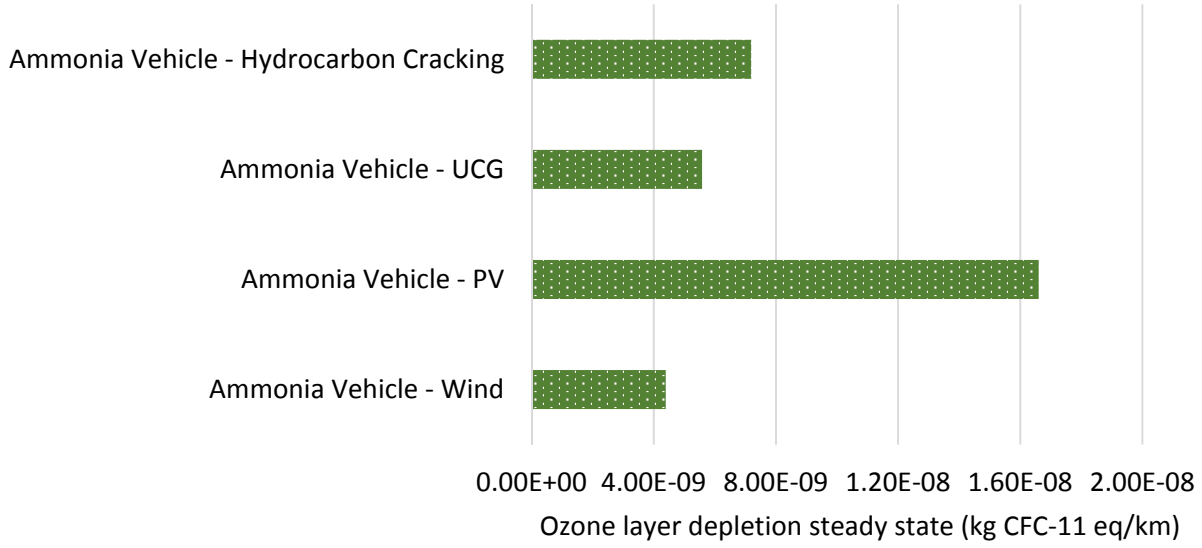

Fig. 15 Ozone layer depletion comparison of various source ammonia vehicles according to CML 2001

When abiotic depletion values of different methods based ammonia vehicles are compared, underground coal gasification (UCG) based method yields highest impact factor followed by hydrocarbon cracking as shown in Fig. 14. On the other hand, ozone layer depletion value of ammonia vehicles where ammonia comes from PV electrolysis has the highest value. It is noted that underground coal gasification based ammonia driven vehicle yields the lowest impact as Fig. 15 shows.

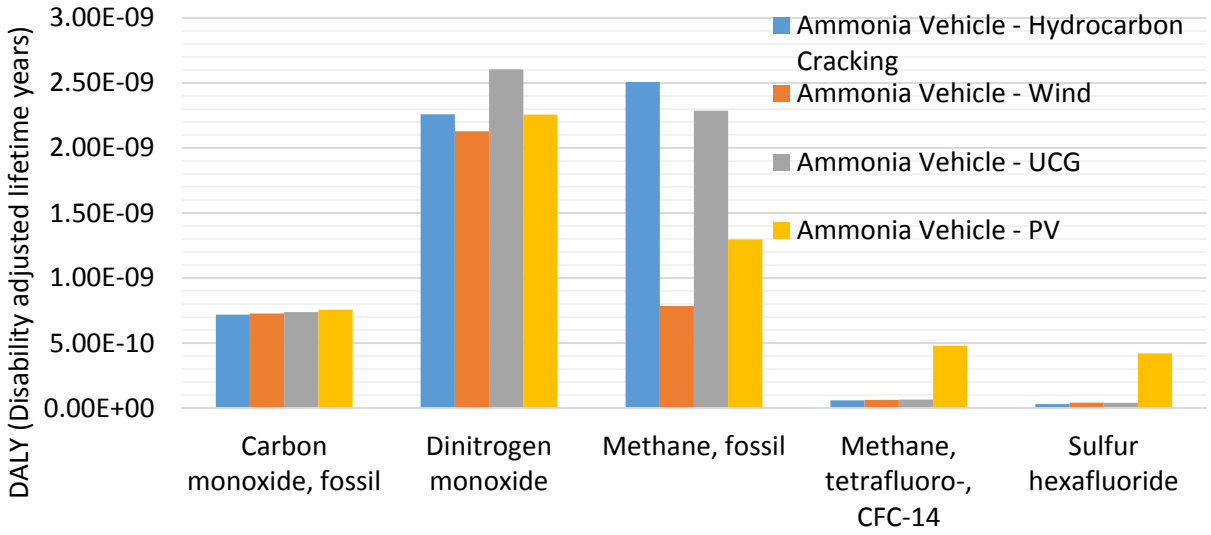

Fig. 16. Climate change impacts of various source ammonia vehicles according to Eco Indicator-99

The emissions from various source ammonia vehicles are shown in Fig. 16. Methane emission is highest in hydrocarbon cracking option while wind energy based option has lowest dinitrogen monoxide emission.

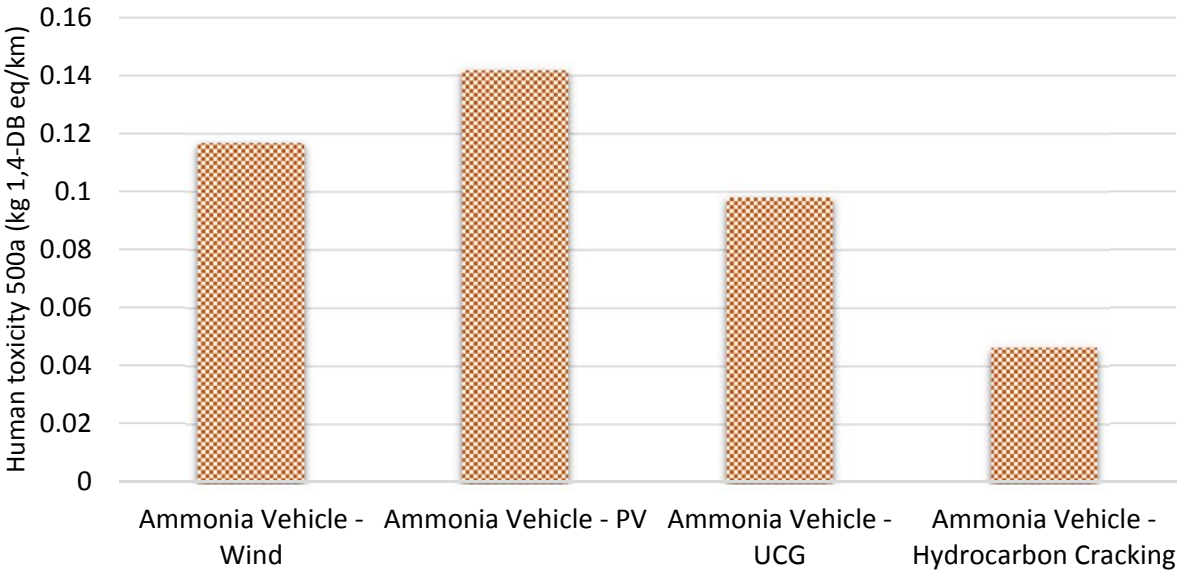

Fig. 17 Human toxicity comparison of various source ammonia vehicles according to CML 2001

The PV manufacturing process includes many toxic materials, hence ammonia vehicle from PV electrolysis option has the highest human toxicity value followed by wind electrolysis as shown in Fig. 17.

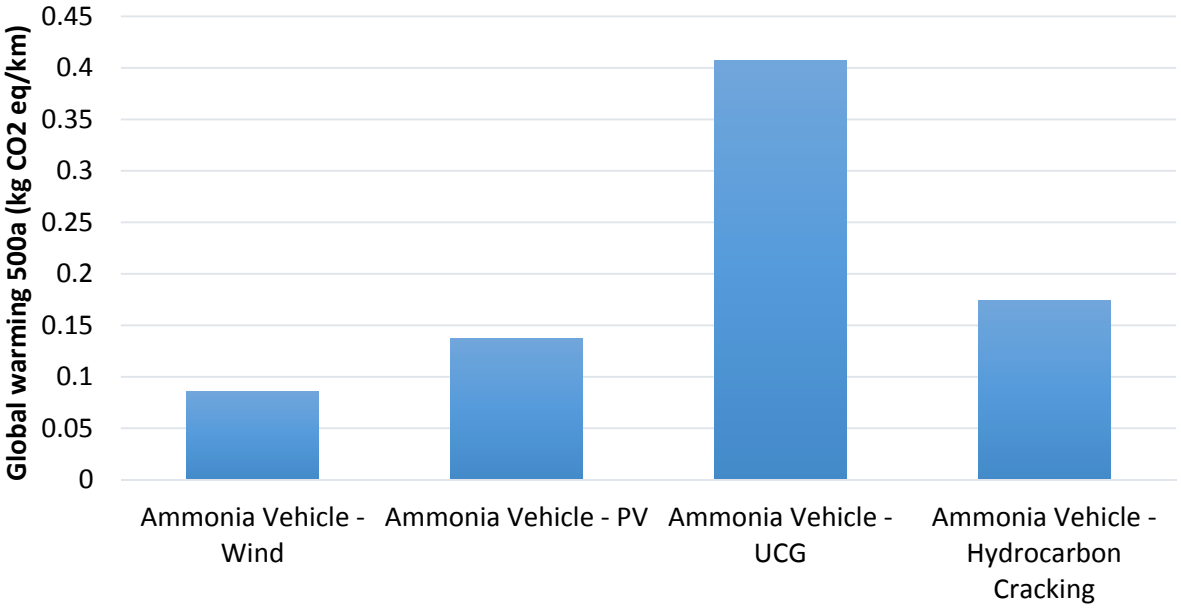

Fig. 18 Global warming comparison of various source ammonia vehicles according to CML 2001

Overall, life cycle global warming potential of ammonia driven vehicles from various methods are shown in Fig. 18 where renewable based options have less GHG emissions. However, hydrocarbon cracking option present only 23% difference from solar PV option.

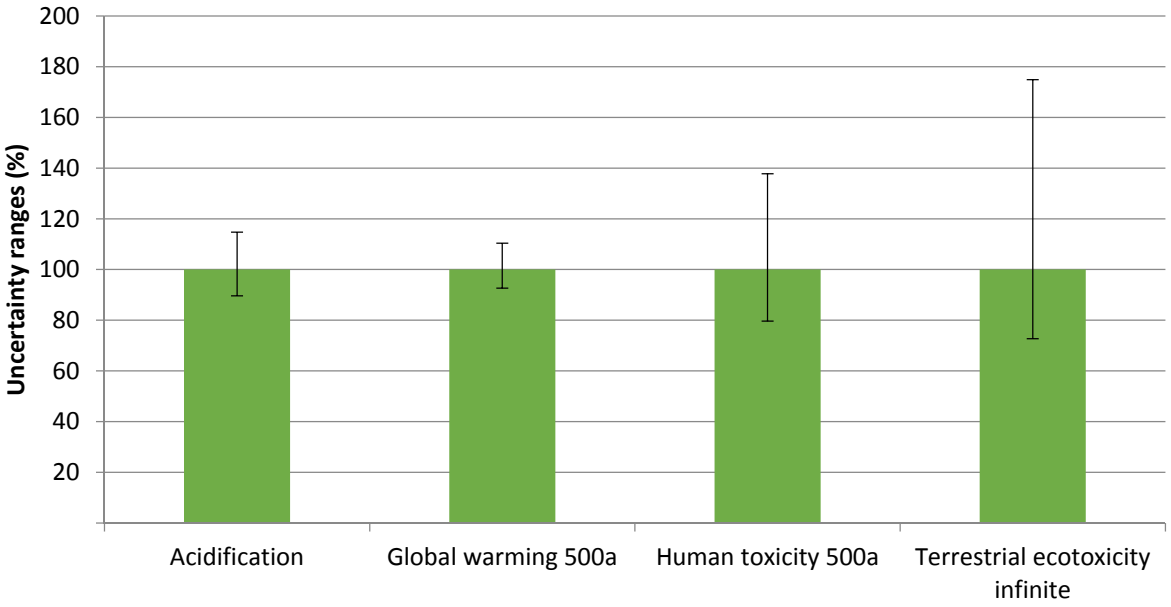

Fig. 19. Uncertainty analyses results of selected categories for ammonia vehicle (ammonia from UCG)

The uncertainty results are tabulated in Tables 2 and 3 for UCG and hydrocarbon options, respectively. As Figs. 19 and 20 show, the uncertainty ranges are not huge for the selected categories which implies more reliable results..

Table 2. Uncertainty results of ammonia vehicle for selected categories (ammonia from UCG)

Impact category	Unit	Mean	SD	CV	2.50%	97.50%	Std.err.of mean
Global warming 500a	kg CO2 eq	4.08E-01	1.89E-02	4.64%	3.76E-01	4.48E-01	0.00147
Acidification	kg SO2 eq	2.65E-03	1.83E-04	6.93%	2.36E-03	3.02E-03	0.00219
Human toxicity 500a	kg 1,4-DB eq	9.84E-02	1.59E-02	16.10%	7.69E-02	1.33E-01	0.0051
Ozone layer depletion steady state	kg CFC-11 eq	5.59E-09	1.31E-09	23.50%	3.74E-09	8.91E-09	0.00743
Terrestrial ecotoxicity infinite	kg 1,4-DB eq	8.40E-04	2.20E-04	26.10%	5.75E-04	1.38E-03	0.00826

The lowest uncertainty range is seen in global warming impact category and abiotic depletion for UCG and hydrocarbon option, respectively. The coefficient of variance (CV) of global warming category is 4.64% and 9.36% for UCG and hydrocarbon based methods, respectively.

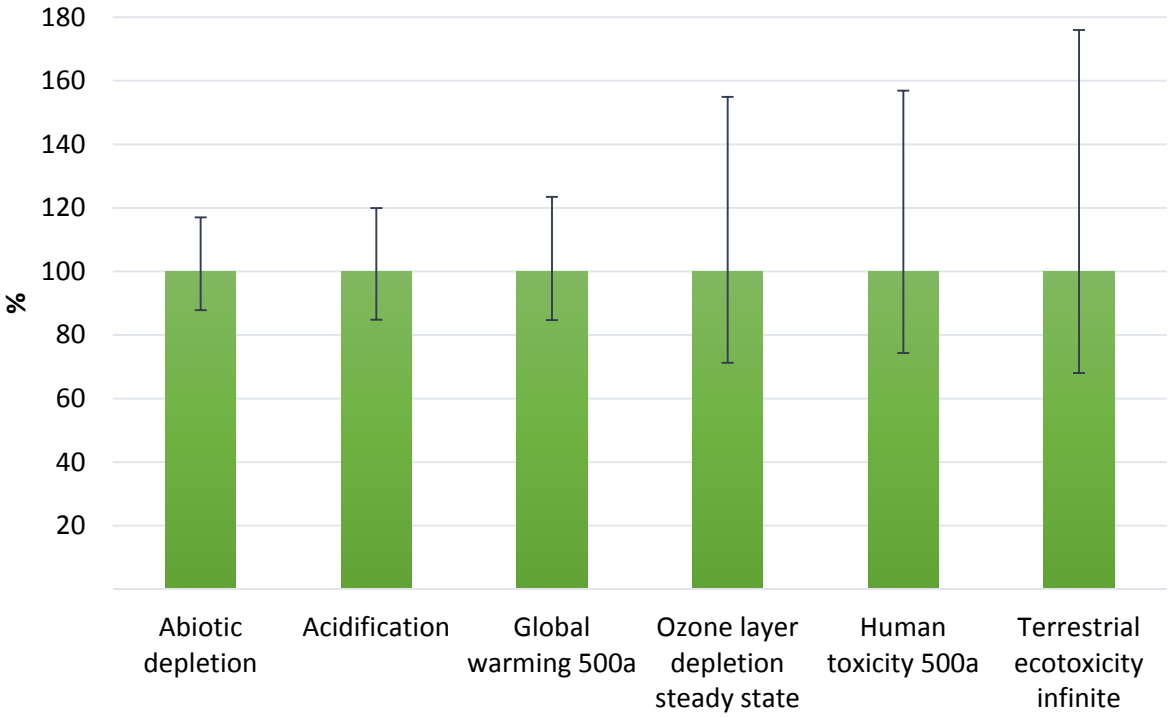

Fig. 20. Uncertainty analyses results of selected categories for ammonia vehicle (ammonia from hydrocarbon cracking)

Table 3. Uncertainty results of ammonia vehicle for selected categories (ammonia from hydrocarbon cracking)

Impact category	Unit	Mean	SD	CV	2.50%	97.50 %	Std.err.of mean
Abiotic depletion	kg Sb eq	0.0017	0.000126	7.43 %	0.00148	0.00198	0.00235
Acidification	kg SO2 eq	0.00104	9.03E-05	8.66 %	0.00088	0.00124	0.00274
Global warming 500a	kg CO2 eq	0.174	0.0163	9.36 %	0.146	0.213	0.00296
Ozone layer depletion steady state	kg CFC-11 eq	7.22E-09	1.47E-09	20.40 %	4.99E-09	1.09E-08	0.00644
Human toxicity 500a	kg 1,4-DB eq	0.0463	0.00988	21.30 %	0.033	0.0695	0.00675
Terrestrial ecotoxicity infinite	kg 1,4-DB eq	0.00063	0.00016	25.30 %	0.000409	0.00106	0.00802

4.1 Comparison of Various Fuels Production

Besides the vehicles, the production processes of various fuel s are also compared in terms of environmental impact in this section.

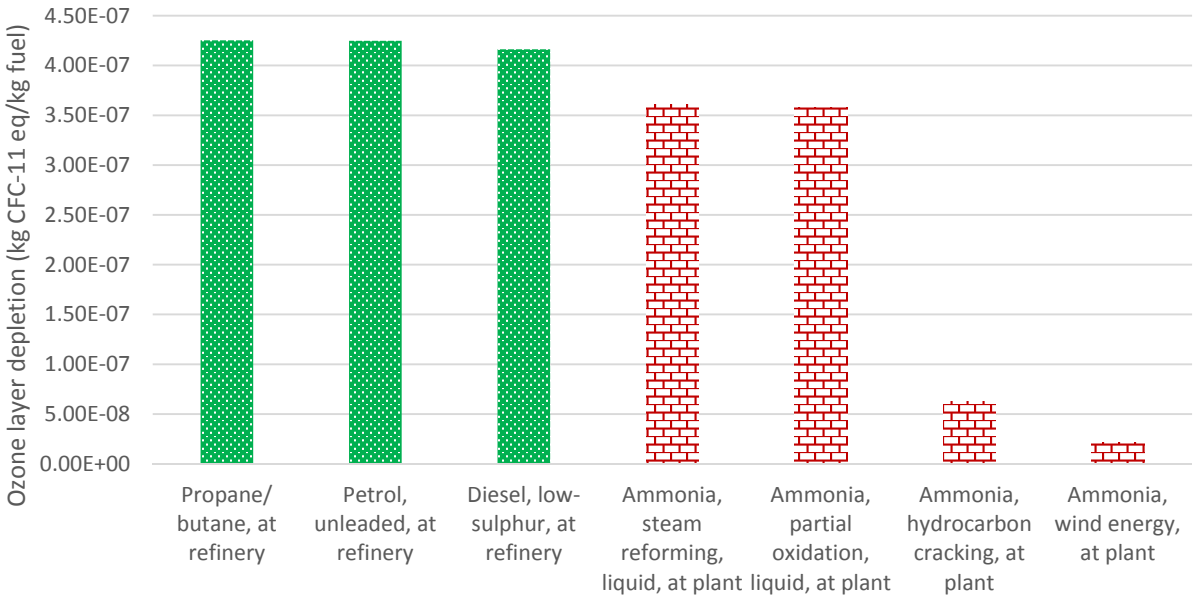

Fig. 21. Ozone layer depletion during productions of various fuels

Fig. 21 shows the comparison of ozone layer depletion values for various transportation fuels. Ammonia has lowest ozone layer depletion even if it is produced from steam methane reforming and partial oxidation of heavy oil. Production of fuel ammonia yields lower greenhouse gas emissions compared to petrol and propane production as shown in Fig. 22.

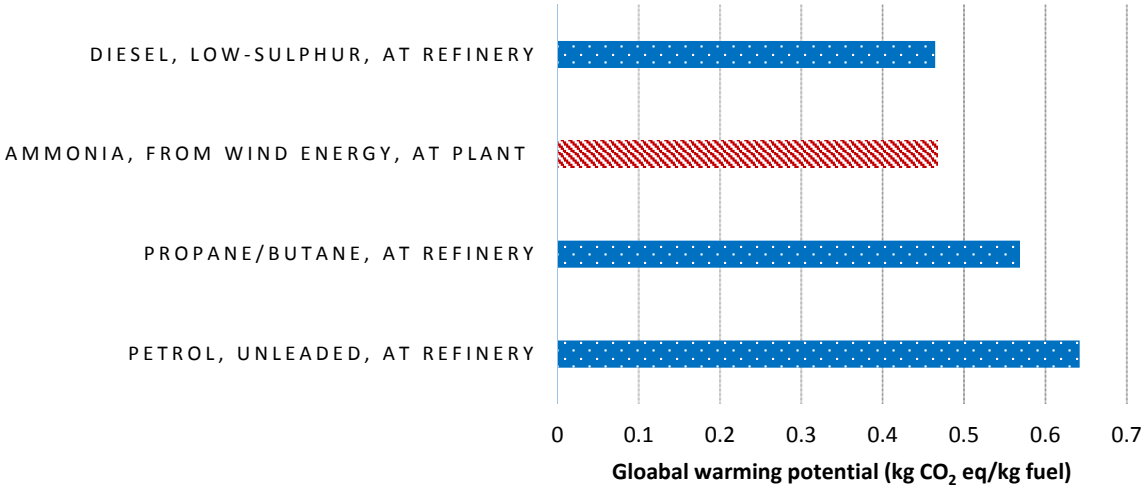

Fig. 22. Greenhouse gas emissions during production of various fuels

The ammonia production from various resources have lower abiotic depletion and ozone layer depletion values compared to other fuels such as propane, petrol, diesel and natural gas as shown in Figs. 23 and 24. Ammonia production from wind energy has the lowest ozone layer depletion impact.

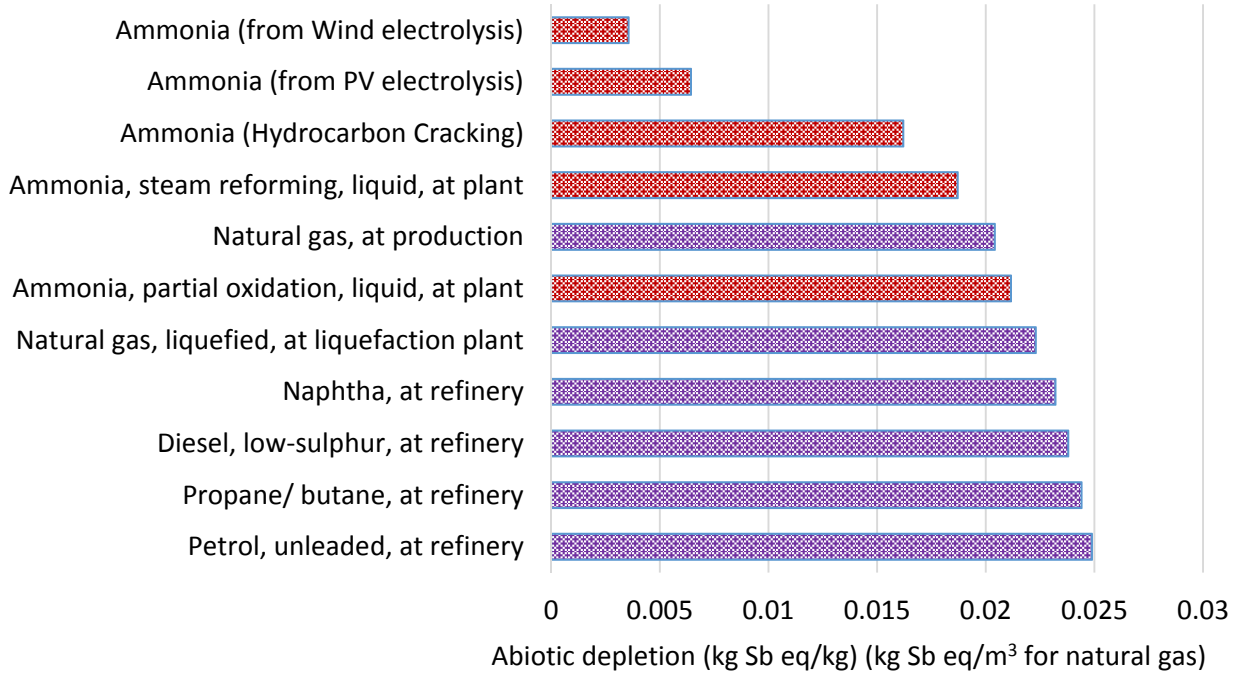

Fig. 23. Abiotic depletion values during production of various fuels

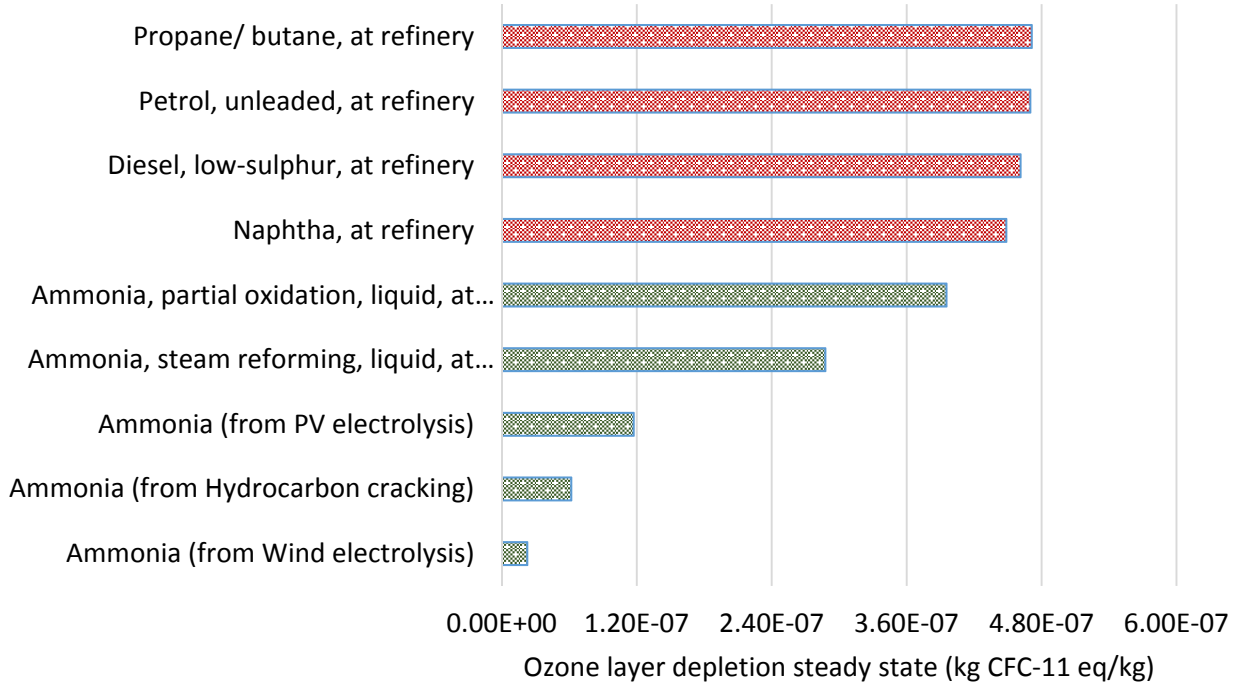

Fig. 24. Ozone depletion values during production of various fuels

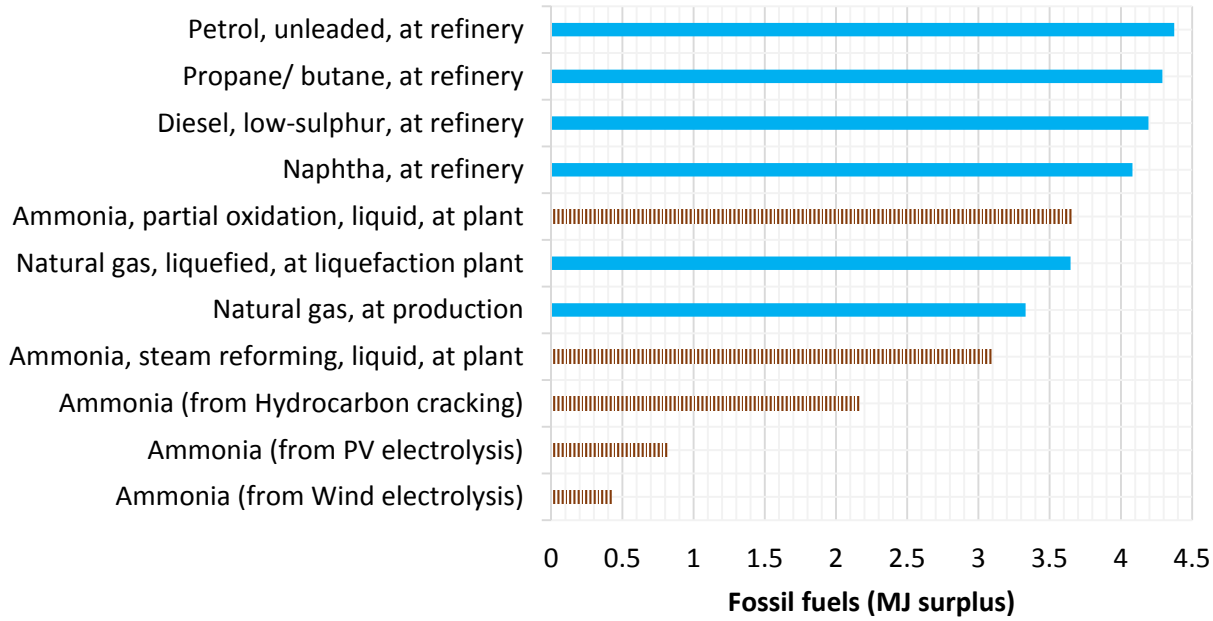

Fig. 25. Fossil fuels depletion impact values per MJ surplus for various fuels according to Eco Indicator 99

As seen in Fig. 25, fossil fuels depletion is the lowest for ammonia production according to Eco Indicator 99 LCA method.

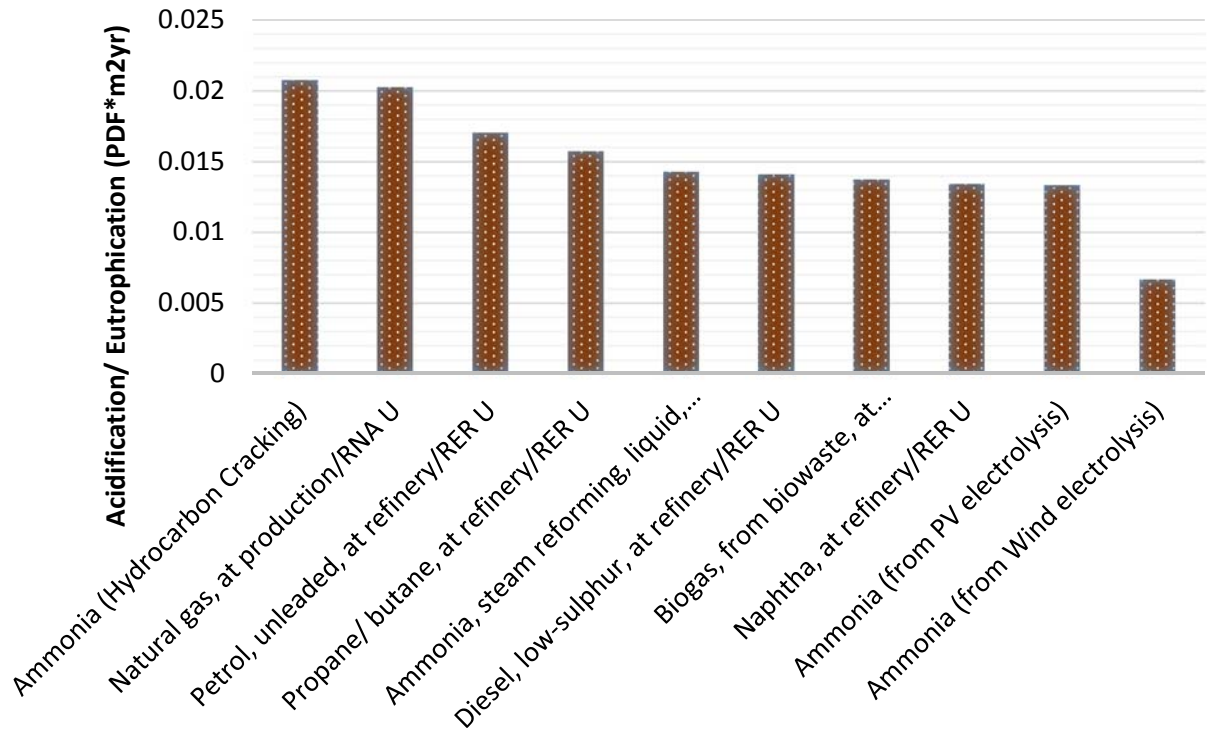

Fig. 26 Acidification/Eutrophication values of various fuels according to Eco Indicator 99

Similar to ammonia driven vehicles, production processes of ammonia from renewable resources have less acidification and eutrophication values although current steam methane reforming option yields lower than natural gas, petrol and propane as illustrated in Fig. 26.

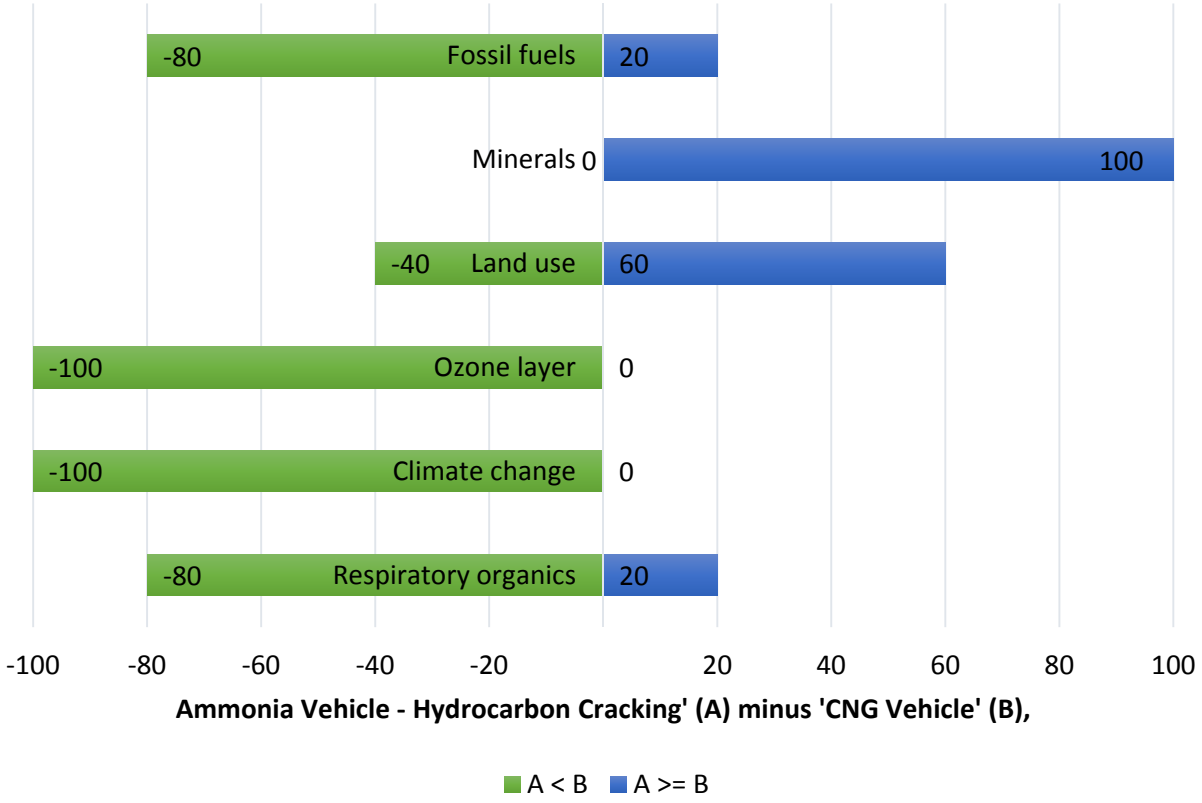

Fig. 27. Monte-Carlo simulation results of characterized LCA comparison between ammonia and CNG vehicle

4.2 Ammonia vs. Natural Gas

Compared to liquefied natural gas, there are more environmentally friendly fuels such as ammonia. Ammonia does not emit direct greenhouse gas emissions when utilized in the vehicles. Furthermore, production process of ammonia yields lower global warming impact compared to LNG production. Ammonia can also be produced from natural gas and hydrocarbons such as bitumen. Henceforth, in the ideal case, if Alberta oil sands bitumen can be converted into ammonia and then transported via pipelines to the ports, it would have lower total environmental impact both in the production process and utilization process. Furthermore, ammonia is liquid at higher temperatures (-33°C) than natural gas (-162°C) which implies lower energy requirement in liquefaction process. The other option for a more environmentally friendly process can be conversion of LNG to ammonia after being produced and transported via pipelines. Natural gas can be cracked into carbon black and hydrogen using plasma dissociation technique. In this case, carbon black is also utilized as a useful output for tire, plastic etc. industry. Instead of emitting CO2 to the environment, produced carbon black is used for various sectors, and greenhouse gas emissions are lowered. Produced hydrogen can be used for ammonia synthesis and stored in the vessels for the overseas transportation. In this manner, a cleaner alternative fuel is consumed and

total greenhouse gas emissions are significantly decreased. Henceforth, establishing an ammonia production plant using either tidal energy (British Columbia has significant potentials) or hydropower electricity would be more cost effective and environmentally friendly.

In Fig. 27, the green bars on the left represent the number of times ammonia vehicle had a lower environmental impact than CNG vehicle. For instance, it shows that in 100% of the cases the climate change impact score is lower for ammonia. In about 20% of the cases, the fossil fuels category is lower in CNG vehicle. Overall, it is noted that ammonia driven vehicle is more environmentally friendly compared to CNG vehicle.

5. Conclusions

Alternative fuels for transportation sector are intensively investigated by researchers in recent years. The main criteria for a sustainable fuel is to be environmentally friendly and cost effective. In this study, a comparative environmental impact assessment of alternative and conventional fueled vehicles is conducted using cradle to grave approach via life cycle analyses under seven different environmental impact categories. Conventional vehicles considered in this study include diesel, gasoline, CNG and LPG. Alternative vehicles comprise of hydrogen, ammonia, methanol, EV and HEV. The analyses are conducted from manufacturing of passenger cars to disposal including operation of the vehicles. Monte Carlo uncertainty analyses of hydrogen vehicle results are also conducted in order to investigate the reliability of the outcomes. The results show that hydrogen vehicle is the most environmentally benign one in all environmental impact categories. Ammonia as a sustainable and clean fuel has lowest global warming potential after EVs and yield lower ozone layer depletion values than EVs. Although EVs do not emit direct CO_2 during operation, the production and disposal processes of batteries bring some consequences which harm the environment in terms of acidification, eutrophication and human toxicity. Since methanol production is dependent on mainly natural gas, it has highest global warming potential. It is concluded that in order to have sustainable and clean transportation, production pathway of vehicles, batteries and alternative fuels need to be environmentally friendly.

CHAPTER 2. AMMONIA FROM HYDROCARBON DISSOCIATION

In this section, dissociation of hydrocarbons including oil sand bitumen and natural gas for ammonia production in Alberta is investigated.

Hydrocarbons can be used as a source of hydrogen which is required for ammonia synthesis. There are various alternative pathways for hydrogen production from hydrocarbons. In this section, a detailed literature review is presented for ammonia production via hydrocarbons. The source of hydrogen needs to be only the hydrocarbon itself, which experiences thermal decomposition:

$$C_nH_m \rightarrow nC + \frac{m}{2} H_2$$

In the case of methane, steam conversion is twice as endothermic as thermal decomposition per unit volume of methane as shown below:

$$CH_4 + 2H_2O \rightarrow CO_2 + 4H_2 \; ; \; \Delta H = 163 \text{ kJ}$$
$$CH_4 \rightarrow C + 2H_2 \; ; \; \Delta H = 75.6 \text{ kJ}$$

If the hydrocarbon itself is used as the thermal energy supply of the processes, the consumption of hydrocarbon feedstock per unit of the product hydrogen in both cases is comparable.

The thermal dissociation of methane is a recognized process. It has long been used for the production of soot. The process is multi-step containing the contact heating (a fire-brick) up to 1500°C and methane dissociation with the yield of soot and methane-hydrogen combinations. It can be seen that the route necessitates elevated temperatures.

Muradov [11] implied that the thermodynamic data show that methane dissociation can be done at reasonable temperatures. For example, at 800°C, the equilibrium concentration of hydrogen in H_2-CH_4 gaseous mixes matches 94% by volume. Thus, for the application of thermal dissociation of methane at relatively low temperatures, the use of catalysts is necessary.

Efforts were made to utilize catalysts for the cracking of methane and light hydrocarbons. The "HYPRO" process was established for the generation of hydrogen from refinery gases and it was shown that the method is financially appropriate for the concentration of hydrogen in gas streams [11]. The method is based on the basic catalytic cracking of methane and other gaseous hydrocarbons. The catalyst is conveyed by the gas streams. The process temperature is up to 980°C and the pressure is atmospheric. The carbon placed on the catalyst was then burned to restore the catalyst and to source the heat of the process. The "HYPRO" process lets the conversion of "dry" refinery gases into a gaseous stream holding 90 vol% hydrogen and 10 vol% methane.

The temperature dependency of hydrogen concentration in methane cracking gas using iron catalyst and other contacts is presented in Fig. 28. It is obvious that the iron catalyst discloses a high catalytic activity at temperatures above 600°C, and at 800°C the composition of the cracking gas approaches the equilibrium value.

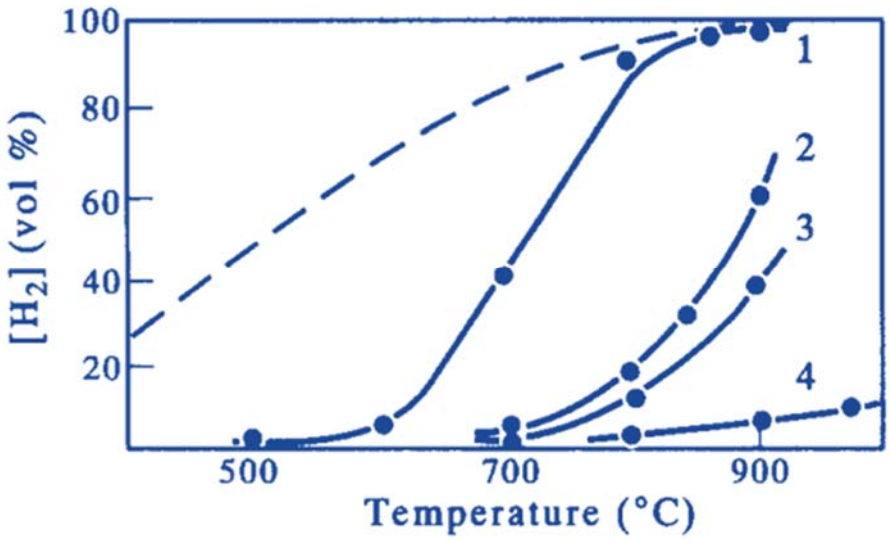

Fig. 28 Temperature dependence of hydrogen concentration in gas of methane decomposition using various catalysts and contacts: (1) iron oxide; (2) alumina; (3) graphite; (4) quartz; (--) equilibrium curve (from Ref. [11])

1. Thermo-catalytic Decomposition of Liquid Hydrocarbons

Thermo-catalytic decomposition of light liquid hydrocarbons (boiling point 50-200°C, average ratio H:C = 2:1) can be carried out with the production of carbon and hydrogen:

$CH_{2.1} \rightarrow C + 1.05\ H_2$

In some situations such as using aromatic-containing fractions, this reaction is thermo-neutral. The volume of hydrogen achieved is slightly less than in the occasion of gaseous hydrocarbons. The process does not vary significantly in its technical features from thermo-catalytic decomposition of methane and other gaseous hydrocarbons. The technical structure of the procedure varies considerably in the circumstance of heavy residual fractions (HRFs: boiling point higher than 350°C), which are used in industry as fuel and as a feedstock for the steam-oxygen gasification process. It is known that HRFs comprise huge amounts of sulfur and metals, which in the case of direct dissociation will transfer into the coke and will reduce it useless for further use. Moreover, the process of coke separation from the catalyst will also turn into a complex type. Hence, it is practical that the process be carded out in a two-step scheme, as in the case of the "HYDROCARB" process [11]:

$CH_{1.6} + 1.2\ H_2 \rightarrow CH_4$: hydrogasification

$CH_4 \rightarrow C + 2\ H_2$: methane cracking

and for the overall process

$CH_{1.6} \rightarrow C + 0.8\ H_2$

The quantity of hydrogen generated is less than in the case of light hydrocarbon fractions. Nevertheless, the procedure has substantial benefits, specifically, that it lets the co-production of valuable by-products: sulfur (or sulfuric acid) and metals (vanadium, nickel and others). The temperature of hydrogasification is about 750°C, pressure 1 - 10 GPa, and the hydrogenating gas contains 95 vol% hydrogen. The occurrence of sulfur mixes in HRFs, as well as in the hydrogenating gas, does not affect the product yields since the method is not catalytic. The yield of liquid products changes from 2-3 to 21-23% by mass, depending on hydrogasificator

construction, using crude oil as a feedstock. Methane and ethane are the key yields of hydrogasification of crude oil [11].

Methane decomposition reaction is moderately endothermic process. The energy requirement per mole of hydrogen produced is considerably less than that for the steam reforming process. Due to this relatively low endothermicity of the process, less than 10% of the heat of methane combustion is needed to drive the process. There have been attempts to use different catalysts to reduce the maximum temperature of thermal decomposition of methane. Metal catalysts, including Ni, Fe, Co, Pd and others, have been most commonly used for methane decomposition. However, there was a catalyst deactivation problem associated with the carbon build up on the catalyst surface. In the vast majority of related publications, carbon produced was burned off the catalyst surface in order to remove it from the reactor and regenerate the original activity of the metal catalyst. Alternatively, carbon could be gasified with steam to produce additional amount of hydrogen. In either case, the amount of CO_2 produced is comparable with that of the conventional processes such as SMR or partial oxidation [12].

Besides methane, as a main component, other heavier hydrocarbons such as ethane, propane, butane and others, constitute natural gas. It was important, therefore, to investigate the behavior of these hydrocarbons in the presence of different carbon catalysts at elevated temperatures (800–900°C). Propane was selected as a representative hydrocarbon. Due to a relatively weak C–H bond in propane molecule (402.2 kJ/mol), it is somewhat easier to split propane than methane molecule (methane C–H bond energy is 440.0 kJ/mol). 26.0 kJ is required to produce one mole H_2 from propane, comparing that to 37.8 kJ for methane (at standard conditions):

$$C_3H_8 \rightarrow 3C + 4\,H_2\,;\ \Delta H_0 = 103.9\ \text{kJ/mol}$$

However thermal cracking of propane at high temperatures could also proceed via a thermodynamically more favorable formation of methane and ethylene

$$C_3H_8 \rightarrow CH_4 + C_2H_4\,;\ \Delta H_0 = 81.3\ \text{kJ/mol}$$

As a result, pyrolysis of propane at relatively low residence times produced gaseous mixtures containing hydrogen, methane, ethylene and small amounts of ethane and propylene. Fig. 29 depicts the experimental results of propane catalytic pyrolysis over carbon black (a) and activated carbon (b) type catalysts at 800°C using a packed bed reactor. Activated carbon demonstrated high initial activity in propane decomposition reaction followed by the rapid drop in catalytic activity which is similar to methane decomposition [12].

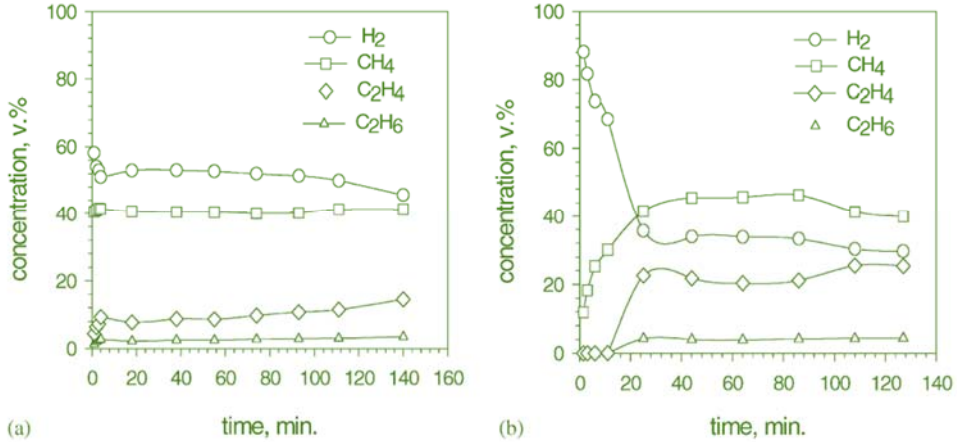

Fig. 29 Propane pyrolysis over carbon black catalyst (a) and activated carbon catalyst (b) at 800°C (from Ref. [12])

There are several technological options for methane dissociation to hydrogen and carbon, which are summarized in Fig. 30.

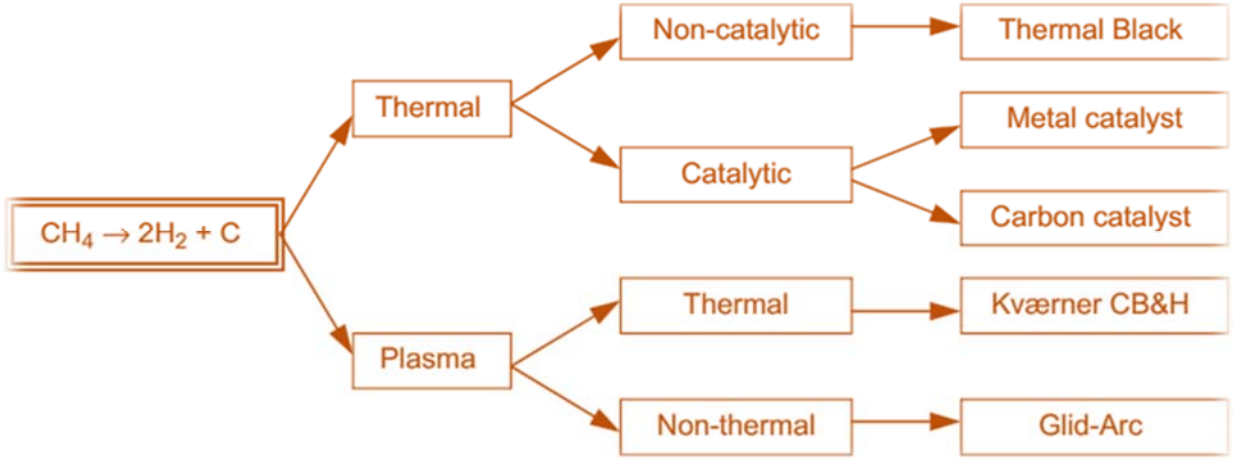

Fig. 30 Main routes for decomposition of methane to hydrogen and carbon (from Ref. [13])

Kværner company of Norway developed and operated on a limited commercial scale a thermal plasma process for decomposition of methane and other hydrocarbon feedstocks to hydrogen and carbon black [14]. Although technologically simple, the process is energy intensive: it was estimated that up to 1.9 kWh of electricity is consumed per one normal cubic meter of hydrogen produced [15].

Hydrogen via thermal (catalytic) dissociation of hydrocarbons represents an alternative solution. One approach that recently attracted the attention of researchers is CO_2-free production of hydrogen and carbon via thermal decomposition (or pyrolysis, cracking) of methane. Methane decomposition over metal catalysts due to a very strong C–H bond, methane is one of the most stable organic molecules hence, thermal dissociation of methane would require temperatures in excess of 1000°C. Different transition metal catalysts were used to reduce the maximum temperature of methane thermal decomposition.

Fig. 31 summarizes the bulk of the available literature data on the catalysts, preferred temperature range and carbon products of catalytic decomposition of methane. Here, 1:Ni-based, 2:Fe-based, 3:carbon-based, 4:summary of data related to Co, Ni, Fe, Pd, Pt, Cr, Ru, Mo, W catalysts, 5:non-catalytic decomposition, CF: carbon filaments, TC: turbostratic carbon, GC: graphitic carbon, AmC: amorphous carbon. Ni-based catalysts attracted an attention of a majority of the researchers in the field due to their high catalytic activity and the capability of producing carbon filaments (CF) or carbon nanotubes (CNT) at moderate temperatures (500–700°C). Fe-based catalysts efficiently operate at a somewhat higher temperature range and also are able to catalyze the formation of CNT [16].

The use of carbon-based catalysts offers certain advantages over metal catalysts due to their availability, durability and low cost. In contrast to metal-based catalysts, carbon catalysts are sulfur resistant and can withstand much higher temperatures. The concept is based on catalytic decomposition of methane over catalytically active carbon particles with the production of hydrogen-rich gas and carbon deposited on the surface of original carbon particles. The most important features of the process are as follows: (i) it can be catalyzed by carbon produced in the process, so that an external catalyst would not be required (except for the start-up operation), and (ii) the separation of carbon product from the carbon catalyst is not necessary. The technical

feasibility of the concept and the data on catalytic activity of a variety of carbon materials of different origin and structure, including a wide range of activated carbons (AC), carbon blacks (CB), microcrystalline graphite and nanostructured carbons toward methane decomposition reaction are reported [16].

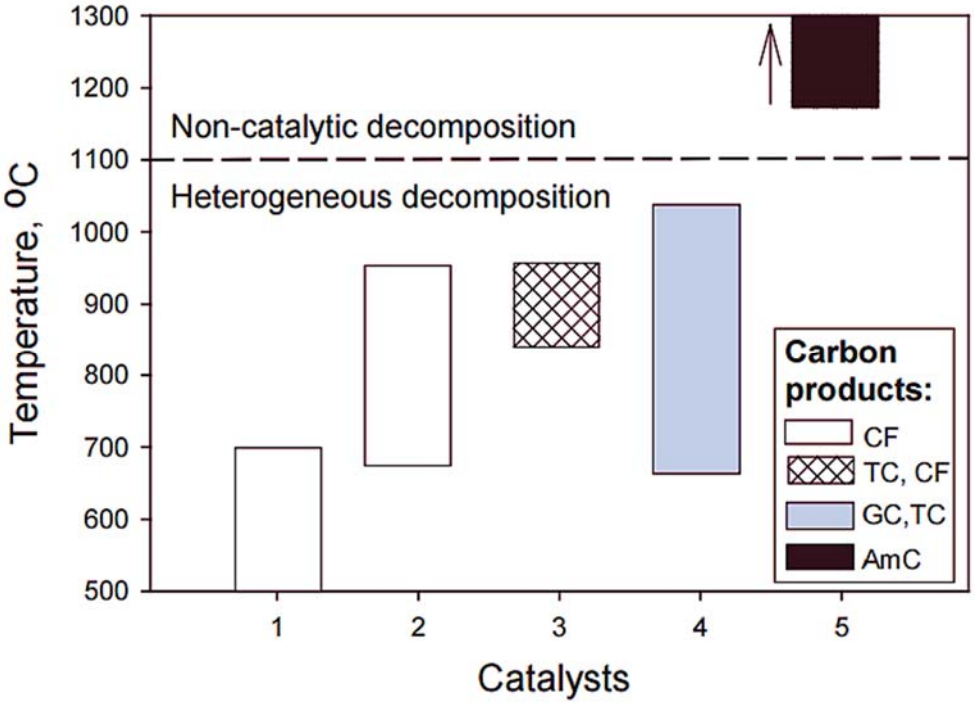

Fig. 31 Comparison of catalysts, preferred temperature range and carbon products related to catalytic methane decomposition reaction (from Ref. [16])

On perspectives of large-scale hydrogen production via catalytic decomposition of natural gas, there are a number of ways to arrange hydrogen production by catalytic decomposition of methane. In the 1960s, Universal Oil Products (UOP) operated a pilot plant with the capacity of 118 l/min for the continuous production of hydrogen via catalytic decomposition of methane in a moving bed of Ni-catalyst particles at 815–1093°C [17]. The process, however, targeted the production of only one product which is hydrogen. Carbon deposited on the catalyst was combusted to provide the process heat causing important amounts of CO_2 byproduct.

Lamacz and Krzton [18] presented a paper dealing with the catalytic decomposition of hydrocarbons (methane and toluene) in the aspect of H_2 production and types of obtained carbon deposits. The catalyst used in the studies was nickel supported on ceriaezirconia ($Ni/CeZrO_2$). Hydrogen production was found to be higher for CH_4 decomposition. Both types of carbon deposits (filamentous and pyrolytic) were found to be very reactive with H_2O, which is due to their activation by the ceriaezirconia support.

An alternative method of hydrogen production from hydrocarbons is their thermal decomposition which is accompanied by the formation of carbon deposits. Methane can be thermally or thermocatalytically decomposed (TCD) into carbon and hydrogen without CO or CO_2 production. Hence, the need for water gas shift (WGS) and CO_2 removal is eliminated, and obtained in TCD hydrogen can be supplied directly to the fuel cells. Takenaka et al. [19] reported that the supported Ni catalyst is one of the most effective catalysts for the methane decomposition.

The catalytic performance of Ni-based catalysts for the decomposition of hydrocarbons of C_3–C_8 into CO-free hydrogen and carbon fibers was investigated in order to produce CO-free hydrogen as a fuel. Ni–Pd/SiO_2 catalyst showed a high activity and a long life for the decomposition of LPG (propane and n-butane) into CO-free hydrogen and carbon fibers [19]. Chai et al. [20] investigated that the size of NiO crystallites is a meaningful parameter in the formation of particular types of filamentous carbon. Methane decomposition carried out at 550°C on the large size NiO (supported on SiO_2, HZMS-5 and CeO_2) lead to CNFs (carbon nanofibers) while the formation of multi walled CNTs (carbon nanotubes) was observed on the small size NiO supported on Al_2O_3.

Gac et al. [21] studied methane decomposition performing over nickel alumina catalysts modified with magnesia between the temperatures of 500-700°C. The catalysts were obtained by the co-precipitation method. Catalytic methane decomposition was studied over metal catalysts, based on Ni , Co or Fe, different supports, including SiO_2, TiO_2 and Al_2O_3, MgO or metallic foams. In spite of the intensive research of the numerous processes of hydrocarbons conversion and synthesis of carbon nanomaterials, some questions still remain open; such as the influence of the size of the crystallites, metal-support interactions, diffusion phenomena, reaction temperature or the nature of carbon deposits. It was found out that the activity of catalysts and the properties of carbon deposits were related to the catalysts composition and the reaction temperature. Carbon filaments with fishbone-like packed graphitic layers were formed at 500°C, while the multi-walled nanotubes were observed after reaction performed at 700°C.

Zhang et al. [22] investigated the catalytic cracking of methane as an alternative route for the production of hydrogen from natural gas. Nickel supported on silica was found to be active for this reaction producing stoichiometric amounts of hydrogen and carbon. While commercial processes exist that utilize thermal cracking of methane at extremely high temperatures for the production of acetylene and carbon black, hydrogen production via the catalytic cracking of methane was only briefly considered in the past. Silica-supported nickel catalysts are active for this reaction at relatively low temperatures around 550°C. These catalysts maintain their activity for a sustained period of time because of their capability to accumulate large amounts of carbon on their surface in the form of long cylindrical hollow ®laments, with a nickel particle located at the front tip of each individual ®lament. Deactivation eventually occurs due to spatial limitations imposed on the ®lament growth, which lead to the loss of exposed nickel surface.

2. Comparison of Furnace and Plasma Processes

If it is assumed that typical electro-thermic efficiency of modern plasma arc devices is over 80%, it can be estimated that the electric energy supply needed for the cracking operation varies between 4 and 7 kWh per kg of carbon produced or between 1 and 1.9 kWh per normal cubic meter of hydrogen produced [23]. Because of the wide range of grades of carbon black, the comparison will only concern a well-defined product, whose industrial name is super abrasion furnace black (SAF). This grade corresponds to an average structured black, used essentially as reinforcing filer to improve abrasion properties. The average commercial price is about US $1000-1400 per ton. Production temperature of this product is about 1600°C, so the theoretical energy supply, as defined above, may be estimated at 5000 kWh per ton of carbon produced. It was presented in Fig. 32 the input/output mass and energy balances for the two processes which is related to one ton of product. Hence, for a typical capacity of 100,000 tons per year with a 0.68 utilization rate, total electric power of a plasma black installation will be 83 MW [23].

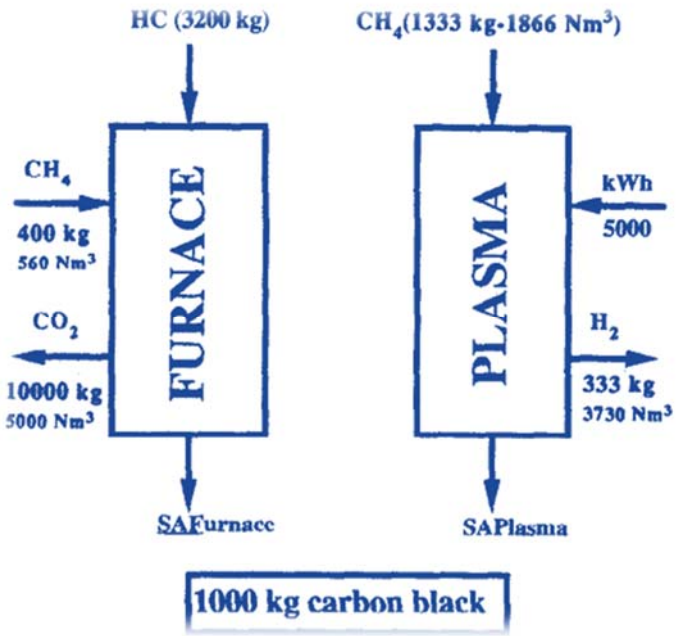

Fig. 32 Input-output balance for furnace and plasma processes (from Ref. [23])

This result compared well with conclusions of a study presented in 1983 [24], as the authors, who were using a 15 kW radio frequency (RF) plasma, obtained with methane carbon yields of about 96% with a lower energy of only 2.2 kWh per kg of carbon.

Plasma technology has been used since 1980 as an alternate method for generating carbon black that takes advantage of the plasma's high enthalpy property [25]. The principle of carbon black manufacture, by the "cracking" of a hydrocarbon vapor using a plasma source, was patented in France in 1980 [26], and several studies have since been dedicated to this subject. Thus in 1983, Ibberson et al. [27] used a 15-kW RF induction plasma reactor to process various hydrocarbons. Methane, n-hexane and benzene were fed to the reactor and carbon black, in high yields, of up to 98%, were obtained, and with a corresponding low energy requirement per kg of carbon produced (2.2 kWh per kg of carbon). Bolouri and Amouroux [28] described carbon (acetylene) black production by direct processing of natural gas in an argon RF plasma reactor. Overall, their results showed that, with a well-designed reactor, almost all input methane can be converted to carbon and acetylene. The carbon yield reached about 45% when the total methane conversion rate approaches 100%. The solid product obtained presented similar qualities to those of acetylene black obtained by the classical processes.

Two, more recent laboratory-scale investigations of carbon black production have been conducted using a HF plasma reactor at the Plasma Technology Research Center in Canada [29, 30]. Light hydrocarbons were used as the feedstock in the process and plasma power levels of between 25 and 70 kW were used. In the first process stage, propane was fed to the system. The injection method employed was found to be the most important parameter in this plasma process. These authors found a relationship between the particular carbon black morphology and the method of feed injection. For example, radial injection produced "flat" form particles similar to those present in acetylene black produced at high frequency (HF). Axial injection produced very spherical form particles, comparable to those carbon blacks with specific surfaces in the order of 75 to 100 m^2/g. A carbon black production rate of 0.35 g/s was obtained for the radial injection. Propane decomposition rates of between 70 and 100% were observed during these experiences. In

the second described process, methane was fed to the plasma system, generating methane decomposition yields of about 100% and carbon black yields of about 55% at 60 kW. Carbon black, with particle sizes of between 20 and 80 nm and specific surfaces up to 250 m^2/g was obtained. The feed rates and the particular injection method employed were found to be the most important parameters determining the morphology of the carbon black produced. Specifically, smaller size particles, with higher specific surfaces, were found when the feed rate was increased. Impurities levels of below 100 ppm were found during these experiences. In 1990, Kvaerner started the development of the innovative Kvaerner CB&H process [30]. This process was considered primarily as a hydrogen-supply process [31]. By pyrolysis of the hydrocarbon feedstock, the process produces two valuable products: hydrogen and carbon black. The process yields almost 100% in feedstock efficiency and the impurity levels of the process products are restricted to only those impurities introduced in the feedstock. Although the Kvaerner Engineering organization represents this technology for industrial scale application [32], no evidence has been forthcoming so far to demonstrate that the process can economically produce carbon black of commercial interest [25].

Among the original potential reforming choices, plasma systems can deliver creative answers to the disadvantages in terms of reactivity, compactness and efficiency. Various ways were explored for the two last decades by means of various plasma techniques such as plasmatron, gliding arc, dielectric barrier discharge (DBD), corona, microwave, pulsed discharge and reformed hydrocarbons, such as methane, diesel and bio fuels [33]. The reforming method targeting hydrogen generation is the conversion of a hydrocarbon into a more valued product in terms of higher heating value. The difficulty is to achieve the process with the best energetic efficiency. Due to the capability to relief high energetic densities, plasmas have then been considered with interest for reforming uses. Based on their energy level, temperature and electronic density, plasma state is typically categorized as a high temperature (or thermal) plasma and a cold (or non-thermal or non-equilibrium) plasma. For example, neon lights are non-thermal plasmas and the sun is a thermal one.

The hydrocarbon reforming is an oxidation reaction in which oxygen, water or carbon dioxide have the responsibility of the oxidant. Plasma is an ionized gas that can be generated by a number of ways, like combustion, flames, electrically heated furnaces, electric discharges (corona, spark, glow, arc, microwave discharge, plasma jets and radio frequency plasma), and shocks (electrically, magnetically and chemically driven) [34]. Consequently, plasma media shows a high energetic state of substance, described by a high electrical conductivity. Traditionally, first plasma assisted reformers were thermal ones, e.g. direct current (DC) plasma torch. Chemical reactions were hence improved due to the presence of very reactive species (ions, electrons) in a very hot intermediate but the energy consumption was high.

Non-thermal plasmas [34] have been used for fuel gas treatment and have been accepted very promising for organic synthesis because of its non-equilibrium features; low power requirement and its capacity to make physical and chemical reactions within gases at comparatively low temperatures. The electrons in non-thermal plasma may extent temperatures of 10 000–100 000 K (1–10 eV) while the gas temperature can stay as low as room temperature. It is the high electron temperature that controls the uncommon chemistry of non-thermal plasmas. Based upon techniques of which plasma is produced, pressure used and the electrode geometry, non-thermal plasmas involve very diverse kinds containing glow discharge, corona discharge, silent discharge, DBD, microwave discharge and radio frequency discharge.

The RF discharge functions at high frequencies (several MHz) and very low pressure to attain the non-equilibrium situations. This discharge is likewise not appropriate for chemical synthesis. The microwave discharge works at very high frequencies, e.g. 2.45 GHz in the range of microwaves, with which only light electrons can track the oscillations of the electric field. Thus, this discharge is far from local thermodynamic equilibrium and may be functioned in a wide pressure range. Lately, gliding arc discharge, a mixture of high power equilibrium arc discharge and better selectivity of non-thermal plasmas was stated to be used for reforming uses [33]. An illustrative comparison of specific energy requirement and efficiencies for various research results is shown in Figs. 33, 34 and Table 4.

Gliding arc discharge reactor assisted the experimental study of methane conversion. It consists of a 2.5 l reactor walled with quartz where 8 cm is inner diameter and 50 cm is the length. Two 7 mm thick, 2 cm wide and 9 cm long diverging electrodes were utilized. They were hold by a stainless steel plate situated at the top of the setup. Reactant types were preheated at temperatures in the range 573–873K before entering the test chamber. Experimental runs circumstances were atmospheric pressure, specific energy input in the range 3–12.1 MJ/kg (ratio of the input electric power on the inlet gas flow rate), and partial oxidation was considered both for the air and 50% oxygen enriched air [33].

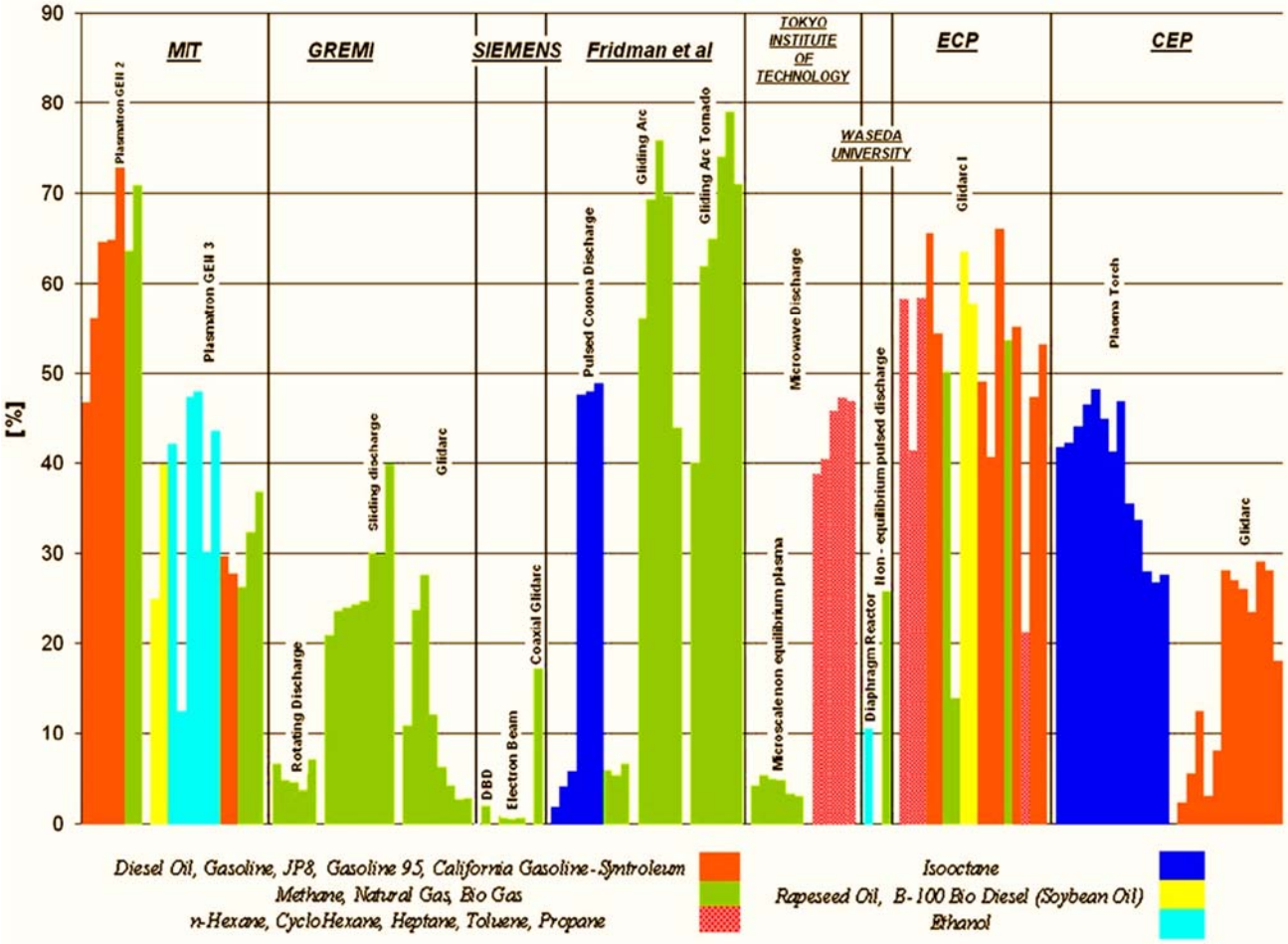

Fig. 33 Comparative efficiencies of non-thermal plasma processes (from Ref. [33])

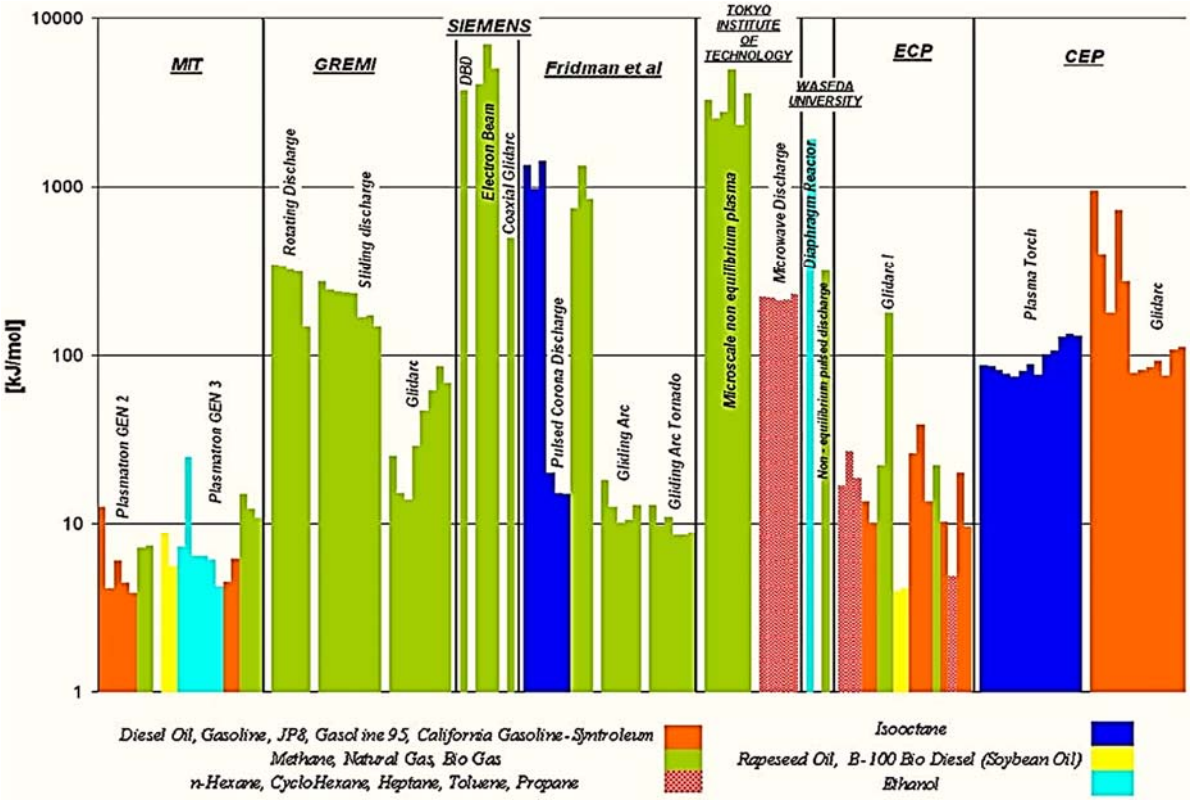

Fig. 34 Specific energy requirement of non-thermal plasma processes (from Ref. [33])

Table 4. Performances of some non-thermal plasma assisted reforming processes (from Ref. [33])

Ref.	Reactor	Fuel	Fuel injected (kW)	Reforming process	Plasma power (W)	Efficiency (%)	Efficiency ratio	Conversion rate (%)	Power density (kWH_2/L)
[35]	GEN 2	Diesel	10.78	Pox	270	46.67		80.9	2.6
[35]	GEN 3	Methane Ethanol Methane	11 26 22.5	ATR+catal. Pox+catal. Pox	210 200 375	63.59 43.5 36.70	0.84 0.84 0.57	103.98 73.38	3.57 57 42
[36,37]	Glidarc	Methane	1.52	Pox	50	75.81	0.98	87	0.476
[36,37]	GAT	Isooctane Methane	0.02	ATR+catal. Pox	4 200	48.78 74	0.70 0.93	75	0.004
[38,39]	Sliding discharge	Methane	2.68	ATR	830	24.59	0.40	22.53	7.8
[38,39]	Sliding discharge	Methane	4.63	Pox	75	27.53	0.42	58.55	11.8
[40,41]	Glidarc	Gasoline	7	SR	1000	29		65.8	0.86
[40,41]	Plasma torch	Isooctane	5.72	ATR	1000	41.78	0.72	90.55	8
[42,43]	Glidarc I	Diesel	12.01	Pox	280	54.28		100.14	4.44
[42,43]	Glidarc I	Gasoline 95	6.23	Pox	350	49.06		95.78	2.15

Table 5. Performances of catalytic reforming systems (from Ref. [33])

Ref.	Fuel	Power injected (kW)	Reforming process	Efficiency (%)	Efficiency ratio	Power density (kWH_2/L)	Start up time	Time to full power
[44]	Indolene 30	42.63	Pox, nickel based catalyst	78.5	0.96	16.12		
[45]	$C_{7.494}H_{14.53}$	86.15	ATR, monolith catalyst	78		53.4	20s	140s
[46]	Octane	1.44	ATR, house catalyst	68–70		0.4		
[46]	Gasoline	1.56	ATR, house catalyst	62–65		0.3	5min	50min

The performance values of some non-thermal plasma assisted reforming processes are shown in Table 4. At the Institute for Advanced Sustainability Studies (IASS), an alternative technology for methane decarbonisation applying liquid metal technology was proposed in collaboration with the Karlsruhe Institute of Technology (KIT) [47]. They comprised the following steps: conceptual design of a liquid metal bubble column reactor and material testing, process engineering incorporating carbon separation and hydrogen purification, and a socio-economic analysis. The results from the experimental tests showed that the liquid metal reactor design works effectively in producing hydrogen and carbon separation. Other aspects of the technology such as socio-economics, environmental impact, and scalability also appeared to be satisfactory making methane decarbonisation based on liquid metal technique a possible candidate for CO_2-free hydrogen production [47].

The decarbonisation of fossil fuels, particularly, natural gas, is a promising alternative and compromises definite benefits over the use of carbon capture storage (CCS) technologies. Methane decarbonisation by pyrolysis also called as methane cracking includes the dissociation of methane (CH_4) into its molecular particles: solid carbon (C) and hydrogen (H_2). Its key benefit lies in the lack of CO/CO_2 emissions. Conversely to CCS, it substitutes the managing of CO_2 with a much lower quantity of easier-to-handle solid carbon. Hydrogen signifies a significant clean energy carrier, with an already substantial demand and capable projections for the future energy system. Moreover, carbon is hypothetically marketable as a product for both current and envisaged usages such as carbon fibres, materials and nanotechnology.

The methane dissociation reaction is initiated with the formation of a free radical $CH_4 \rightarrow CH_3^* + H^*$ that dominates the kinetics of the reaction splitting the C-H bond (dissociation energy: 434.72 kJ/mol), which necessitates high temperature levels [48]. The evaluation of the reaction thermodynamic equilibrium mole fraction with Cantera library [49] was depicted in Fig. 35. It could be seen that above 1000°C, nearly comprehensive conversion of methane into hydrogen is theoretically feasible. Performances of catalytic reforming systems are listed in Table 5.

Noteworthy effort was formerly devoted to offer catalysts to the reaction to attain a feasible application below 1000°C. In particular, metallic catalysts based on Ni and Fe have attained quite motivating conversion rates at temperatures of the order of 600-700°C. Carbon based catalysts such as black carbon or activated carbon have been also proposed. Fig. 36 gives a schematic view of the application range of the main catalyst types.

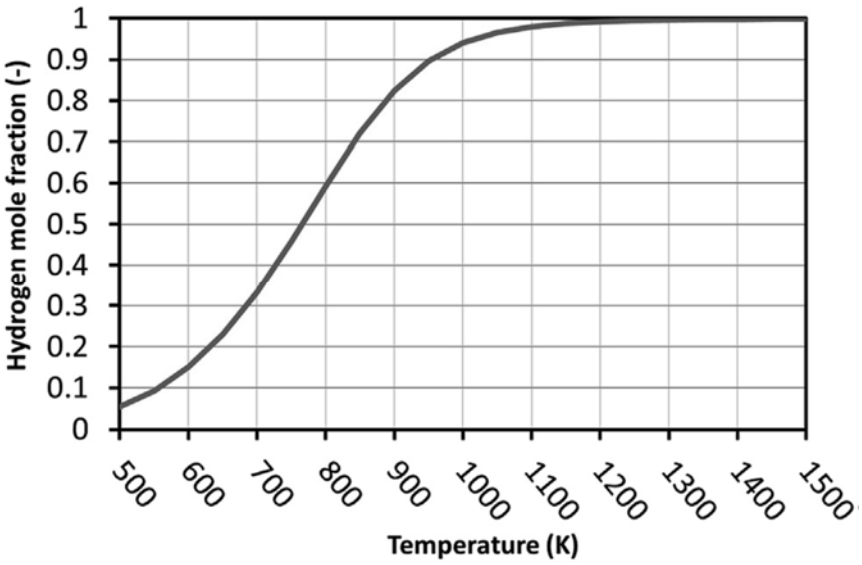

Fig. 35 Hydrogen mole fractions attained during thermodynamic equilibrium of the methane cracking reaction at various temperatures and 1 bar pressure (from Ref. [47])

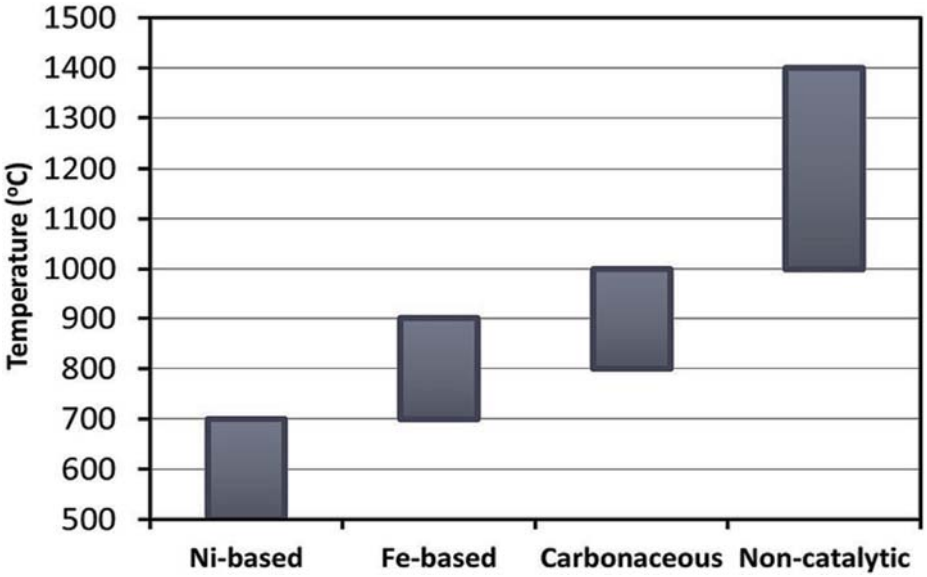

Fig. 36 Catalyst types used for methane cracking and their temperature range of applicability (from Ref. [47])

The practical industrial implementation in the case of catalyzed reactions is limited by the deactivation of the catalyst and its cost. The deactivation of the catalyst is a process resulting from the formation of coke on the surface of the catalyst during its operation and its control is a very important challenge. In the case of carbonaceous catalysts, carbon from the pyrolysis process decreases the active surface, and lastly abolishing its catalytic effect [47].

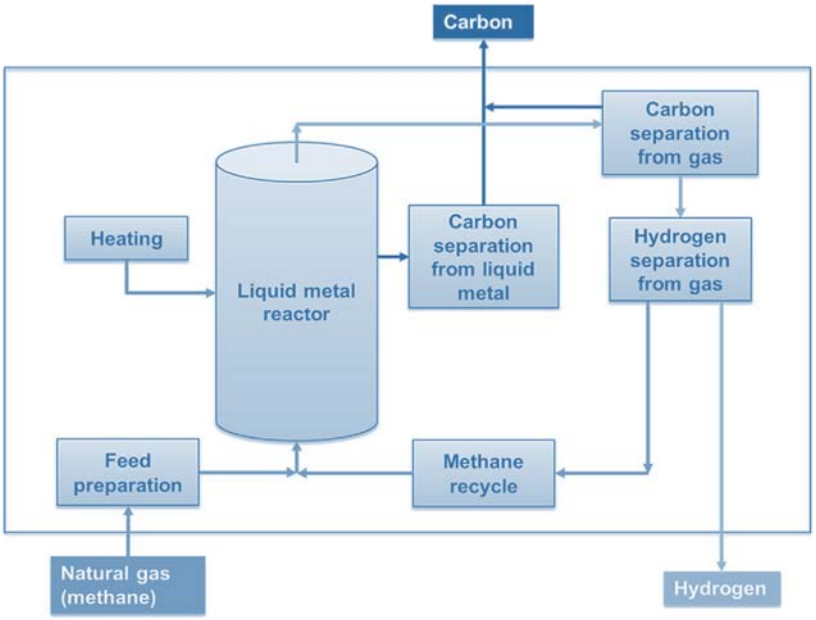

Fig. 37 Basic methane decarbonisation process definition (from Ref. [47])

The schematic diagram of the experimental setup conducted by Abanades et al. [47] is shown in Fig. 37. The steps followed in that study are explained shortly here.

- Feed preparation: The raw natural gas can need a preparation unit to increase the methane content and to remove impurities.
- Reactor: The liquid metal bubble column reactor is envisaged to be made of quartz glass and operated at temperatures above 1000°C.
- Heating: The heating to deliver the energy for the reactor is based on two selections for an industrial application: a hydrogen burner or a methane burner. Moreover, the combination with solar technology is envisioned for further steps, but that will bring higher capital costs.
- Carbon removal from the reactor: The carbon obtained from the experiments is characterized.
- Carbon separation from the gas stream: A filter is planned to eliminate small amounts of carbon elements from the gas stream.
- Hydrogen separation from the process stream: There are two core selections under consideration: pressure swing absorption (PSA), a developed method applied for CO_2 sequestration, and metallic membranes. Unreacted methane after separation from the process stream will be recycled back to the reactor.

The comparison of methane pyrolysis with other developed methods for hydrogen production from fossil-fuels is displayed in Table 6. From this theoretical comparison, that should be checked in a demo facility, the production of 100 Mtoe (toe = tonne of oil equivalent) of hydrogen will produce 103.8 Mtonnes of carbon with methane cracking, avoiding the production of 255.18 Mtonnes of CO_2 with steam methane reforming, or 626.85 Mtonnes CO_2 in comparison with coal gasification. The volume of CO_2 to be sequestrated and managed in supercritical state will be 10 times larger than the volume of carbon produced for the same hydrogen energy generation, substituting the management of carbon dioxide with solid carbon, which may have additional applicability as well. The application of methane decarbonisation can be especially convenient in industrial sectors, as in the case of ammonia production, in which huge amounts of hydrogen are required. From the preliminary economic analysis, the H_2 production cost that can

be expected from industrial methane cracking could be of the order of 1.5 $/kg [47]. In a previous analysis of methane decarbonisation [13], a H_2 cost of around 3.0 $/kg for solar methane pyrolysis was reported. However, the higher cost was mainly due to the solar field, which represents a significant capital cost of the facility.

Table 6. Comparison of hydrogen production technologies from fossil-fuels (data from Refs. [47 ,50, 51])

Process	**Methane steam reforming**	**Coal gasification**	**Methane pyrolysis**
Reaction Heat of reaction (kJ/mol-H_2)	$CH_4+2H_2O \rightarrow CO_2+ 4H_2$ 63.25	$Coal+2H_2O \rightarrow CO_2+ 2H_2$ 89.08	$CH_4 \rightarrow C + 2H_2$ 37.43
Energy efficiency in transformation (%)	74	60	55
Energy efficiency with CCS (%)	54	43	55
CO_2 emission (mol-CO_2/mol-H_2)	0.34	0.83	0.05
Carbon production (mol-C/mol-H_2)	0	0	0.5

In another study by Abanades et al. [52], the following experimental setup was used for methane cracking as shown in Fig. 38.

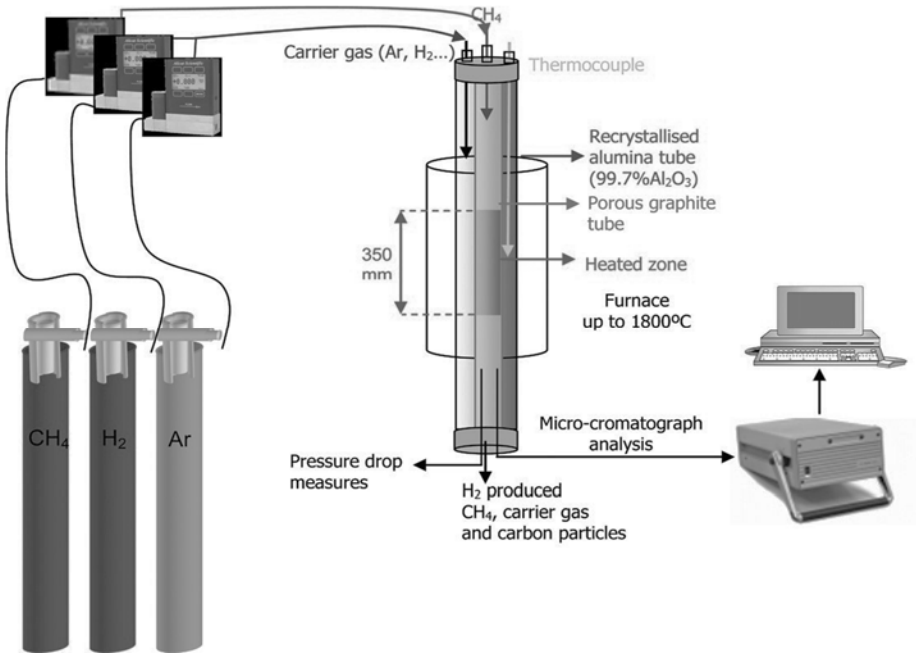

Fig. 38 Schematic diagram of the experimental setup for methane cracking (from Ref. [52])

At temperatures higher than 1350°C, the decomposition is practically complete, and the main component of the outgoing gas is H_2, with almost no traces of hydrocarbon gases. A cloud of carbon powder still goes out, but a huge fraction of the produced carbon appears as solid deposits securely adhering to the wall. Elimination of the deposit by simple mechanical pushing is very difficult, at least in cold conditions. That carbon deposit can be eliminated by combustion, just by blowing air into the hot oven, so producing CO_2, which is undesirable. Their experimental results showed the amount of hydrogen at the tube outlet in volume ratio percentage which is depicted for three flow rates implying three residence times of 16, 32 and 96 s in normal conditions (25°C, 1 bar) and at a temperature range between 875-1065°C as illustrated in Fig. 39. The summary of their experimental results are shown in Table 7 where they observed 100% dissociation at 1400°C.

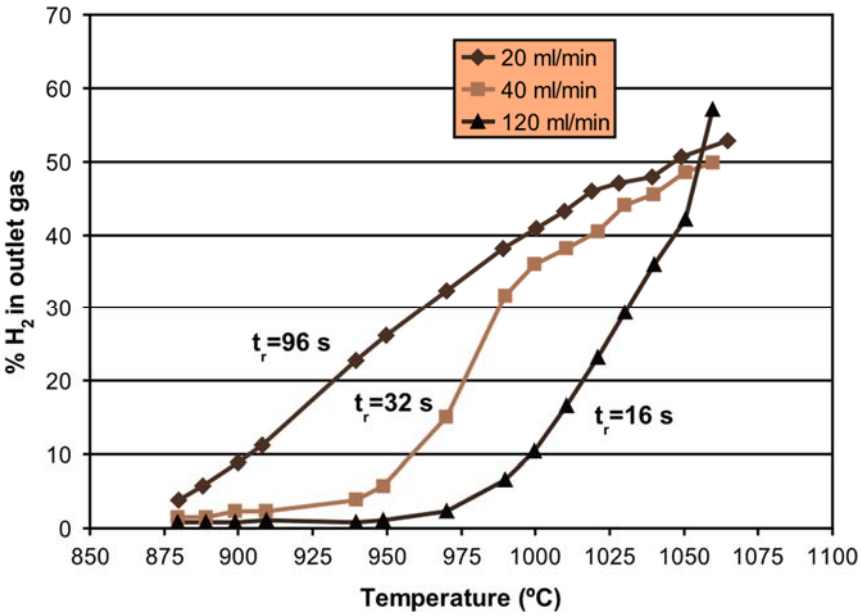

Fig. 39 Hydrogen volumetric ratio at the outlet gas as a function of the temperature and the flow rate (from Ref. [52])

Wei et al. [53] studied methane cracking over different coal chars in a fixed bed reactor. Their purpose was to study methane cracking on different coal chars with an aim to explain the changes in the catalytic activity of different coal chars for methane cracking and to speculate the mechanism of methane cracking. The chars have a profound catalytic effect on the methane cracking, with the catalytic activity varying with different types of coal chars. The catalytic activity of char in methane cracking decreases with increasing coal rank, with the Shengli lignite char being the most active and the Jincheng anthracite char being the least active. Methane conversion and hydrogen yield decrease with the time on stream as the coal char becomes deactivated and the carbon deposition from methane cracking is primarily responsible for the loss of catalytic activity of the chars with the time on stream. The methane cracking is a surface reaction controlled by the gas phase diffusion and therefore is influenced by both reaction temperature and methane concentration. The methane conversion increases with increasing temperature and decreasing methane concentration. The catalytic effect of char decreases with increasing pyrolysis temperature in the char preparation but is less affected by the pyrolysis time indicating that the catalytic activity depends not only on the porous structures but also on the chemical nature of the char surface [53].

Table 7. Summary table of the SiC tube experiments (from Ref. [52])

Experiment no.	**1**	**2**	**3**	**4**
T (°C)	1200	1300	1400	1400
Tube CH_4 flow (l/min)	SiC 1	SiC 1.1	SiC 1	SiC + Boron Nitrate layer 1
Ar flow (l/min)	1	0.9	1	
Time (h)	3	3	3	3
Dissociation rate	10% methane in exit. Hydrocarbons presence. Unknown H_2 production.	3% methane in exit. H_2 presence 60-70%. Very Low hydrocarbons presence.	0% methane in exit (complete dissociation) H_2 presence 93-94%	0% methane in exit (complete dissociation) H_2 presence 93-94%
Carbon deposit	Soft carbon black	Soft dust carbon black Carbon black Hard carbon black	Soft dust carbon black Carbon black Hard carbon black	Soft dust carbon black Carbon black Hard carbon black

3. Microwave Usage for Hydrocarbons Applications

Microwaves are electromagnetic waves with a frequency range between 300 MHz to 300 GHz, equivalent to wavelengths of 1 mm to 1 m. Further than 30 GHz, the microwave frequency range overlays with the RF range. Since the type of microwaves, they are ruled by the Federal Communications Commission (FCC). In North America, the single permitted frequencies for industrial usage are 915, 2450, 5800, and 22,000 MHz [54]. For usage in laboratory and testing applications, a 2450 MHz is preferred. Because this frequency carry suitable diffusion depth for many laboratory reaction situations. Microwaves are produced if electrons resonate at high frequencies. The electric field is formed by an internal cathode and external anode with a huge potential variance in-between. The magnetic field is forced by perpetual magnets situated typically on the bottom of the magnetron. The electrons in this atmosphere go from the cathode in an external spiraling path, finally reaching to the anode. While the electrons pass by resonance chambers, energy is released. This energy is collected by an antenna as microwaves. They are usually used for a cavity via waveguides. The essentially dissimilar technique of transporting energy from the resource to the sample is the key advantage of using microwave energy in comparison to standard thermal processing. By distributing energy to microwave-absorbing materials, problems like long heat up periods, thermal gradients, and energy lost to the system environment can often be avoided. Moreover, the penetrating ability of microwave permits volumetric heating of sections. Hence, these advantages of microwave energy create attractiveness for industrial uses as a substitute to standard thermal processing options. In lots of the situations, the usage of microwave energy creates dissimilar results in comparison with the standard thermal reactions allowing a decreased heating time or decreased reaction temperature [55]. Additionally,

the sample heating encouraged by microwave fields is firmly affected by the capability of the material to captivate microwave energy which consents samples to be selectively heated by improving the efficiency of giving energy into the system.

The essential appliance of microwave heating contains agitation of polar molecules or ions which oscillate under the influence of an oscillating electric or magnetic field. In the occurrence of an oscillating field, particles attempt to position themselves to be in phase with the field. Nevertheless, the movement of the particles is limited by resisting forces, which restrict the movement of particles and make arbitrary motion, creating heat. Microwave heating for industrial processing is categorized by numerous features which lead the method basically altered from standard heating options because of physical and chemical changes in products. As the reply of several materials to microwave radiation is different, not all materials are agreeable to microwave heating. Depending on the response to microwaves, materials may be generally categorized as follows: materials that are transparent to microwaves, e.g., sulfur; materials that reflect microwaves, e.g., copper; and materials that absorb microwaves, e.g., water. So, materials that absorb microwave radiation are related to microwave chemistry. Microwave heating arises via three tools [56–58] dipolar polarization, ionic conduction, and interfacial polarization.

Dipolar polarization is a procedure by which heat is produced in polar molecules. The main obligation for dipolar polarization is that the frequency range of the oscillating field need to permit suitable inter-molecule interaction. If the frequency range is too high, intermolecular forces will end the motion of a polar particle before it attempts to track the field, causing insufficient interaction. Conversely, if the frequency range is low, the polar molecule acquires adequate time to line up itself in phase with the field. Therefore, no arbitrary interaction occurs between the adjoining particles. Microwave radiation has the suitable frequency (0.3–30 GHz) to fluctuate polar particles and permit inter-molecular interaction. This oscillation rises the kinetic energy and collisions of all particles in the structure. As temperature is the degree of the mean kinetic energy of elements in a body, microwaves efficiently rise the temperature of dielectric medium. For instance, food involves commonly water, a polar particle, therefore microwave ovens are operative for heating in the kitchens.

The conduction procedure produces heat via resistance to an electric current. The fluctuating electromagnetic field produces an oscillation of electrons or ions in a conductor, causing an electric current. This current aspects interior resistance, which heats the conductor. The key restriction of this technique is that it is not appropriate for substances which include high conductivity, as this type of substances reflect most of the energy falling on them. At lesser temperature levels and high frequencies, heating is realized typically by dipole rotation. As temperature rises and frequency declines, ionic conduction keeps the importance in heating.

The interfacial polarization process can be deliberated as a mixture of the conduction and dipolar polarization techniques. It is significant for heating arrangements that include a conducting material detached in a non-conducting ambient. For instance, if the diffusion of metal elements in sulfur is considered, sulfur does not react to microwaves, and metals reflect supreme of the microwave energy they are faced to, but merging the two creates a microwave-absorbing material. Nevertheless, for the occurrence of this, metals need to be utilized in powder form. This is due to metal powder which is a good absorber of microwave radiation dissimilar than metal surface. It absorbs radiation and is heated by a process which is comparable to dipolar polarization. The surroundings of the metal powder actions as a solvent for polar particles and restricts motion by forces that are correspondent to inter-molecular exchanges in polar solvents. The limiting forces,

under the influence of an oscillating field, make a phase lag in the movement of ions. The phase lag produces an arbitrary movement of ions and causing the heating of the system [54].

The abilities of microwaves such as fast heating, penetration, and choosiness of impacted materials lead them to be a promising substitute in the applications of oil sands separation and making of hydrocarbons. Most of the heating techniques are based on convection in which heat is passed to the surface of a body, stimulating the external particles or elements. The kinetic energy is progressively transported to the internal particles or atoms till the entire body is heated.

Lower frequencies may penetrate more than higher frequencies. Because of this, radio waves can be more favorable in underground heating of bitumen. A few materials are microwave transparent. This implies that microwaves may transmit through without any effect. Some substances heat quicker than others when applied to the same electromagnetic field, implying that microwaves can deliver selective heating. Microwaves make temperature gradients which can help in separation. For example, microwaves were utilized to detach water-in-oil emulsions by evaporating the water whereas the oil leftovers in its original state, being mainly not affected by the radiation [59]. This feature can possibly save energy by merely heating what is essential to be heated in a combination or heterogeneous system.

4. Microwaves and Radio Frequency Applications in Oil Sands

There are 1.7 trillion barrels of bitumen in place in Canadian oil sands [60] and the source will be a key resource of petroleum yields in the coming years [61]. Heavy oil has been commercially made from Alberta's huge oil sands sources for four decades. Although the development of technology, the effectiveness of oil sands extraction, separation and upgrading technology has progressive, as operating costs have fallen. In 2005, Alberta made more than 1 million barrels per day of upgraded crude oil and bitumen from oil sands, and estimates are that over three million barrels per day could be produced in 2030.

5. Microwave-Assisted Oil Sands Separation

Many of the inorganic particles in processed oil sands carry a charge, and could be influenced by electromagnetic radiation. They are thrilled at an altered rate than the water and bitumen when irradiated, making a temperature gradient between the different components of the oil sands. The surfactants and other forces cannot cope with this gradient and the solids are able to break free [62]. Since all oil sands are dissimilar, a single frequency or power of microwaves are not available which functions best for all.

In 2003, samples of Lloydminster oil sands (oil–water–solids ratio of 19:40:41) considered principally stubborn to separation were tested with exposure to adjustable frequency microwaves [62]. The tests were able to avoid the FCC regulations because of distinct apparatus to comprise the electromagnetic waves. The aim was to explore what microwave frequency is best for this type of oil sands. All samples separated into a liquid upper layer and a mostly solid lower layer. The degree of separation was calculated by evaluating the oil content of the lower layer. The lower layer of the control specimen, which was not irradiated, had 27% oil content by weight. Tests were achieved by changing frequency and exposure time. Most of the samples presented marginally lower oil content. The best result occurred when the sample was irradiated for a duration of 10 min at 6400±100 MHz, where the lower layer only had 19% oil content.

Pierre et al. [63] used a 915 MHz microwave to separate a 570 g sample of oil sands. This sample was exposed for 5 min at 500W and extended a last temperature of 315°C. This resulted in numerous layers comprising a bottom layer of sand with an asphaltene-like material on top. A

second, noticeably bigger specimen with a volume of about 20 L was exposed for 9 min at 1500W at the same frequency. It got a temperature of 142°C where it exhibited three distinct layers. The bottom layer was typically sand, but also included other solids. The second layer contained a yellowish solution, accounting for all the water and other impurities in the oil sand. The top layer was black, viscous oil.

Bosisio et al. [64] considered microwave-assisted extraction of oil sands. They conducted oil sand extraction experiments under inert atmosphere in a quartz reactor which was located in a rectangular microwave guide (WR 284 wave guide) built-in with a coupling iris and modifiable short circuit. Instance microwave power of 100W at 2450 MHz frequency was realized to the oil sands samples and the different phases of reaction were perceived. The duration of first was 10 to 15s and second-third step were 15s to 15 min. Microwave radiation of oil sands created a crude oil and also small quantities of gaseous yields. Therefore, electromagnetic heating also proved to increase yields of crude oil from 70% to 86%. Lately, Global Research Corporation technologies declared a method using over 8,700 RF microwave frequencies essential to hydrocarbon elements. About 1.2 gal of diesel fuel was extracted from a tire after microwave radiation under vacuum at different frequencies. The company requested to extract oil and gas from diverse feedstocks by microwave radiation such as oil sands, oil shale, used plastics, or rubber with little or no additional processing. Initial testing results formed great amounts of hydrogen and methane gases without CO or CO_2 contaminants [65, 66].

6. Microwave-Assisted Oil Sands/Oil Shale Extraction

Balint et al. [67] described microwave assisted extraction to recover hydrocarbon substances from oil shale, oil sands and lignite in the U.S. Patent 4,419,214. The patent describes how oil sand, oil shale rock and lignite samples were irradiated in a pressure vessel with gaseous or liquefied carbon dioxide and other gaseous or vapor hydrocarbon solvents. For example, oil sand was taken into a microwave feeder pipe and irradiated at 5.8 GHz frequency. Further, BTX (benzene-toluenexylene-ethylbenzene) was pumped through the sand. The extraction solution contained green oil on the top and bitumen was obtained at the bottom. In another example, crushed oil shale rock was irradiated at 915 MHz frequency. After radiation, carbon tetrachloride was impelled to extract kerogen and the projected isolated kerogen was 65% of initial organic content of the rock.

Dumbaugh et al. [68] specified that oil sands and oil shale samples irradiated to microwaves produced the required heat to dissociate bitumen components to produce a crude oil and distilled kerogen. A laboratory microwave oven was utilized to test oil sand samples from Athabasca and oil shale specimens from Green River and Sunnyside. The authors found that a 128 g sample of oil sand separated into its components when irradiated at 800W for 10 min, followed by 1500W for 15 min.

7. In-Situ Recovery of Oil By Electromagnetic Heating

About 20% of the oil sand confirmed sources of 174 billion barrels is reachable by open-pit mining, therefore other approaches have been advanced to extract the other 80% of the source. In the main in-situ methods, steam is injected into the ground to rise bitumen temperature and reduce viscosity to the point where the additional heavy oil can be pumped out. Unconventional procedures advanced for heating heavy oil reservoirs can be economically feasible options to steam in definite circumstances. Due to the abilities of microwaves, research was performed regarding the usage of electromagnetic energy to heat the bitumen to the essential temperature. For oil sands or enormously high viscosity reservoirs, where the temperature influence on viscosity is important,

electromagnetic heating can be applied as a preheating purpose. Because lower frequency waves carry less energy, heating times are significantly longer compared to the higher energy microwaves. In preference to using electromagnetic energy to do all the heating, it was proposed to use it only for preheating. This makes the recovery by the standard steam method more economical by demanding less heating by steam and increased yield per well [69]. Microwaves have not been utilized commercially because of the initial setup costs and undefined potential. If microwaves proved to increase yields and profits on a large scale, they could have a substantial influence on the petrochemical and petroleum industry [54].

Cho et al. [70] developed a microwave plasma-catalytic reaction method to generate hydrogen and carbon black from natural gas. In the plasma system of high power discharge, hydrogen and carbon black is generated by the dissociation of methane, which is almost similar to thermal cracking. Methane is a favored raw material for the generation of hydrogen from a hydrocarbon due to its high H to C ratio, availability and low cost. Moreover, the carbon obtained can be traded as a co-product into the carbon black market for ink, paints, tires, batteries etc. applications. Numerous routes of carbon black production are presently used to make furnace black, lampblack, channel black, thermal black, and acetylene black, which represent 95% of world production and consume mainly petroleum derivatives. A plasma black was used as a for lithium ion battery. The carbon black is not only performances as an electron path by creation of a conducting network of active substance but also develops electrical conductivity of interfacial electrode surface. According to Fulcheri and Schwob [15], the total enthalpy of methane decomposition at 1600℃ is 181.8 kJ/mol, and the energy associated with carbon mass changes about between 3 and 5 kWh per kg of carbon produced. In the experiments, microwave plasma (2.45GHz) was utilized to generate hydrogen and carbon black from methane. The maximum microwave power was 6 kW. Plasma reactor is made of quartz tube of 6” outer diameter which is coupled to a microwave waveguide and resonator. It is primarily composed of 6 kW magnetron power source and plasma generator (resonance), cold plasma reactive zone where methane is sent, separation bag filter of hydrogen and carbon, water and air cooling and gas supply systems.

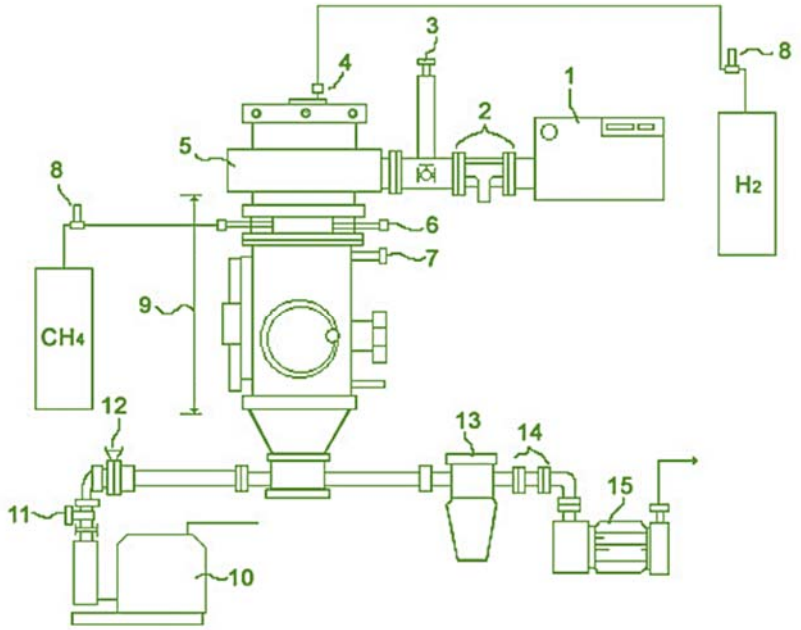

Fig 40. Experimental set for microwave plasma and catalytic reaction process (from Ref. [63])

The components in Fig. 40 are explained as follows: magnetron (1), waveguide (2), e-h tuner (3), microwave quartz tube (4), plasma generator (5), jet inlet nozzle (6), cooling line inlet (7) MFC (8), microwave plasma reactor (9), vacuum pump (10), control valve for pressure (11, 12), cyclone (13), filter (14), mechanical diaphragm pump (15).

Thermal conductivity analyzer analyzed the reaction products which are hydrogen, methane and C2+ chemicals. In their results, conversion of methane and yield of hydrogen and carbon black as a function of applied power were exhibited in Fig. 41. The conversion of methane obtained up to 96% of a plasma and catalytic reaction at 3 kW of applied power. Furthermore, the yield of hydrogen was from 83% to 95% at above condition. The yield with respect to carbon black and hydrogen increased with increasing applied power. When an input of 1 mole of methane was introduced, 0.6 mole of carbon and 1.62 mole of hydrogen were produced. Also, they carried out the microwave heating catalysis in order to advance the performance of methane conversion. The microwave heating of the catalysts might have an important advantage over conventional thermal heating. The catalyst can act as extracting more hydrogen from methane as improving the reactions of radicals between catalyst surface and reactant gas. They observed that hydrogen and carbon black were produced at the rate of almost 2:1.

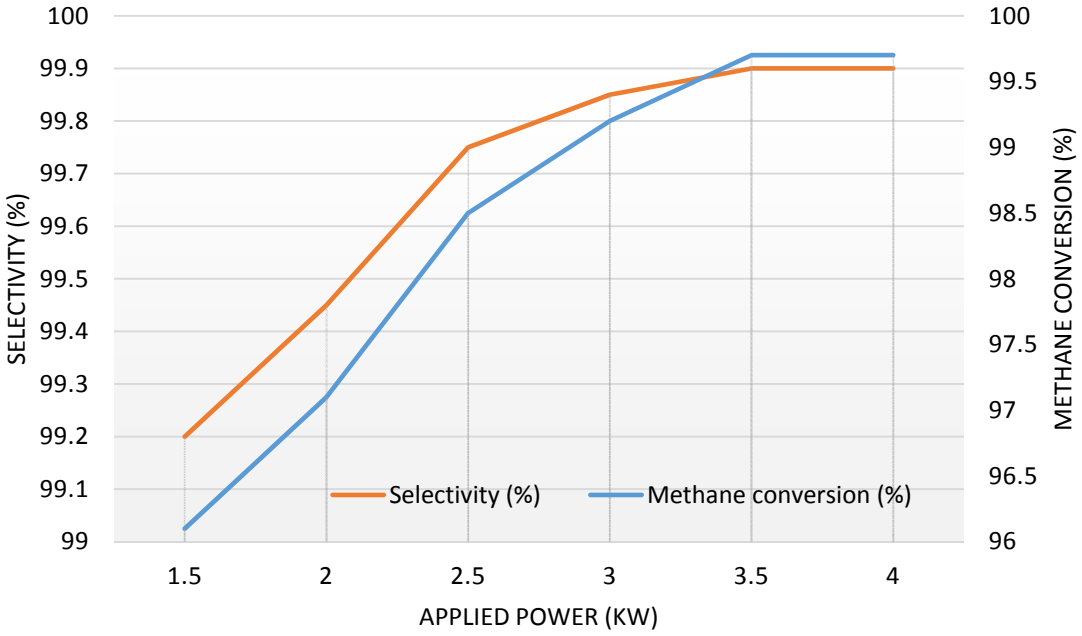

Fig. 41 Conversion of methane and yields of hydrogen and carbon black as a function of applied power (data from Ref. [70])

Fig. 42 illustrates the comparison of various catalysts in the plasma-catalytic reaction of methane decomposition. Among them, Pt-Rh catalyst is good for methane decomposition and production H_2/carbon black. Conversion methane to hydrogen is 72% and to carbon black is 54%. They resulted that the high frequency discharge is an effective method to decompose methane to hydrogen and carbon black in the present catalyst. The catalytic reaction enhances the decomposition of methane to hydrogen and carbon black due to abstract more hydrogen electron from methane as activating the reaction of radicals. The plasma process appears to have better than conventional hydrogen production processes. The performance of plasma black has almost the same electronic resistivity with that of acetylene black [70].

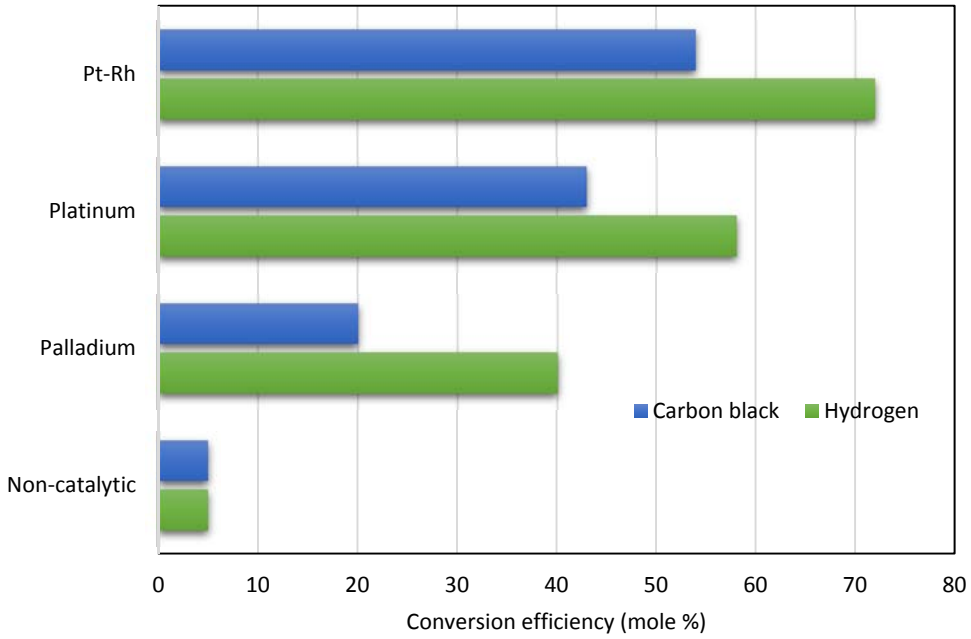

Fig. 42 Comparison of various catalysts in the plasma-catalytic reaction; 200ml/min of flow rate, 4 kPa of system pressure and applied plasma power is 3.0 kW (from Ref. [70])

For the microwave dissociation of hydrocarbons for ammonia production, the following advantages and disadvantages can be listed:

Advantages

- The microwave energy may be of sufficient power and duration to cause microwave depolymerization of the high molecular weight materials such as bitumen.
- Bitumen, which is the end product from oil sand, can be decomposed using microwave energy.
- Microwave energy is environmentally friendly since it has no harmful effect during hydrocarbon cracking process.
- Optimized ammonia synthesis using the excess heat in Haber-Bosch ammonia plant for oil sand bitumen extraction which is used for hydrogen production via microwave dissociation process is possible.

Disadvantages

- The reaction requires catalysts which are mainly Fe and Ni based materials.
- The solid residues could be problematic which may cause an interrupted operation for reactor cleaning purposes.
- The cost of electricity used to create the microwave radiation is a major factor for efficient and low cost processes.
- Only about 10% of oil sand represents the bitumen as hydrocarbon. Alberta oil sand bitumen includes about 10% hydrogen where the remaining 80-85% is mostly carbon.

There are some research papers and patents in the literature regarding the application of microwave energy for hydrocarbons [71-78]. They have shown that bitumen, which is the end product from oil sand, can be decomposed using microwave energy. Many of the inorganic particles in processed oil sands hold a charge, and could be influenced by electromagnetic

radiation. They are excited at a different rate than the water and bitumen when irradiated, creating a temperature gradient between the different components of the oil sands. The reaction also requires catalysts which are mainly Fe and Ni based materials. However, the solid residues could be problematic which may cause an interrupted operation for reactor cleaning purposes. Alberta oil sand bitumen includes about 10% hydrogen where the remaining 80-85% is mostly carbon. Furthermore, only 10% of oil sand represents the bitumen as hydrocarbon [79]. An illustrative layout of ammonia synthesis process using microwave decomposition of bitumen is shown in Fig. 43. The excess heat in the Haber-Bosch reactor can be utilized via heat recovery steam generator (HRSG). The produced steam is injected underground to extract bitumen using a specific pump arrangement for high dense liquids. Application of microwave energy can yield production gases where a portion is hydrogen. The generated hydrogen can be utilized in a conventional Haber-Bosch process for ammonia synthesis.

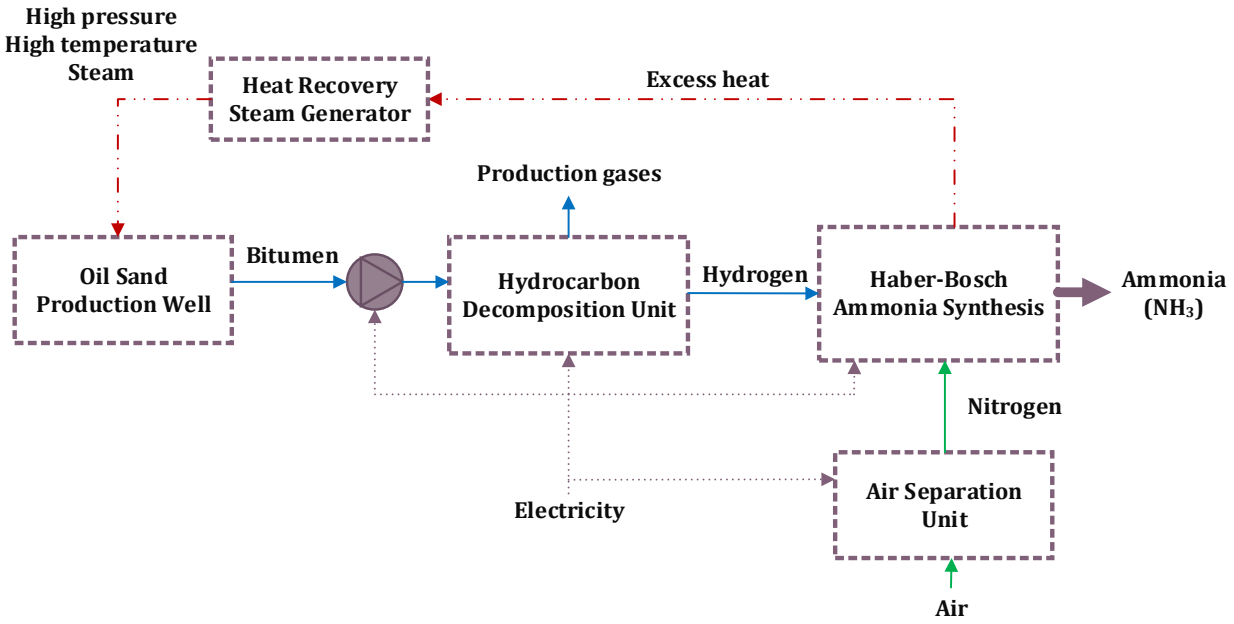

Fig. 43 Illustrative schematic layout of ammonia synthesis using hydrocarbon decomposition via heat recovery from Haber-Bosch process

The ammonia synthesis via Haber-Bosch process releases approximately 2.7 GJ/tonne NH_3 heat. This is equivalent to about 8% of the energy input for the entire process. It means that heat dissipation from Haber-Bosch ammonia process is about 2700 kJ/kg ammonia. When 300 tonne/day ammonia is produced, the Haber-Bosch reactor releases 9375 kW heat. A small temperature approach (about 10–20°C) along the low temperature heat exchanger is possible and then a substantial (90–95 %) part of the reaction heat could be utilized. But the temperature level of heat utilization is low and the exergy efficiency of the entire heat utilization system is not high.

The Haber Bosch process converts atmospheric nitrogen (N_2) to ammonia (NH_3) by a reaction with hydrogen (H_2) using a metal catalyst under high temperatures and pressures:

$N_2 + 3H_2 \rightarrow 2\ NH_3$ ($\Delta H = -92.4$ kJ/mol or $\Delta H = -5435$ kJ/kg)

Presumably 50% of the reaction heat is recovered. In this case, the excess heat for various capacity ammonia production plants are listed:

- 300 tonne/day: 9,375 kW
- 600 tonne/day: 18,750 kW
- 900 tonne/day: 28,152 kW

In the previous studies for Alberta bitumen extraction [80, 81], it was shown that in order to extract about 0.15 m^3/s bitumen via SAGD based process, the required energy input to the production well is approximately 15,600 kW. Bitumen extraction requires continuous production of high temperature high pressure steam. The required pressure of the steam being sent to SAGD (steam assisted gravity drainage) oil sand plant is about 1000 kPa and the temperature is about 380°C. Including the pressurization and evaporation of water, the total required power is about 18,000 kW. This amount of power can be recovered from approximately 600 tonne/day ammonia production plant. The calculations do not include the possible energy losses, hence a detailed exergy analyses are beneficial for practical applications.

Based on the references [82-84], the microwave disassociation of methane requires the equivalent of between 3-4 kWh/m^3 of pure H_2 which can be evaluated as 0.08 kg/h can be produced with a power input of 4 kW. For a 600 tonne/day ammonia plant, about 4248 kg/h hydrogen is needed. Therefore, the total required power input for hydrogen production via microwave energy yields about 212 MW. The same amount of hydrogen can be produced by water electrolysis with a power input of about 240 MW when electrolysis efficiency is assumed to be about 70%. This implies about 10% less power input. The excess heat can be utilized for bitumen extraction, but there is still important amount of required power input for disassociation of methane into hydrogen.

8. Conclusions

Utilization of hydrocarbons in an environmentally friendly manner becomes more significant day by day. Dissociation of hydrocarbons such as methane and bitumen is a promising option especially for Canada. Based on the extensive literature review and assessments, the following concluding remarks can be noted.

- Hydrocarbons can be used as a source of hydrogen which is required for ammonia synthesis. There are various alternative pathways for hydrogen production from hydrocarbons such as thermal, non-thermal, plasma routes.
- Methane decomposition reaction is moderately endothermic process. The energy requirement per mole of hydrogen produced is considerably less than that for the steam reforming process.
- Using different catalysts, the maximum temperature of thermal decomposition of methane can be decreased. Metal catalysts, including Ni, Fe, Co, Pd were most commonly used for methane decomposition.
- Ni catalyst is one of the most effective catalysts for the methane decomposition.
- Metallic catalysts based on Ni and Fe have achieved quite remarkable conversion rates at temperatures of the order of 600-700°C.
- Hydrogen via thermo-catalytic dissociation of hydrocarbons represents an alternative solution. It is accompanied by the formation of carbon deposits. Methane can be thermally or thermocatalytically decomposed into carbon and hydrogen without CO or CO_2 production.
- It can be estimated that the electric energy supply needed for the cracking operation varies between 4 and 7 kWh per kg of carbon produced or between 1 and 1.9 kWh per normal cubic meter of hydrogen produced.

- The microwave energy may be of sufficient power and duration to cause microwave depolymerization of the high molecular weight materials such as bitumen.
- Many of the inorganic particles in processed oil sands hold a charge, and could be influenced by electromagnetic radiation. They are excited at a different rate than the water and bitumen when irradiated, creating a temperature gradient between the different components of the oil sands.
- Lower frequencies can penetrate further than higher frequencies. For this reason, radio waves may be better in underground heating of bitumen.
- For oil sands or extremely high viscosity reservoirs, where the temperature effect on viscosity is significant, electromagnetic heating could be used as a preheating purposes. Because lower frequency waves carry less energy, heating times are considerably longer compared to the higher energy microwaves.
- Gliding arc discharge reactor is one of the highest efficient route for methane conversion which was experimentally tested by many researchers.
- H_2 production cost that can be expected from industrial methane cracking could be of the order of 1.5 $/kg and NH_3 in the range of 0.3-0.5 $/kg.
- Optimized ammonia synthesis using the excess heat in Haber-Bosch ammonia plant for oil sand bitumen extraction which is used for hydrogen production via microwave dissociation process is possible.

CHAPTER 3. CASE STUDIES

In this section, a set of case studies for production and utilization of ammonia in Canada are proposed and analyzed in terms of feasibility, sustainability, environmental impact and cost.

1. Experimental Investigation of Ammonia Synthesis via Molten Salt Electrolyte Based Electrochemical Route

The synthesis of ammonia from electrochemistry is based on electrolysis where electric current is supplied to a reactor consisting of a cathode, anode, and ionic conducting membrane. The chemical reactions consist of reduction on one side and oxidation on the other with an important component being the membrane which will only conduct a special kind of ion such as protons in the form of H^+, this allows the reactor to work continuously. There are many variations of types of cathodes, anodes, and membranes however the principle remains the same where two reactants and an activation potential are applied to generate a chemical reaction resulting in ammonia synthesis. These reactions have been shown to work in a wide range of pressures and temperatures making it viable when working with atmospheric conditions. In the current electrochemical system, molten salt is utilized as electrolyte. The required hydrogen is initially supplied from tanks but in the final case, photoelectrochemically produced hydrogen is used for ammonia synthesis. The list of the materials used in the experiments are shown in Table 8.

Table 8. Material list for the experimental study

Material Name
1. Nitrogen tank and regulator
2. Hydrogen tank and regulator
3. Ammonia sensor or pH meter when ammonia collected in the water
4. Temperature sensors (3)
5. Pressure sensors (3)
6. Flowmeters (3)
7. Data loggers
8. Plate Heater (for the mixture) or Band heater for surface heating
9. Power supply (potentiostat)
10. Stirring device
11. Reactor
12. Insolation material for covering the reactor
13. Stainless steel top lid with holes for electrodes, inlets, and outlets.
14. Stainless Steel bottom lid
15. 4 bolts-rod assemblies to connect the lids together
16. Tubes (alumina material) for inlet and outlets
17. A gasket between the reactor and lid
18. Potassium hydroxide and sodium hydroxide for the electrolyte
19. Nickel electrodes and nickel-monel meshes
20. Nickel wires for connecting the electrode and mesh to power supply
21. Nano iron oxide (of specified grain size)
22. Gas storage tank for the products

The following steps present the process of the experimental study:

- Phase 1: Construction of new PEC (photoelectrochemical) reactor
- Phase 2: Ammonia synthesis using hydrogen and nitrogen in the molten salt reactor
- Phase 3: PEC hydrogen production coupled with ammonia synthesis
- Phase 4: Concentrated light PEC hydrogen production coupled with ammonia synthesis

For the purpose of conducting the experimental setup, the following materials are required and supplied.

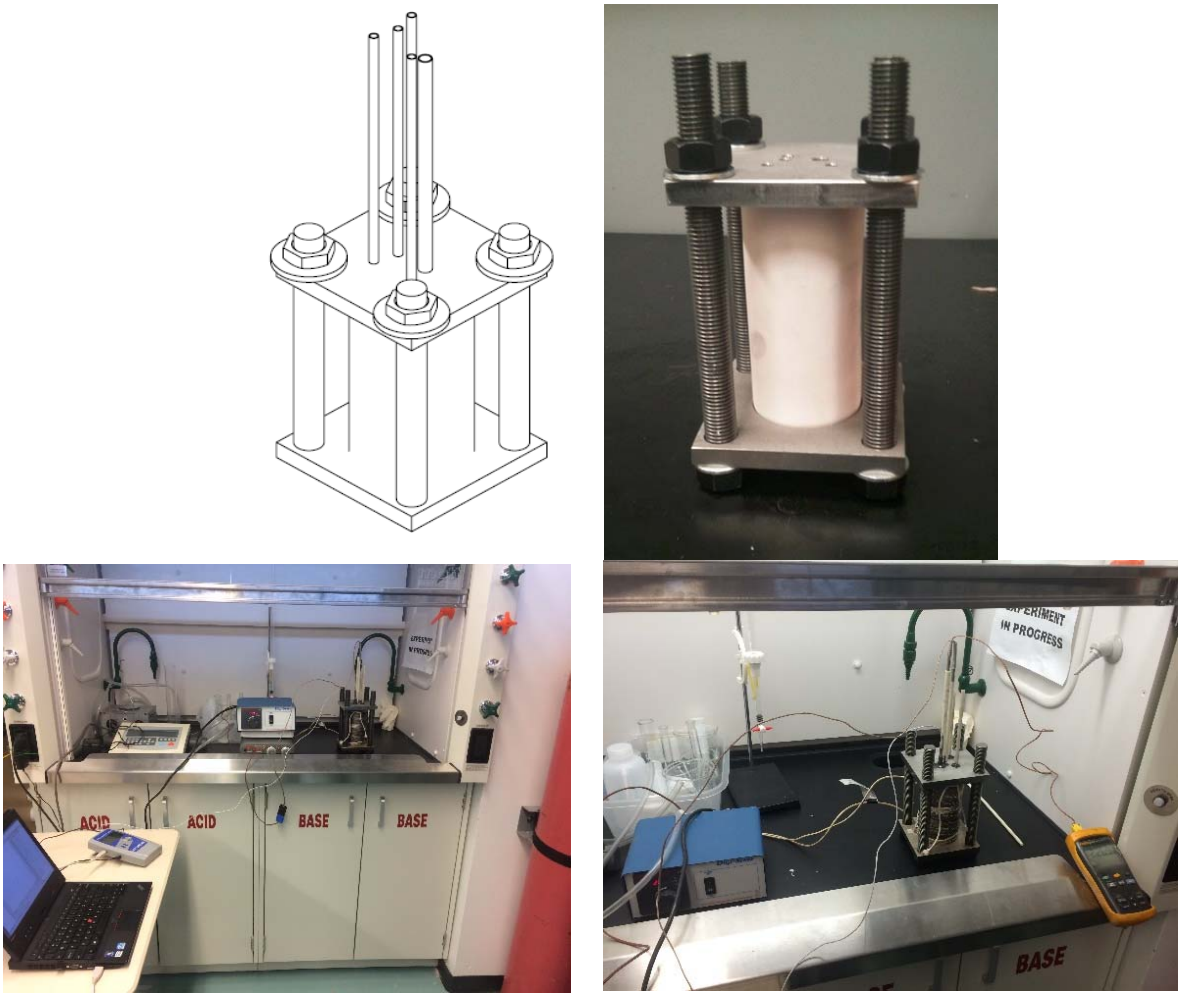

Fig. 44 Ammonia synthesis reactor and setup for electrochemical synthesis

The reactor details used in the experiments are as follows**:**

- 500ml crucible made out of Alumina (99.6% pure)
- Cover plates stainless steel (316 alloy)
- Salts: Sodium Hydroxide (NaOH) and Potassium Hydroxide (KOH), both come in pellet form
- Nano Iron Oxide (20-40nm per particle)

Table 9. The dimensions of the reactor

Top Diameter	Bottom Diameter	Height	Capacity
100 mm	60 mm	116 mm	500 mL

The dimensions of the reactor is listed in Table 9. In addition, the materials used in the experimental setup need to be resistive to corrosivity. The specifications of the selected equipment are given below:

- **Wiring**
  - Nickel Wiring
    - Melting point 1455°C, boiling point 2732°C
    - Non-corrosive applications
    - Conductive
- **Electrodes**
  - Nickel Rod (Anode)
    - High melting point
    - Non-corrosive
    - Conductive
  - Nickel-Monel Mesh (Cathode)
    - Stable in molten salt
    - Non-corrosive
    - Conductive
- **Reactor casing**
  - Alumina Crucible (Al_2O_3)
  - High melting point, strong hardness
  - Chemical Stability
  - Non-corrosive
- **Reactor Lids**
  - Stainless steel (316 Alloy) or Aluminum
  - Withstand high temperature (pressure if applicable)

Experimental procedure

The reactants travel through a copper coil of 10 turns positioned on top of a hot plate. The hot plate heats the nitrogen and hydrogen to around 200°C which is required to prevent cooling the reactor down as the reactants are supplied. Using power source, direct current (DC) is supplied to both electrodes inside the reactor via nickel wires. By adjusting voltage and current values, the rate of change in the reaction can be determined. A potentiometer adjusts the potential and resistance of the circuit. Both reactants enter into the ammonia reactor. Here the two preheated reactants nitrogen and hydrogen mix with a eutectic mixture composed of KOH-NaOH. An electrochemical pathway is created to produce ammonia by the reaction of nitrogen and hydrogen in a molten hydroxide salt solution (with a molar ratio of 0.5 NaOH/0.5 KOH). This eutectic mixture is prepared prior to the start of the experiment and preheated to form the molten salt. The reactor will remain at atmospheric pressure and is leak-free because of a gasket used to maintain the seal. The picture of the eutectic mixture preparation inside the reactor is also shown in Fig. 44.

The suspension of nano-Fe_2O_3 within the melted salts acts as a catalyst for the reaction to occur. The reactants inside the crucible are separated by a partition to allow the ammonia produced

to flow through the output tube and are sprinkled into deionized water. Ammonia test strips with a range of 0 – 6 mg/l and then it is used to identify/give a good estimate of ammonia. The strips work by detecting the change in PH as a result of the added ammonia. Furthermore, an Arduino ammonia sensor is also utilized for measurements.

Power supply can also be realized by PV modules that are in direct contact with sunlight. The deionized water needs to be changed regularly during testing to ensure accurate test results. Supplying air instead of nitrogen could also be a modification to the system using fans. The reactor is designed to eliminate any leakage from the joints. It is designed to contain a molten salt mixture with the catalyst as well as the electrode set up carefully supported by supplying rods with nickel wire. There is also a wall designed into the reactor set up to separate the production gases at the anode and cathode which are nitrogen and ammonia/hydrogen respectively.

Forming the eutectic molten salt mixture with the nano-Fe_2O_3 catalyst

When creating the molten salt mixture, it is important to take into account the boiling points of the certain salts that is intended to melt within the crucible before melting. The melting point of NaOH is about 318°C, and the melting point of KOH is about 406°C. Taking the temperatures into account, it is required to heat the crucible up to 450-500°C to ensure that the salts are fully melted. A mass ratio of 0.5 NaOH/0.5 KOH within the reactor is formed. Depending on the production rate of ammonia, the amount of electrolyte is adjusted for parametric studies.

After achieving the temperature, the temperature is taken down to about 350°C and the catalyst is added. The iron oxide mixes are catalysts for the traditional chemical synthesis of ammonia and will undoubtedly help in producing it. The high surface area of the nano-Fe_2O_3 in the electrochemical synthesis, will be critical for the reaction to not only occur, but also for the ammonia to be produced at a higher rate. As the reaction continues, adding more catalyst will be important to see the effect on the production rate. After the addition of the catalyst, the eutectic molten salt mixture temperature will be stabilized at various temperatures starting with 350°C and ready for the electrochemical reaction to occur with the other reactants of the ammonia synthesis procedure.

The electrolyte used in this experiment consists of a 1:1 ratio of potassium hydroxide and sodium hydroxide, as was previously discussed. The two form a eutectic mixture when they both melt at the melting temperature of the highest melting point salt which is potassium hydroxide at about 400°C. They combine physically but not chemically, and so they retain their properties except their melting points which overall is decreased to about 170°C. The mixture is originally prepared at room temperature, putting the mixture together to melt in the crucible when heated up to 500°C. However due to the drastic change in density, the initial volume of salts will not be the same volume as the final and working volume. Since the liquid level is an important component of the system, it is required to estimate to a very high degree of accuracy what the volumes will be before and after. The calculations yield that 3.15 moles of each of the salts fill the desired volume of 274 ml as shown in Table 10.

Since the crucible is the main component of the reactor and the reactions occur if it is heated to the correct temperature, a test to ensure that the crucible is being heated to at least 450°C was conducted. In order to analyze the temperature within the crucible, a thermocouple is used to provide the temperature inside the rector. A temperature controller is used for stabilizing the required temperature at the desired level. The experiment was successful in terms of durability and reliability.

Table 10. The density-volume change depending on the temperature for the salts

Temperature (°C)	NaOH Density (kg/m^3)	KOH Density (kg/m^3)	NaOH Volume (ml)	KOH Volume (ml)
20	1.663	2.333	84.5	84.5
200	1.03	1.445	136.4	136.4
250	1.307	0.9318	150.8	150.8

The steps of the experimental tests are listed here:

1) Nickel wire connections to meshes and potentiostat (Cathode: Hydrogen side)
2) Preparation of electrolyte
   - Measure the salts in the scale (140.5 g of NaOH=150.8 mL and 197.1 g of KOH=150.8 mL)
   - Measure the iron oxide in the scale (10 g)
   - Put the salts in the reactor
   - Turn on the heater and melt the salts until 450°C (May take up to 2.5 hours)
   - Mount the temperature sensor and measure the temperature in the reactor using thermocouple
   - Wait until the temperature decreases to 350°C
   - Add the nano iron oxide catalyst
   - Stir the mixture
   - Wait until the electrolyte temperature reaches 250°C
3) Mount the flowmeters for hydrogen and nitrogen inlets
4) Mount the gas inlet piping to reactor
5) Mount the ammonia sensor at the outlet stream
6) Connect the potentiostat to the reactor electrodes
7) Run the potentiostat at 1.44 V.
8) Prepare the nitrogen supply, adjust the volume flow rate and run the nitrogen tank
9) Prepare hydrogen supply and run the hydrogen production unit
10) Collect the flow meter data
11) Vent the ammonia to fume hood

In order to investigate the effect of various conditions on the performance of the reaction and ammonia yield, the following parametric studies are planned to be conducted:

1) Change the nitrogen flow rate and measure the NH_3 outlet, current and temperature
2) Change the hydrogen flow rate and measure the NH_3 outlet, current and temperature
3) Increase the nano iron oxide mass in the reactor and measure NH_3 outlet, current and temperature
4) Change the supplied voltage and measure the current, NH_3 and temperature
5) Change the operation temperature to 225°C and conduct experiments
6) Change the operation temperature to 200°C and conduct experiments
7) Change the molten salt electrolytes masses and conduct experiments
8) Change the molar concentrations of salts and conduct experiments

2. Ammonia Production Using Water Electrolysis from Low-Cost Hydropower and Wind Energy

The system modeled is a standalone grid powered PEM electrolyzer system with a total hydrogen production capacity of 50,000 kg/day. This corresponds to about 280 tonne/day ammonia production plant. The system is based on a generic system using input from several key industry collaborators with commercial experience in PEM electrolysis. The electrolyzer units use process water and grid electricity for electrolysis. Two different electrolysis process namely high pressure electrolysis and standard electrolysis are considered in the assessments where the parameters are given in Table 11.

Table 11. Analysis parameters for electrolysis based methods

Energy Efficiency Calculations			
	H_2 Outlet Pressure	psi	1000
Stack Electrical Usage			
	Cell voltage	volts/cell	1.6625
	Voltage Efficiency	% LHV	74.0%
	Dryer Loss	% of gross H_2	1.5%
	Permeation Loss	% of gross H_2	2.0%
	Total Stack Energy Usage per mass net H_2	$kWh_{elec}/kg_{Net\ H2}$	46.67
BOP Loads			
	Power Inverter Efficiency	%	97%
	Inverter Electrical Load	$kWh_{elec}/kg_{Net\ H2}$	1.44
	Dryer Thermal Load	$kWh_{therm}/kg_{Net\ H2}$	0.31
	Dryer Efficiency	kWh_{elec}/kWh_{therm}	3.30
	Dryer Electrical Load	$kWh_{elec}/kg_{Net\ H2}$	1.02
	Misc Electrical Load	$kWh_{elec}/kg_{Net\ H2}$	1.08
	Total BOP Electrical Load	$kWh_{elec}/kg_{Net\ H2}$	3.54
Summary			

	Stack Electrical Usage	kWh_{elec}/kg_{H2}	46.67
	BOP Electrical Usage	kWh_{elec}/kg_{H2}	3.54
Total System Electrical Usage per mass net H_2		$kWh_{elec}/kg_{Net\ H2}$	50.2
Total System Electrical Usage per mass net H_2 (High pressure electrolysis)		$kWh_{elec}/kg_{Net\ H2}$	40.6
Reference year		2007	
Assumed start-up year		2020	
Basis year		2012	

The required power for 300 tonne/day ammonia plant was calculated as 145 MW. Around 7.7 MW of this power corresponds to synloop compressors. Therefore, if high pressure electrolysis is utilized, the required power will decrease 5.3% for the overall plant. The average cost of ammonia production from the electrolysis based systems are approximately 20-25% of hydrogen production cost as previously given in Ref. [85] for various ammonia production methods. 17.8% of ammonia is hydrogen in weight, and around 3% of ammonia production cost comes from air separation based nitrogen production. In the current analyses, ammonia production costs are calculated as the 20% of hydrogen production cost. The source of electricity is taken as wind energy and hydroelectric power plant. These two renewable sources are significant and dominant in various locations of Canada. In the case studies, hydropower plant is located in Ontario whereas wind power plants are located in Newfoundland and Labrador. The province has high potential of wind energy as compared in the Fig. 45 and Table 12. The average wind capacity factor for Newfoundland is taken to be as 40% [86].

Table 12. Comparison of cost of wind energy based electricity for various locations in Canada (data from Ref. [86])

Location	Capital Cost of Wind Turbine ($/kW)	Transmission distance (km)	Capital Cost of Transmission Line ($/kW)	Capacity factor	Cost of transmission (cents/kWh)	Cost of electricity (cents/kWh)
Vancouver	1862	677	839	0.460	1.11	5.29
South Alberta	2059	365	683	0.402	1.02	6.03
Regina	2165	2043	1521	0.506	1.86	6.39
Winnipeg	1593	3401	2200	0.527	2.54	6.11
S. Ontario	2083	1820	1410	0.531	1.61	5.79
S. Quebec	1952	1465	1232	0.512	1.46	5.49
New Brunswick	1872	832	933	0.492	1.15	5.14
Nova Scotia+PEI	2014	831	916	0.529	1.05	5.04
Newfoundland	1648	87	544	0.458	0.72	4.50

Table 13. The electricity prices taken for the analyses of electrolysis based ammonia production

Method	Province	Electricity price ($US/kWh)
Low-cost hydropower high pressure electrolysis	Ontario	0.0275
Low-cost hydropower electrolysis	Ontario	0.0275
Wind high pressure electrolysis	Newfoundland	0.045
Wind electrolysis	Newfoundland	0.045

Hydroelectric and wind energy based electricity production costs are taken as shown in Table 13.

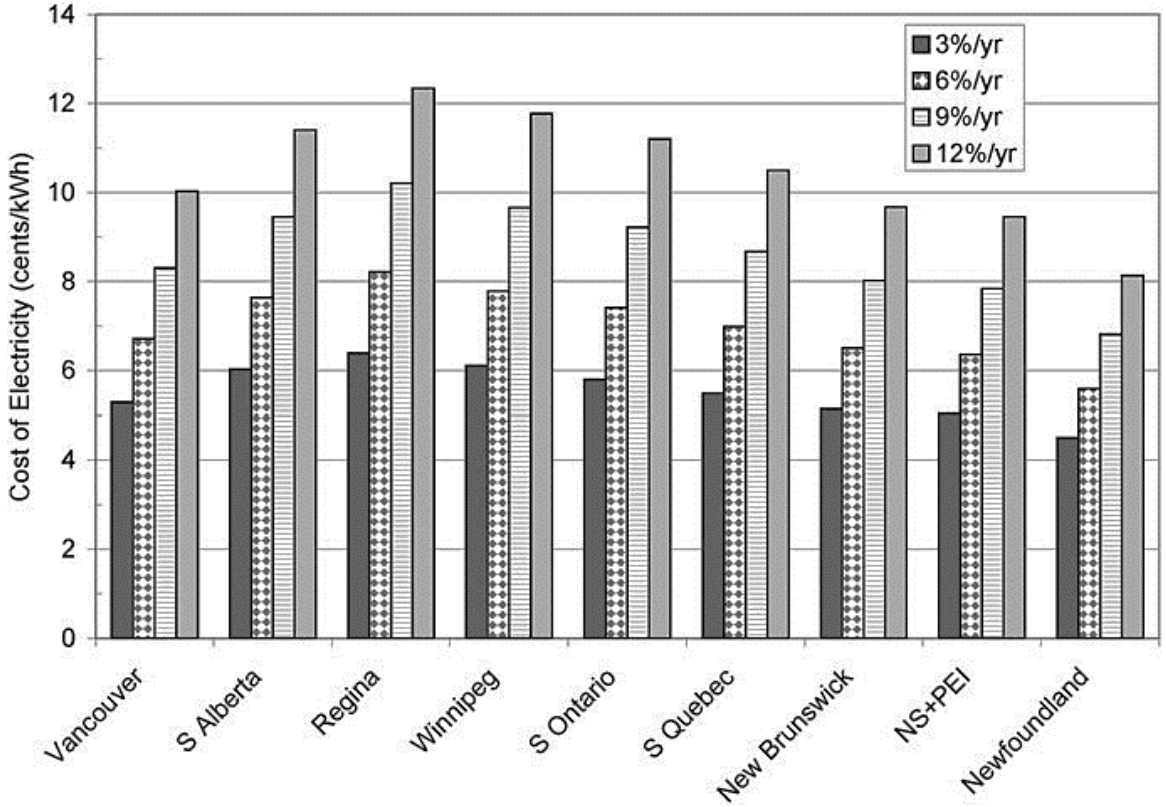

Fig. 45 Cost of electricity with rates of return on the capital investment of 3%/yr to 12%/ yr for the base case (from Ref. [86])

A project is on the way by Siemens for green ammonia with wind as fertilizer. They plan to utilize the excess wind power in ammonia production by investing wind powered electrolysis for hydrogen production and then ammonia synthesis. They propose it as a fuel blending for vehicles. Building of a 30 kW trial with an approximate cost of $2.8 million will start. Since the electrolysis is costly, they presume to have ammonia commodity in 10 years [87].

3. Ammonia Production From Steam Methane Reforming (SMR) with CO_2 Capture and Sequestration

Since steam methane reforming is currently the primary production route of ammonia, a comparative assessment can give important insights for alternative methods. The following processes are followed for massive ammonia production. In this method, natural gas is fed to the plant from the pipeline at a pressure of 31 bar. The desulfurized natural gas feedstock is mixed with process steam to be reacted over a nickel based catalyst contained inside of a system of high alloy steel tubes. The reforming reaction is strongly endothermic, and the metallurgy of the tubes usually limits the reaction temperature to 760-926°C. The flue gas path of the fired reformer is integrated with additional boiler surfaces to produce steam. A portion of this steam is superheated to 31 bar and 399°C, to be added to the incoming natural gas. Additional steam from the boiler is used to regenerate the CO_2. After the reformer, the process gas mixture of CO and H_2 passes through a heat recovery step and is fed into a water gas shift reactor to produce additional H_2. Two different locations are chosen for SMR based ammonia production options namely Edmonton, Alberta and Toronto, Ontario. The following grid electricity prices are taken into account in the analyses as shown in Fig. 46. The assumptions and design parameters are given in Table 14.

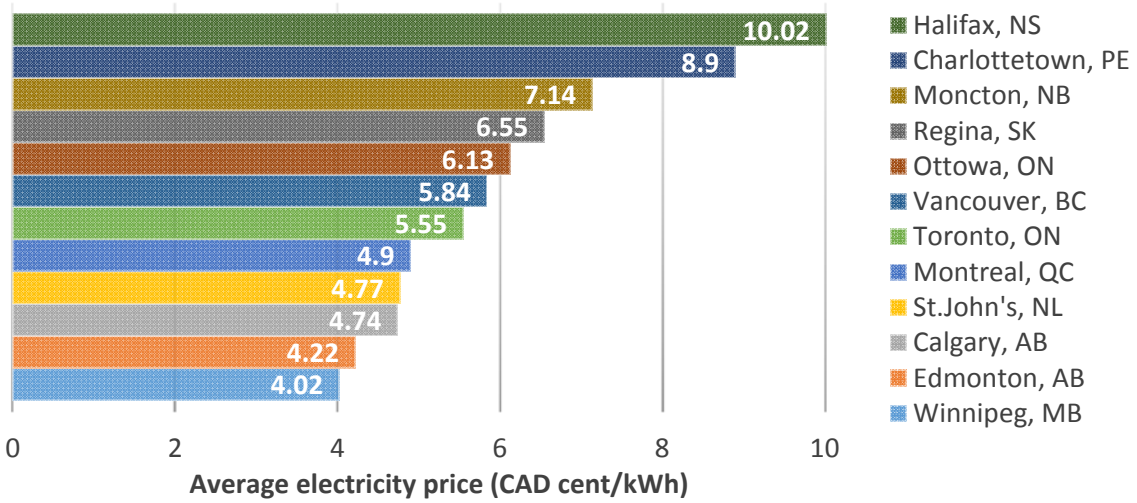

Fig. 46. Comparative index of electricity prices for large-power customers with a monthly consumption of 3,060,000 kWh and a power demand of 5,000 kW (data from Ref. [88])

Table 14. Analysis parameters for steam methane reforming method

Energy efficiency of SMR	0.82
Energy efficiency of Shift Reactor	0.95
Energy efficiency of PSA Hydrogen Separation	0.8
Reference year	2007
Assumed start-up year	2020
Basis year	2009
Usage (kWh/kg H_2)	0.6
Pressure (bar)	20

Current ammonia retail prices

The ammonia prices have fallen to the lowest levels since April 2009. Ammonia prices fell primarily due to lower natural gas costs. There are positives and negatives for falling ammonia prices. Since most of the ammonia is upgraded to other fertilizers, lower prices benefit companies that do not sell it directly to the market. However, the low price also makes higher cost producers more competitive [89]. The following Figs. 47 and 48 show the retail fertilizer prices in comparison with ammonia in the market. The currency is US$. Ammonia has the highest prices among other fertilizers.

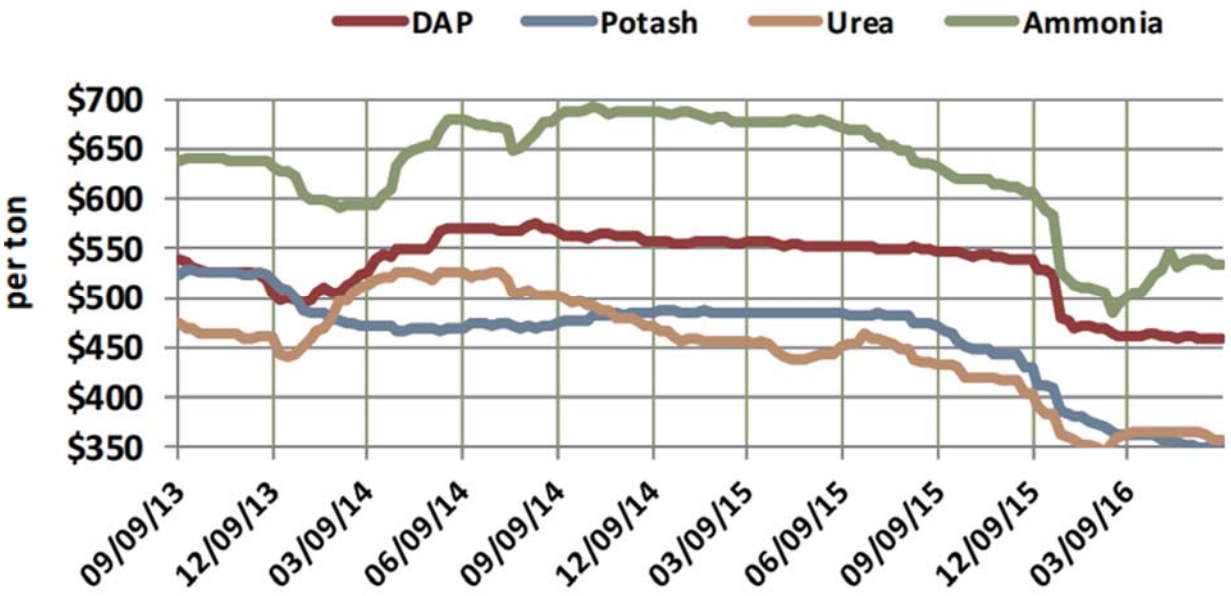

Fig. 47 Average retail fertilizer prices in US (from Ref. [90])

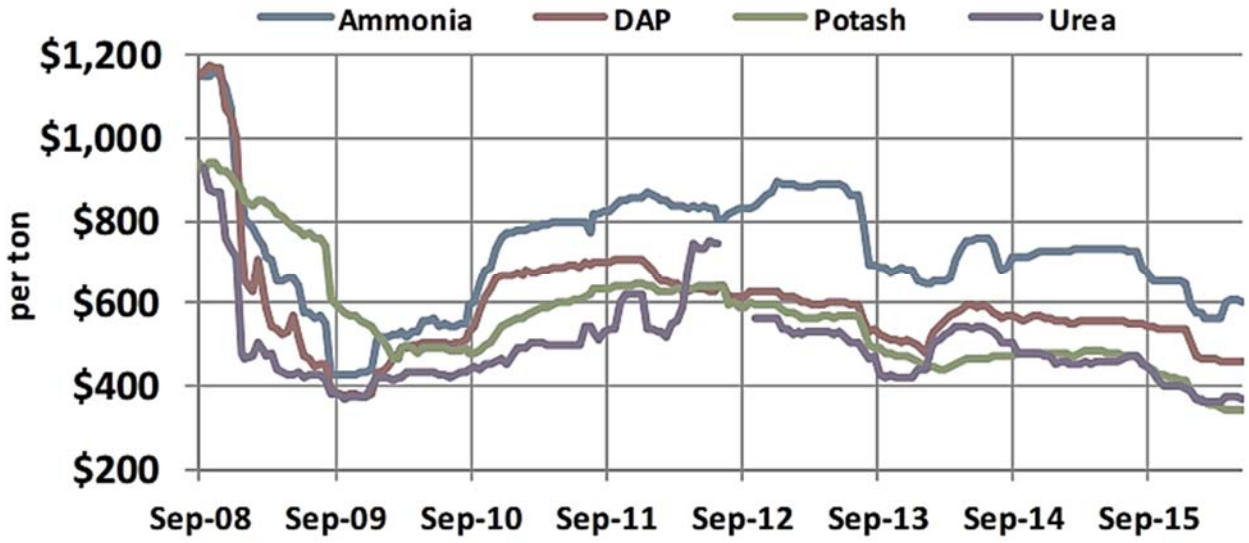

Fig. 48 Illinois fertilizer prices including ammonia since 2008 (from Ref. [90])

4. Cost Analyses Results

Based on the previously mentioned assumptions and calculations, the following ammonia production costs are obtained for various scenarios in Canada as shown in Table 15.

As comparatively shown in Table 15 and Fig. 49, the highest ammonia cost is calculated for wind electrolysis route in Newfoundland. However, by using high pressure electrolysis the cost of ammonia can be decrease down to 0.46 which is quite closer to conventional SMR method. The lowest cost is observed in hydrocarbon dissociation based on the price given in Ref. [91].

The hydrogen production costs are calculated using H2A Central Hydrogen Production Model, Version 3.1 of U.S. DOE. On the other hand, the cost of SMR with CCS based ammonia is slightly lower in Alberta because of lower electricity prices and distance to the natural gas wells. Still using the high pressure electrolysis, the cost is lower than conventional SMR.

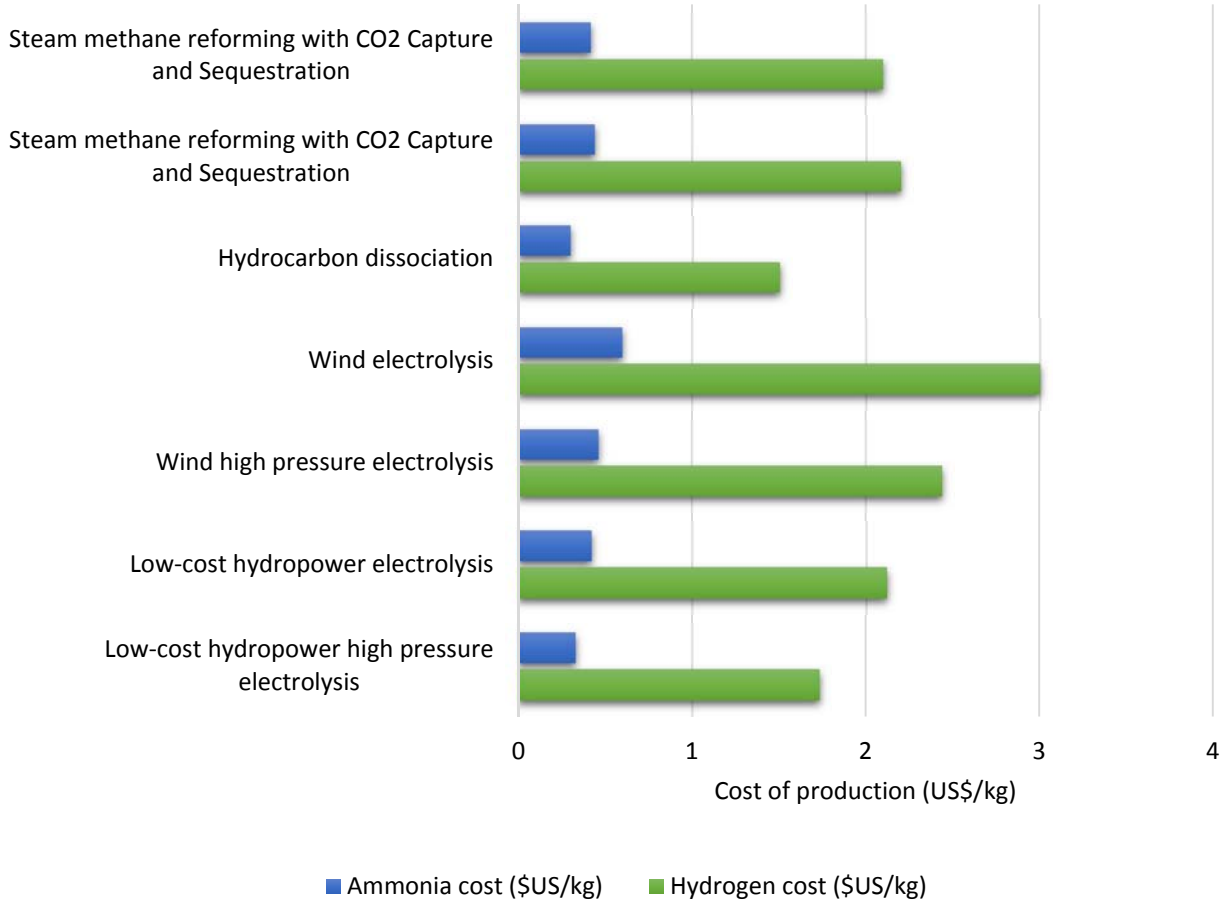

Fig 49. Comparison of cost of production for ammonia and hydrogen using various routes

Table 15. Cost of ammonia production for various scenarios in Canada

Method	Province	Electricity price ($US/kWh)	Hydrogen cost ($US/kg)	Ammonia cost ($US/kg)	Reference
Low-cost hydropower high pressure electrolysis	Ontario	0.0275	1.73	0.3287	H2A Model [92]
Low-cost hydropower electrolysis	Ontario	0.0275	2.12	0.424	H2A Model [92]
Wind high pressure electrolysis	Newfoundland	0.045	2.44	0.4636	H2A Model [92]
Wind electrolysis	Newfoundland	0.045	3	0.6	H2A Model [92]
Hydrocarbon dissociation	Alberta	-	1.5	0.3	Abánades et al. [91]
Steam methane reforming with CCS	Ontario	0.05	2.2	0.44	H2A Model [92]
Steam methane reforming with CCS	Alberta	0.042	2.1	0.42	H2A Model [92]

3.1 Storage cost

Besides the production costs, various scenarios for storage and transportation of ammonia are developed in these section. The storage of ammonia requires not only a capital cost for the facility, but also an operating energy cost depending on if pressurized or low-temperature storage is used. The energy use and efficiency of low-temperature storage was analyzed for both hydrogen and ammonia transportation fuels in Ref. [85]. For large-scale storage of ammonia or hydrogen, low-temperature storage is typically used based on cost considerations. For example, both ammonia and hydrogen can be stored as a liquid at atmospheric pressure if a low enough temperature is maintained.

The low temperature storage system consists of a large insulated tank and a refrigeration system to maintain the fuel as a liquid at the low temperature. The insulated vessel is only designed with the structural strength to withstand the static pressure of the fluid, which greatly reduces the steel content of the vessel compared to pressure storage. Ammonia storage vessels are constructed in a range of sizes from 4,500 tonne to 45,000 tonne, although typical facilities store between 15,000 tonne and 60,000 tonne. The ammonia storage capacity selected for the analyses was 15,000 t, which is the smallest sized commercial facility commonly used by industry. The length

of storage was assumed to be about 6 months, which is based on representing a storage period between summer and winter seasons.

The storage vessel would be able to store the fuel between seasons to allow for a reliable supply of fuel for vehicles. Efficiency was defined as the chemical energy stored in the vessel divided by the sum of both the energy input to the system and the chemical energy stored in the vessel. The storage efficiency calculated for ammonia was 93.6%. The ammonia also enters the liquefaction process from the ammonia synthesis process as a liquid at -25°C, and therefore the amount of heat removal required to achieve the -33°C storage temperature is minimal compared to the 273°C decrease in temperature and phase change for hydrogen liquefaction.

The energy cost would vary depending on the amount of fuel stored in the vessel at any given time and how often the tank is filled and emptied. If electricity costs 0.08 $/kWh and 6 months of storage is used, then the cost of hydrogen and ammonia storage was calculated as 0.95 $/kg-$H_2$ and 0.03 $/kg-$H_2$, respectively, ignoring the capital cost. Combining the energy cost with the capital cost gives the total storage cost for 6 months of storage to be 14.95 $/kg-$H_2$ for hydrogen, and 0.54 $/kg-$H_2$ for ammonia. Therefore, ammonia has a cost of storage nearly thirty times less than that of hydrogen [85]. The cost of ammonia storage including the capital cost yields 0.095$/kg NH_3.

Table 16. Ammonia storage energy requirements and storage parameters

Total Energy Input (kJ/kg NH_3)	1,532
Total Mass (tonne NH_3)	15,000
Work Input (GJ)	4081
Energy Out HHV (GJ)	59,742
Storage Temperature (°C)	-33
Efficiency HHV	93.6%
Storage cost ($US/kg NH_3)	0.095

Based on the calculations, the total cost of storage for ammonia for a duration of approximately 6 months and 15,000 tonne is found to be 1.425 million $US.

3.2 Transportation cost

The transportation cost of ammonia is calculated based on the following table showing the average costs per km where a truck's payload capacity is 16 tonne. Although, there are alternative ways for the transport of ammonia such as pipelines, since there is no ammonia pipeline infrastructure at the moment in Canada, truck transportation is taken into account. However, for Newfoundland case, ocean transportation is also considered for comparison purposes.

Table 17. Estimated per-km truck cost for sample fleet [93]

Truck Type	Per Kilometer Costs		Congestion Premium
	With Congestion	Without Congestion	
Straight	CA$2.97	CA$2.53	17%
Tractor-trailer	CA$3.58	CA$3.12	14.5%

The above results in Table 17 are for a specific fleet operating within primarily within the GTA and for 16,000 average kg of payload capacity. The cost terms are in Canadian dollar here. The congestion premium noted would obviously be less for fleets that operate for longer periods of time in non-congested traffic areas. The truck transportation cost values are taken from the report of "Transport Canada Economic Analysis Directorate, Estimation of Costs of Heavy Vehicle Use Per Vehicle-Kilometer In Canada".

In the following calculations in Table 18 and 19, it is assumed that 16 tonne ammonia can be carried per truck. The calculations are performed for a total installed power of 20 MW diesel generator running on ammonia. It is assumed that ammonia is produced in GTA and transported to northwestern Ontario with a distance of 1,900 km.

Table 18. Calculations of required transportation for a 20 MW remote community in Northwestern Ontario

Fuel Mass Flow Rate (tonne/day)	Required Fuel Mass in 6 months (tonne)	Required Number of Truck Transportation in 6 months
277	49860	3117

Table 19. Total cost of ammonia transportation for a 20 MW remote community in Northwestern Ontario for 6 months

Required Number of Truck Transportation in 6 months	Transportation Cost (US$/km)	Cost of Transportation (US$/6 months)
3117	2	1,1844,600

It is calculated that unit transportation cost of ammonia per tonne kilometer is 0.125 US$/tkm NH_3. Hence, per kg of ammonia, an additional cost of 0.23 US$/kg NH_3 is required for the transportation when 1,900 km distance is considered.

3.3 Total cost of ammonia in Northwestern Ontario

The total cost of ammonia is calculated using the production, storage and transportation cost of ammonia for various scenarios as illustrated in Fig. 50.

Fig. 50. Selected scenarios for ammonia production in Canada

3.3.1 Ammonia production in Ontario

If ammonia is produced using hydroelectric route from water electrolysis in GTA, Ontario, the approximate distance of transportation is 1900 km as shown in Table 20. The total cost of ammonia is calculated and comparatively shown in Table 21 and Fig. 51.

Table 20. Unit cost of ammonia transportation for a remote community in Northwestern Ontario (ammonia production in GTA, Ontario)

Transportation Cost per Tonne-kilometer (US$/tkm)	Distance (km)	Unit Cost of Transportation (US$/kg)
0.125	1900	0.2375

Table 21. Total cost of ammonia in Northwestern Ontario for various routes (ammonia production in GTA, Ontario)

Cost Contributions	**Low-cost hydropower high pressure electrolysis in Ontario**	**Low-cost hydropower electrolysis in Ontario**	**Steam methane reforming with CO_2 capture and sequestration in Ontario**
Production cost (US$/kg)	0.3287	0.424	0.44
Storage cost (US$/kg)	0.095	0.095	0.095
Transportation cost (US$/kg)	0.2375	0.2375	0.2375
Total cost of ammonia in Northwestern Ontario (US$/kg)	0.6612	0.7565	0.7725

Considering the cost of storage in GTA and transportation to Northwestern Ontario, the total cost of ammonia increases to about 0.75 US$/kg for low cost hydropower electrolysis whereas it is 0.66 US$/kg for high pressure electrolysis option as seen in Fig 7. If the cost of hydroelectric can be decreased lower than 0.2 $US/kWh, it can be the lowest cost ammonia production among other methods.

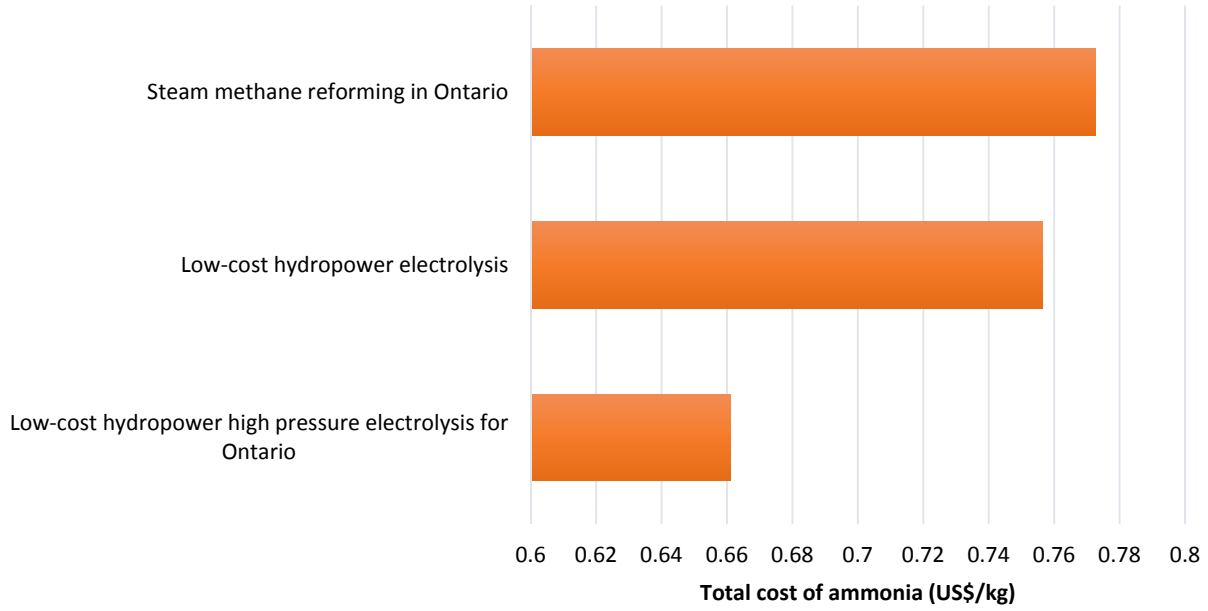

Fig. 51. Total cost of ammonia in Northwestern Ontario for different routes in Ontario

3.3.2 Ammonia production in Newfoundland and Labrador

If ammonia is produced using wind energy route from water electrolysis in Newfoundland, the approximate distance of transportation is 4400 km as shown in Table 22. The total cost of ammonia is calculated and comparatively shown in Table 23 and Fig. 52.

Table 22. Unit cost of ammonia transportation for a remote community in Northwestern Ontario (ammonia production in Newfoundland and Labrador)

Transportation Cost per Tonne-kilometer (US$/tkm)	Distance (km)	Unit Cost of Transportation (US$/kg)
0.125	4400	0.55

Table 23. Total cost of ammonia in Northwestern Ontario for various scenarios (ammonia production in Newfoundland and Labrador)

Cost contribution	Wind energy based high pressure electrolysis in Newfoundland	Wind energy based electrolysis in Newfoundland
Production cost (US$/kg)	0.4636	0.6
Storage cost (US$/kg)	0.095	0.095
Transportation cost (US$/kg)	0.55	0.55
Total cost of ammonia (US$/kg)	1.1086	1.245

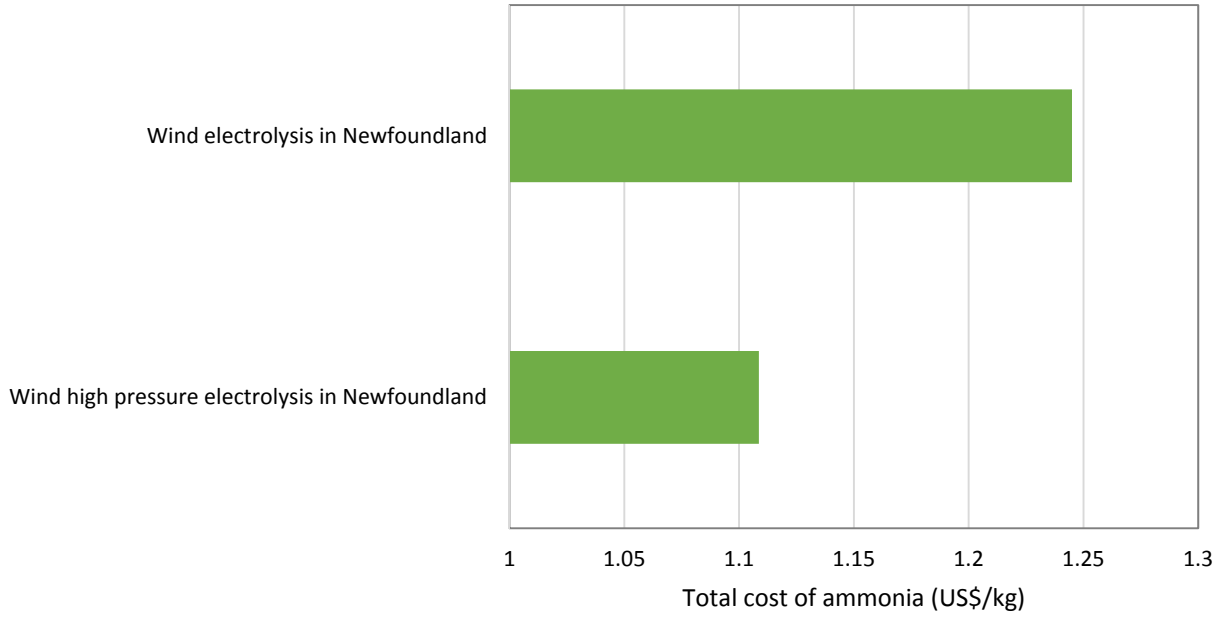

Fig. 52. Total cost of ammonia in Northwestern Ontario for different routes (ammonia production in Newfoundland and Labrador)

Considering the cost of storage in Newfoundland and transportation to Northwestern Ontario, the total cost of ammonia increases to about 1.1 US$/kg for high pressure electrolysis from wind energy route as seen in Fig 8. Although the cost of production is as low as SMR, considering the long transportation distance doubles the cost of ammonia in Northwestern Ontario.

From the perspectives of efficiency, productivity, cost-effectiveness, and reduced emissions, the maritime mode of transportation excels compared to other modes of transportation. For this case, a further study is conducted for an ocean tanker transportation of ammonia from Newfoundland to Northwestern Ontario. The high efficiency of maritime operations also contributes to comparatively lower GHG emissions per tonne-km of cargo moved by ships than by other modes of transportation. This assures the sustainable and viable nature of commercial maritime activity.

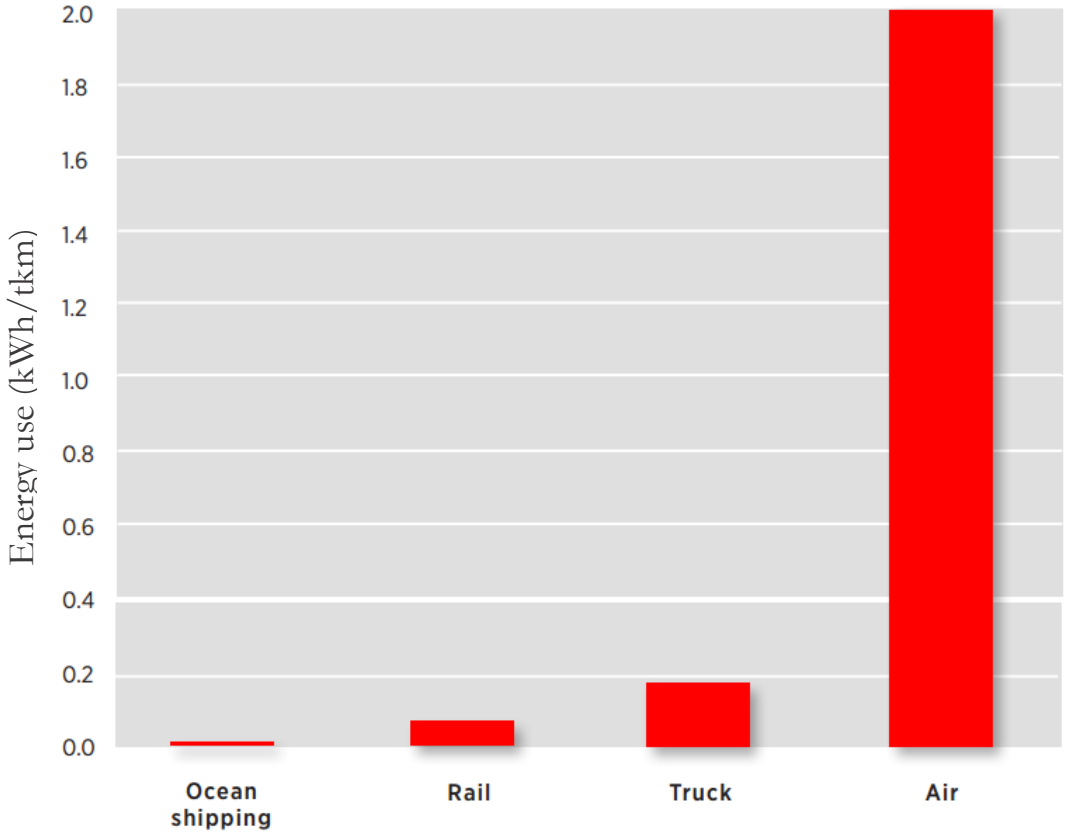

Fig. 53. Comparative energy use of various transportation types (from Ref. [94])

According to Ref. [94] as seen in Fig. 53, the energy use of ocean shipping corresponds to nearly 7% of truck transportation. Hence, the cost of ocean transportation for ammonia is considered to be about 10% of truck transportation for Newfoundland and Labrador case. In this assessment, unit cost of ammonia transportation can be evaluated as 0.055 US$/kg whereas it was 0.55 US$/kg for truck transportation. The total cost of ammonia in Northwestern Ontario can decrease down to 0.62 US$/kg for wind energy based high pressure electrolysis and 0.75 US$/kg for wind energy based electrolysis in Newfoundland and Labrador.

3.3.3 Ammonia production in Alberta

If ammonia is produced using hydrocarbon dissociation route in Alberta, the approximate distance of transportation is 2200 km as shown in Table 24. The total cost of ammonia is calculated and comparatively shown in Table 25 and Fig. 54.

Table 24. Unit cost of ammonia transportation for a remote community in Northwestern Ontario (ammonia production in Alberta)

Transportation Cost per Tonne-kilometer (US$/tkm)	Distance (km)	Unit Cost of Transportation (US$/kg)
0.125	2200	0.275

Table 25. Total cost of ammonia in Northwestern Ontario for various scenarios (ammonia production in Alberta)

Cost contribution	Hydrocarbon dissociation in Alberta	Steam methane reforming with CCS in Alberta
Production cost (US$/kg)	0.3	0.42
Storage cost (US$/kg)	0.095	0.095
Transportation cost (US$/kg)	0.275	0.275
Total cost of ammonia (US$/kg)	0.67	0.79

Considering the cost of storage in Alberta and transportation to Northwestern Ontario, the total cost of ammonia increases to about 0.67 US$/kg for hydrocarbon dissociation route as seen in Fig 10. However, SMR with CCS method represents slightly higher price corresponding to 0.79 US$/kg.

Hydrocarbon dissociation also produces carbon black which is a commercial commodity in the market. Per each kg of ammonia produced, about 0.5 kg of carbon black can be obtained from methane dissociation. If the price of carbon black is assumed to be 1 US$/kg, the cost of ammonia for the hydrocarbon dissociation scenario decreases down to 0.17 US$/kg.

If the ammonia is produced in a mix pathway such as %50 hydro in Ontario, 25% wind in Newfoundland, 25% hydrocarbon in Alberta, the cost of ammonia becomes 0.83 US$/kg. If the price of carbon black is assumed to be 1 US$/kg, the cost of ammonia for the mix scenario decreases down to 0.69 US$/kg.

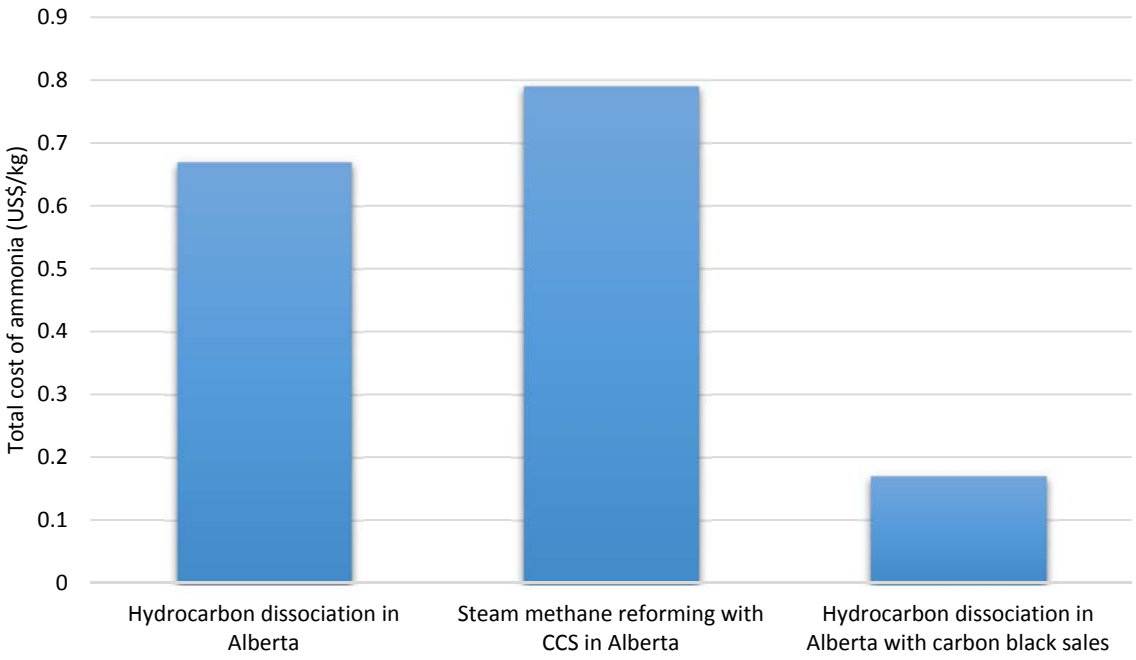

Fig. 54. Total cost of ammonia in Northwestern Ontario for different routes (ammonia production in Alberta)

3.4 On-site ammonia production in Northwestern Ontario using renewable resources

As seen in the calculations, the cost of transportation plays an important role in the overall cost of ammonia. Hence, on-site production of ammonia where it is needed presents promising approach. If it can be realized using low cost renewable resources depending on the region, the cost of ammonia can be decreased substantially as illustrated in Fig. 55 and Table 26.

Table 26. Comparison of ammonia cost produced on-site using wind and hydropower

Method	**Electricity price ($US/kWh)**	**Hydrogen cost ($US/kg)**	**Ammonia cost ($US/kg)**
Low-cost hydropower high pressure electrolysis	0.0275	1.73	0.3287
Low-cost hydropower electrolysis	0.0275	2.12	0.424
Wind high pressure electrolysis	0.063	3.18	0.6042
Wind electrolysis	0.063	3.91	0.782

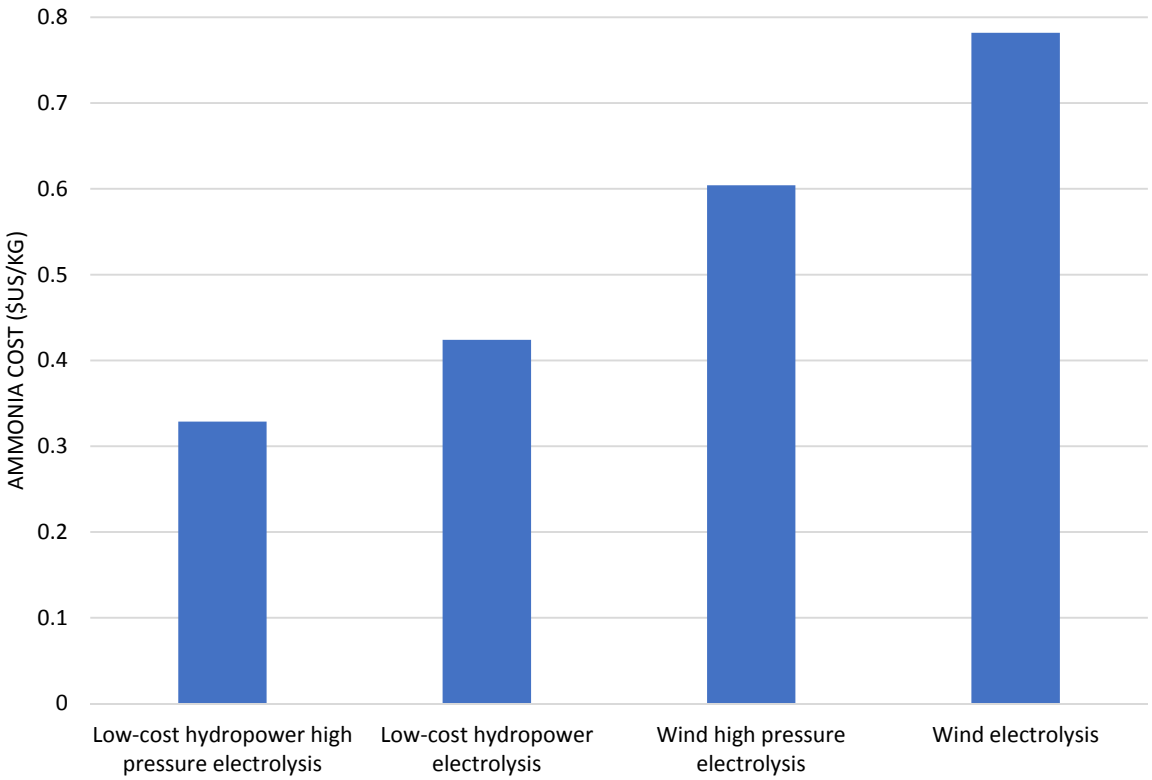

Fig. 55. Comparison of ammonia cost produced on-site using wind and hydropower

5. Environmental Impact Assessment Results

Environmental effect of the selected ammonia routes are also critical for the decision making. Impacts of the environment can be assessed using a life cycle assessment (LCA) approach which is principally a cradle to grave analysis method to examine environmental impacts of a system or process or product. LCA denotes a methodical set of processes for assembling and investigating the inputs and outputs of materials and energy, and the related environmental impacts, directly assignable to the product or service during the course of its life cycle. Hence, a comparative study for the selected routes namely hydro, wind and hydrocarbon under various impact categories is conducted. The units are given per kg of ammonia produced.

Fig. 56 shows the ozone layer depletion (ODP) potential of the routes. Due to stratospheric ozone depletion, a bigger portion of UV-B radiation hits the world surface. It may have damaging properties upon human health, animal health, terrestrial and aquatic ecosystems, biochemical cycles and on materials. Hydrocarbon route has the lowest ODP value whereas wind has the highest since it is mainly caused by the transport of natural gas which is used in the power plants where the electricity is supplied to wind turbine production.

The greenhouse gases to air are related with the climate change. Adverse effects upon ecosystem health, human health and material welfare can result from climate change. Fig. 57 illustrates the global warming potential of the selected routes. As expected hydropower and wind options yield lower than hydrocarbon since they are renewable and more environmentally friendly. However, it is important to note that hydrocarbon cracking has still much lower greenhouse gas emissions compared to conventional SMR method.

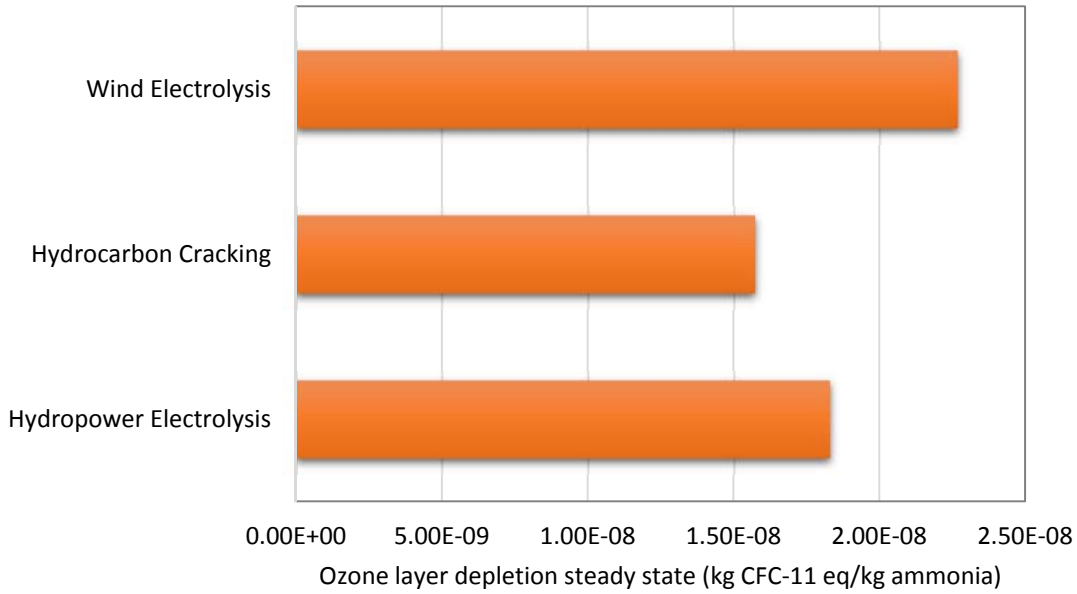

Fig. 56. Ozone layer depletion impact comparison of selected ammonia routes

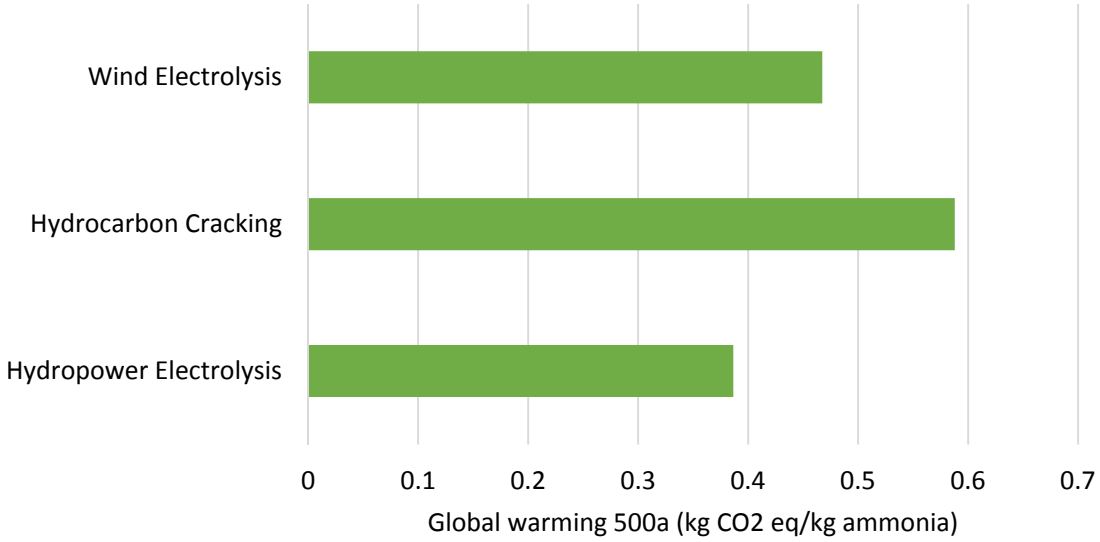

Fig. 57. Global warming impact comparison of selected ammonia routes

Fig. 58 show the acidification potential (AP) for the selected routes. Acidifying substances causes a wide range of impacts on soil, groundwater, surface water, organisms, ecosystems and materials. It is mainly caused by hard coal usage in the electricity grid mixture.

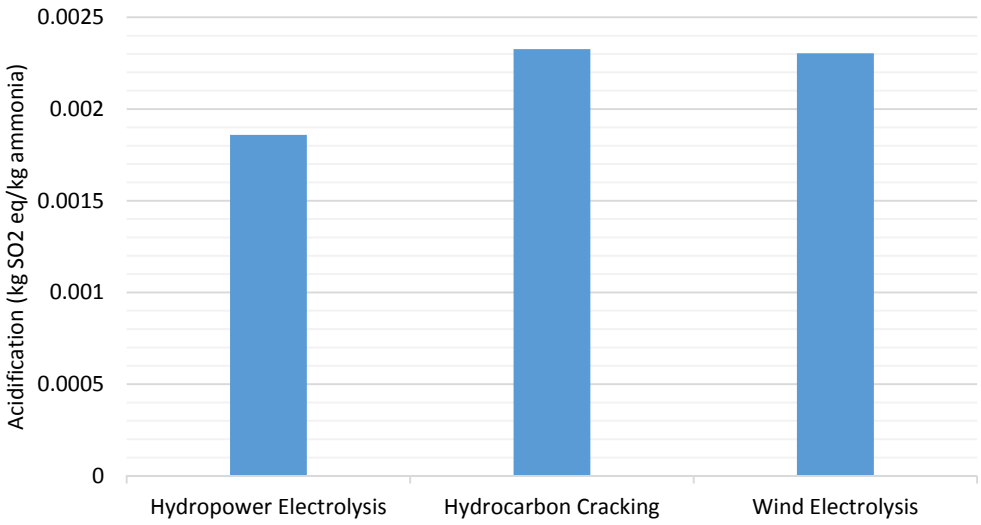

Fig. 58. Acidification impact comparison of selected ammonia routes

Depletion of abiotic sources is one of the sub categories to consider. The key concern of this category is the human and ecosystem health that is affected by the extraction of minerals and fossil as inputs to the system. As shown in Fig. 59, the fossil fuel based hydrocarbon route has the highest impact.

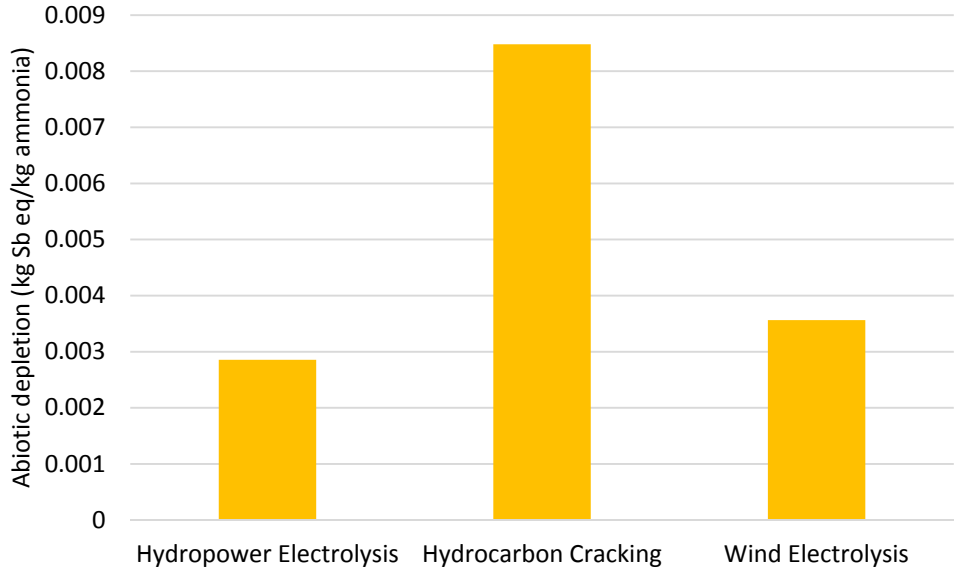

Fig. 59. Abiotic depletion impact comparison of selected ammonia routes

Freshwater aquatic ecotoxicity indicator considers the effect of the emissions of toxic substances to air, water, and soil on fresh water and ecosystems as shown in Fig. 60. It is high for wind electrolysis because of intensive electricity usage in wind turbine production where it is caused by spoil from lignite mining.

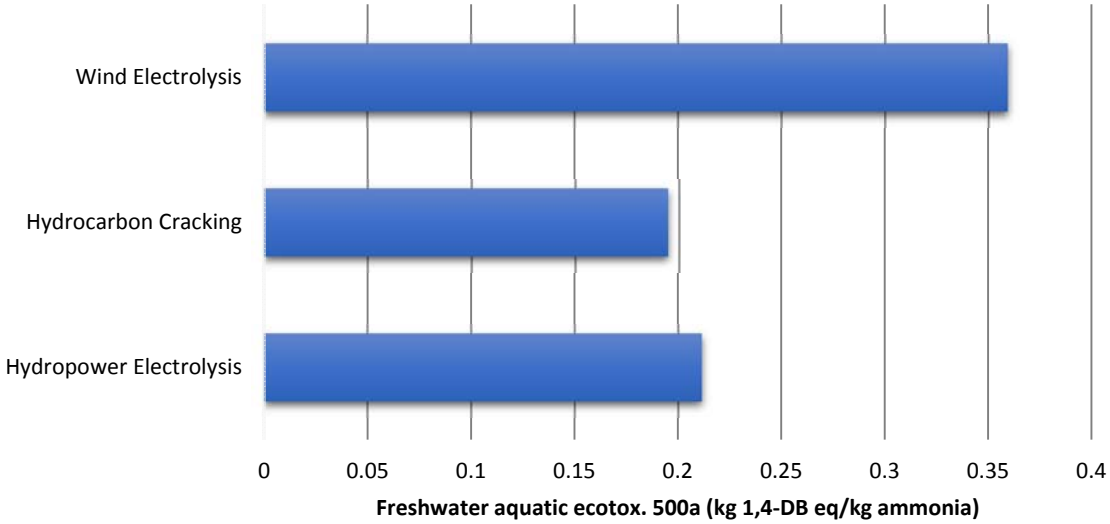

Fig. 60. Freshwater aquatic ecotoxicity impact comparison of selected ammonia routes

Eutrophication category reflects the impacts of to excessive levels of macro-nutrients in the environment caused by emissions of nutrients to air, water and soil. As shown in Fig. 61, the values are close to each other corresponding to 0.0012 kg PO4 eq/kg ammonia for hydropower route.

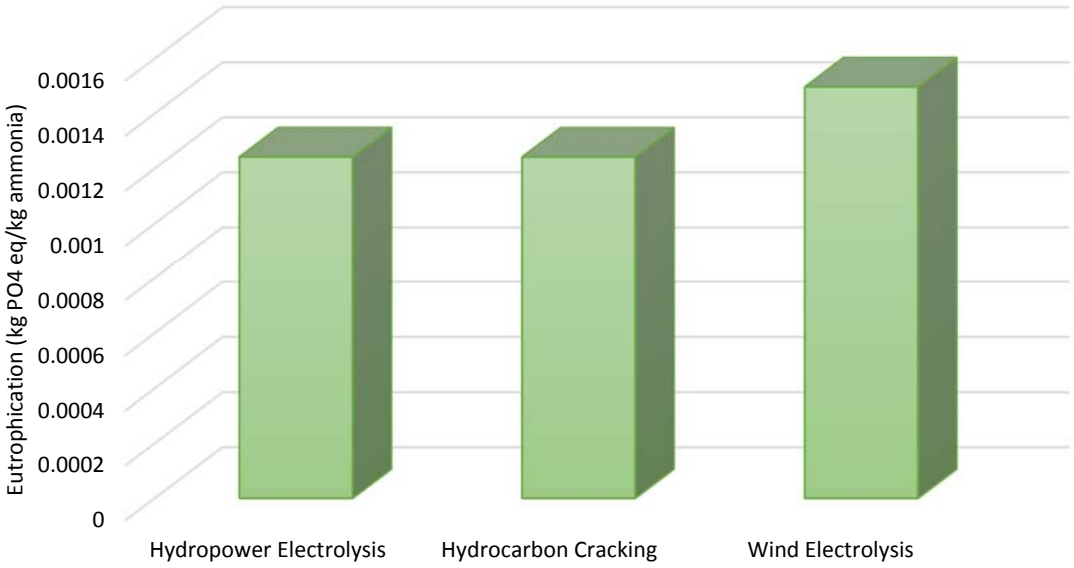

Fig. 61. Eutrophication impact comparison of selected ammonia routes

Ecotoxicology is the study of how chemicals interact with organisms in the environment. Environments that are potentially at risk vary greatly and include marine and freshwater environments, terrestrial environments from the arctic to the tropics, and even the air where respiratory exposures and foliar uptake by plants can occur. Fig. 62 illustrates the ecotoxicity potentials where hydrocarbon route has the lowest impact.

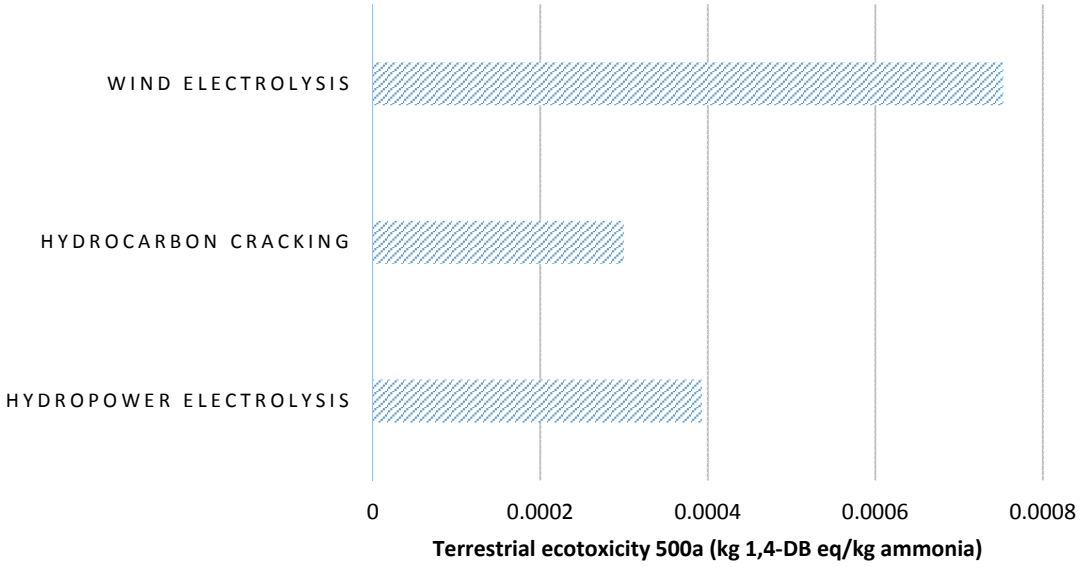

Fig. 62. Terrestrial ecotoxicity impact comparison of selected ammonia routes

It is noted that although hydrocarbon route is a fossil fuel based option, the environmental impacts are not that bad because of the dissociation method used in the analyses. Instead of reforming via steam, methane is decomposed to carbon black and hydrogen yielding lower GHG emissions.

6. Efficiency and Sustainability Assessment Results

The efficiencies are defined as useful output by consumed input. The following equation is used to define the energy efficiency (η_{en}) Of ammonia production facility:

$$\eta_{en} = \frac{\dot{m} \times LHV}{\dot{E_{in}}}$$

where m is the mass flow rate of produced ammonia, LHV is the lower heating value of ammonia and E_{in} is the rate of energy input to the process.

The following equation is used for exergy efficiency (η_{ex})

$$\eta_{ex} = \frac{\dot{m} \times ex_{ch}}{\dot{Ex_{in}}}$$

where ex_{ch} is the chemical exergy of ammonia and Ex_{in} is the rate of exergy input into the process. The sustainability index is used here to determine the sustainability of each option based on the exergy efficiency of ammonia production:

$$\mathrm{SI} = \frac{1}{1 - \eta_{\mathrm{ex}}}$$

The results of energy and exergy efficiencies together with sustainability index are comparatively shown in Table 27 and Fig. 63.

It is seen that hydroelectric based electrolysis method yield slightly higher efficiency than conventional SMR whereas wind route is lower because of less wind-to-electricity efficiency. Based on the Ref. [91], hydrocarbon route has higher efficiencies and sustainability index.

Table 27. Efficiency and sustainability comparison of various ammonia production routes

Ammonia Production Method	Energy Efficiency	Exergy Efficiency	Sustainability index	Reference
Natural Gas Reforming	0.57	0.51	2.04	Acar and Dincer [95], Dincer and Zamfirescu [96], H2A Model [92]
Natural Gas Reforming with CO_2 Capture	0.56	0.50	2.00	Acar and Dincer [95], Dincer and Zamfirescu [96], H2A Model [92]
Coal Gasification with CO_2 Capture	0.52	0.42	1.72	Acar and Dincer [95], Dincer and Zamfirescu [96], H2A Model [92]
Coal Gasification	0.54	0.44	1.78	Acar and Dincer [95], Dincer and Zamfirescu [96], H2A Model [92]
Water Electrolysis - Wind energy	0.32	0.30	1.43	Acar and Dincer [95], Dincer and Zamfirescu [96], H2A Model [92]
Water Electrolysis - Hydroelectric	0.58	0.56	2.27	Acar and Dincer [95], Dincer and Zamfirescu [96], H2A Model [92]
Hydrocarbon dissociation - Methane (Gliding arc reactor)	0.74	0.70	3.33	Petitpas et al.[97]

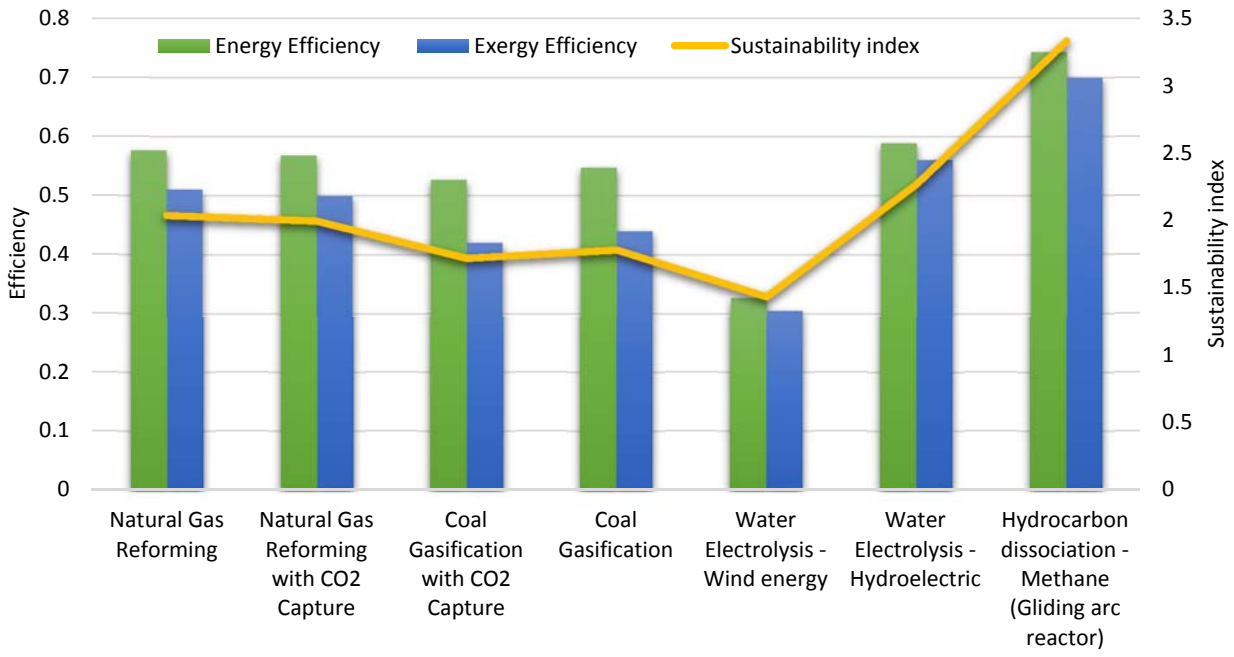

Fig. 63. Efficiency and sustainability comparison of various ammonia production routes

7. Conclusions

The following concluding remarks can be noted in this analyses and assessment study for alternative ammonia production routes.

- A comprehensive cost, sustainability, efficiency and environmental impact assessment of various ammonia production routes namely hydro, wind and hydrocarbon is performed.
- The cost of electricity from wind energy is corresponds to 4.5 cents/kWh in Newfoundland although lower cost grid electricity about 1.8 cents/kWh is available for large scale customers.
- Fortier in Newfoundland and Labrador is the terminal point of the high voltage transmission line from Muskrat Falls. As this is on the coast, it has sea water available for synergistic processes such as HCL and NaOH and a seaport for bulk ocean transport.
- Once the Muskrat Falls hydroelectric facility is completed, Newfoundland can have access to lower cost electricity. This can bring additional advantageous to the natural gas industry in Newfoundland since the gas is stranded and would have to be liquefied in order to transport it to world markets.
- Utilization of high pressure electrolysis required less power input resulting in less cost of hydrogen and ammonia.
- The lowest average cost of electricity for large-scale industrial consumers is seen in Winnipeg, MB and Edmonton, AB.
- The current ammonia retail prices continue to decrease by low natural gas prices. Current retail price is about 550 US$/ton. However, ammonia price is strictly dependent on natural gas price which is not the case for renewable based options.
- Hydrocarbon dissociation and low-cost hydroelectric routes yield the lowest ammonia production cost in the range of 0.3-0.33 US$/kg.
- There are 58.2 trillion cubic feet of proven reserves in Canada and there is potentially 113 trillion cubic feet in Newfoundland's offshore gas fields which can be utilized for the production of ammonia as a sustainable and alternative fuel.
- Renewable based ammonia production routes have comparative costs with conventional SMR.
- Storage and transportation of ammonia brings additional costs after production which is a significant disadvantage for long distance transportation.
- If ammonia is produced in southern Ontario via hydropower and transported to Northwestern Ontario, the total cost of ammonia is found to be in the range of 0.66-0.75 US$/kg.
- When ammonia is produced in Newfoundland via wind energy and transported to Northwestern Ontario, the total cost of ammonia is found to be in the range of 1.1-1.25 US$/kg.
- If ammonia is produced in Alberta via hydrocarbon dissociation and transported to Northwestern Ontario, the total cost of ammonia is found to be in the range of 0.67-0.79 US$/kg. However, since dissociation of methane produced carbon black, considering the carbon black sales, it decreases down to 0.17-0.29 US$/kg.
- Decreasing crude oil prices could be an alternative source of hydrogen and eventually ammonia which are quite satisfactory energy storage mediums. The cost assessment of this process requires a more detailed approach because of the complexity of the method.
- It is seen that on-site production and utilization of ammonia has significant cost advantage.

- Although hydrocarbon dissociation route is a fossil fuel based process, the technology is clean and environmentally friendly close to renewable resources in some environmental impact categories.
- The energy and exergy efficiencies of hydropower and SMR route are quite close. But the hydrocarbon dissociation is higher resulting in more sustainability index.
- Ammonia production form wind energy is suitable for Newfoundland whereas hydropower in Ontario yields lower production cost. Additionally, Newfoundland has high potentials of hydropower which can bring even lower costs compared to wind energy.
- Considering the recent decreasing electricity prices in Ontario ranging between 1-3 cents/kWh, the cost of ammonia production can decline considerably.
- Production, storage and transport of ammonia need to be analyzed and assessed at the same time for feasible scenarios.

References

1. IEA. CO2 emissions from fuel combustion. OECD Publishing. 2009.
2. IEA. CO2 emissions from fuel combustion highlights. OECD Publishing. 2014
3. Rose L, Hussain M, Ahmed S, Malek K, Costanzo R, Kjeang E. A comparative life cycle assessment of diesel and compressed natural gas powered refuse collection vehicles in a Canadian city. Energy Policy. 2013;52:453-61.
4. Li M, Zhang X, Li G. A comparative assessment of battery and fuel cell electric vehicles using a well-to-wheel analysis. Energy. 2016;94:693-704.
5. Argonne National Laboratory. GREET model. 2015. http://greet.es.anl.gov/ .
6. Archsmith J, Kendall A, Rapson D. From Cradle to Junkyard: Assessing the Life Cycle Greenhouse Gas Benefits of Electric Vehicles. Research in Transportation Economics. 2015;52:72-90.
7. Consultants P. SimaPro Life Cycle Analysis Database version 7.3 (software).
8. Duce AD, Egede P, Öhlschläger G, Dettmer T, Althaus HJ, Bütler T, Szczechowicz E. Guidelines for the LCA of electric vehicles. European Union Seventh Framework Programme. 2013
9. Leuenberger M, Frischknecht R. Life cycle assessment of battery electric vehicles and concept cars. Report, ESU-Services Ltd. 2010.
10. Boyden A. The environmental impacts of recycling portable lithium-ion batteries. Australian National University. Thesis Dissertations. 2014
11. Muradov NZ. How to produce hydrogen from fossil fuels without CO2 emission. International Journal of Hydrogen Energy. 1993;18(3):211-5.
12. Muradov N. Hydrogen via methane decomposition: an application for decarbonization of fossil fuels. International Journal of Hydrogen Energy. 2001;26(11):1165-75.
13. Muradov NZ, Veziroğlu TN. “Green” path from fossil-based to hydrogen economy: An overview of carbon-neutral technologies. International Journal of Hydrogen Energy. 2008;33(23):6804-39.
14. Kværner based technologies for environmentally friendly energy and hydrogen production. In: Proceedings of the 12th world hydrogen energy conference. Buenos Aires, Argentina; 1998.
15. Fulcheri L, Schwob Y. From methane to hydrogen, carbon black and water. Int J Hydrogen Energy 1995;20:197
16. Muradov NZ, Veziroğlu TN. From hydrocarbon to hydrogen–carbon to hydrogen economy. International Journal of Hydrogen Energy. 2005;30(3):225-37.
17. Pohlenz J, Scott N. Method for hydrogen production by catalytic decomposition of a gaseous hydrocarbon stream, U. S. patent no. 3,284,161 (UOP), 1966.
18. Łamacz A, Krztoń A. Hydrogen production by catalytic decomposition of selected hydrocarbons and H2O dissociation over CeZrO2 and Ni/CeZrO2. International Journal of Hydrogen Energy. 2013;38(21):8772-82.
19. Takenaka S, Kawashima K, Matsune H, Kishida M. Production of CO-free hydrogen through the decomposition of LPG and kerosene over Ni-based catalysts. Appl Catal A: Gen 2007;321:165e74
20. Chai SP, Zein SHS, Mohammed AR. Synthesizing carbon nanotubes and carbon nanofibers over supported-nickel oxide catalysts via catalytic decomposition of methane. Diamond Relat Mater 2007;16:1656e64.
21. Gac W, Denis A, Borowiecki T, Kępiński L. Methane decomposition over Ni–MgO–Al2O3 catalysts. Applied Catalysis A: General. 2009;357(2):236-43.

22. Zhang T, Amiridis MD. Hydrogen production via the direct cracking of methane over silica-supported nickel catalysts. Applied Catalysis A: General. 1998;167(2):161-72.
23. Fulcheri L, Schwob Y. From methane to hydrogen, carbon black and water. International journal of hydrogen energy. 1995;20(3):197-202.
24. C. Cristofides and V. J. Ilberson, Processing hydrocarbons in a thermal R. F. plasma reactor, ISPC-6, Montreal, paper A-8-2, July 1983.
25. Merlo-Sosa L, Soucy G. Dodecane decomposition in a radio-frequency (RF) plasma reactor. International Journal of Chemical Reactor Engineering. 2005;3(1).
26. Fulcheri, L., Schwob, Y., Variot, B, Flamant, G., Badie, J.M., Fischer, F., Kassabji, F., Saint Just, J., "A 3-Phase A.C. Plasma Process for Carbon Black Production from Methane", 3rd European Congress on Thermal Plasma Processes, VDI Berichte NR. 1166, Aachen, Germany, 525-532 (1995).
27. Ibberson, V.J., Christofides, C., "Processing of Hydrocarbon in a Thermal R. F. Plasma Reactor", ISPC-6 Montreal, Vol. 1, 254-257 (1983).
28. Boulori, K., Amouroux, J., "Reactor Design and Energy Concepts for a Plasma Process of Acetylene Black Production", Plasma Chemistry and Plasma Processing, Vol. 6, No. 4, 335-348 (1986).
29. Bergeron, E., "Production de carbone par pyrolyse du méthane dans un plasma thermique" (in French), M.Sc.A. Thesis, Département de Génie Chimique, Université de Sherbrooke, Canada, (1997).
30. Lynum, S., "System for the production of carbon black", Patent Number WO 93/20153.14/10/93 (1993).
31. Gaudernack, B., Lynum, S., "Hydrogen from Natural Gas Without release of CO2 to the Atmosphere", Int. J. Hydrogen Energy, Vol. 23, No. 12, 1087-1093 (1998).
32. Shaw, D., "Carbon Black process is flexible" in "Carbon Black", European Rubber Journal, Vol. 180, No. 1, 18-27 (1998).
33. Petitpas G, Rollier JD, Darmon A, Gonzalez-Aguilar J, Metkemeijer R, Fulcheri L. A comparative study of non-thermal plasma assisted reforming technologies. International Journal of Hydrogen Energy. 2007;32(14):2848-67.
34. Liu CJ, Xu GH, Wang T. Non-thermal plasma approaches in CO2 utilization. Fuel Process 1999;58:119–34.
35. Bromberg L, Cohn DR, Rabinovich A, Alexeev N, Samokhin N, Hadidi K, et al. Onboard plasmatron hydrogen production for improved vehicles. PSFC JA-06-03, 2006.
36. Kalra CS, Gutsol AF, Fridman AA. Gliding arc discharges as a source of intermediate plasma for methane partial oxidation. IEEE Trans Plasma Sci 2005;33(1).
37. Sobacchi MG, Saveliev AV, Fridman AA, Kennedy LA, Ahmed S, Krause T. Experimental assessment of a combined plasma/catalytic system for hydrogen production via partial oxidation of hydrocarbon fuels. Int J Hydrogen Energy 2002;635–42.
38. El Ahmar E, Met C, Aubry O, Khacef A, Cormier JM. Hydrogen enrichment of a methane-air mixture by atmospheric pressure plasma for vehicle applications. Chem Eng J 2006;116:13–8.
39. Ouni F, Khacef A, Cormier JM. Methane steam reforming with oxygen in a sliding discharge reactor. 17th International symposium on plasma chemistry, Toronto, 2005 [symposium proceedings].
40. Paulmier T, Fulcheri L. Use of non-thermal plasma for hydrocarbon reforming. Chem Eng J 2005;106:59–71.
41. Rollier JD. Theoretical and experimental studies of non-thermal plasma assisted reforming of gasoline. Doctoral thesis, Center for Energy and Processes, Ecole Nationale Supérieure Mines de Paris, 2006.
42. Czernichowski M, Czernichowski P, Czernichowski A. Glidarc assisted reforming of carbonaceous feedstocks into synthesis gas. Detailed study of propane. 16th International symposium on plasma chemistry, Taormina, 2003 [symposium proceedings].
43. Czernichowski M, Czernichowski P, Czernichowski A. Non-catalytical reforming of various fuels into syngas. France Deutschland fuel cell conference on "material, engineering, systems, applications", 7–10 October 2002.
44. Houseman J, Cerini DJ. On-board hydrogen generator for a partial hydrogen injection internal combustion engine, SAE paper 740600, 1974.
45. Goebel SG, Miller DP, Pettit WH, Cartwright MD. Fast starting fuel processor for automotive fuel cell systems. Int J Hydrogen Energy 2005;30:953–62.
46. Qi A,Wang S, Fu G,Wu D. Integrated fuel processor built on autothermal reforming of gasoline: a proof-of-principle study. J Power Sources 2006;2(22):1254–64.
47. Abánades A, Rathnam RK, Geißler T, Heinzel A, Mehravaran K, Müller G, et al. Development of methane decarbonisation based on liquid metal technology for CO2-free production of hydrogen. International Journal of Hydrogen Energy. 2016;41(19):8159-67.
48. Billaud F, Gueret C, Weill J. Thermal decomposition of pure methane at 1263 K. Experiments and mechanistic modelling. Thermochim Acta 1992;211:303-22.

49. Goodwin DG, Moffat HK, Speth RL. Cantera: an objectoriented software toolkit for chemical kinetics, thermodynamics, and transport processes. 2014. vol. Software Toolkit, no. Version 2.1.2, http://www.cantera.org.
50. Abanades A, Rubbia C, Salmieri D. Thermal cracking of methane into hydrogen for a CO2-free utilization of natural gas. Int J Hydrogen Energy 2013;38(20):8491-6.
51. Steinberg M. Fossil fuel decarbonization technology for mitigating global warming. Int J Hydrogen Energy 1999;24(8):771-7.
52. Abánades A, Ruiz E, Ferruelo EM, Hernández F, Cabanillas A, Martínez-Val JM, et al. Experimental analysis of direct thermal methane cracking. International Journal of Hydrogen Energy. 2011;36(20):12877-86.
53. Wei L, Tan Y-s, Han Y-z, Zhao J-t, Wu J, Zhang D. Hydrogen production by methane cracking over different coal chars. Fuel. 2011;90(11):3473-9.
54. Mutyala S, Fairbridge C, Paré JRJ, Bélanger JMR, Ng S, Hawkins R. Microwave applications to oil sands and petroleum: A review. Fuel Processing Technology. 2010;91(2):127-35.
55. J.M.R. Belanger, J.R.J. Pare, Applications of microwave-assisted processes (MAP™) to environmental analysis, Analytical and Bioanalytical Chemistry 386 (4) (2006) 1049–1058.
56. E.D. Neas, M.J. Collins, Microwave Heating: Theoretical Concepts and Equipment Design, in: H.M. Kingston, L.B. Jassie (Eds.), American Chemical Society publishing, Washington DC, 1988, pp. 7–32.
57. Evalueserve's special reports on Developments in microwave chemistry, Chemistry World 2 (4) (April 2005), http://www.rsc.org/chemistryworld/issues/2005/April/ Microwavechemistry.asp.
58. D.M.P. Mingos, D.R. Baghurst, Applications of microwave dielectric heating effects to synthetic problems in chemistry, Chemical Society Reviews 20 (1991) 1–47.
59. IPRC, http://www.iprc.com/oil-recovery-technology.php, 2006–2007 Imperial Petroleum Recovery Corporation, Inc., accessed on February 6, 2009.
60. Alberta's Oil Sands: 1995–2009 Government of Alberta; http://oilsands.alberta.ca/
61. E. Isaacs, Canadian oil sands: development and future outlook, IV International Workshop on Oil and Gas Depletion, October 20–21, 2005.
62. G. Renouf, R.J. Scoular, D. Soveran, Treating heavy slop oil with variable frequency microwaves, Canadian International Petroleum Conference, July 1, 2003.
63. E.P. Pierre, Microwave separation of bituminous material from tar sands, Canadian Patent 1293943, January 7, 1992.
64. R.G. Bosisio, J.L. Cambon, C. Chavarie, D. Klvana, Experimental results on the heating of Athabasca tar sand samples with microwave power, Journal of Microwave Power 12 (4) (1977) 301–307.
65. F.G. Pingle, Microwave based recovery of hydrocarbons and fossil fuels, U.S. Patent application No. 11/610,823 Dec.14, 2006.
66. GRCwebsite: http://www.globalresourcecorp.com/ accessed on December 17, 2007.
67. V. Balint, A. Pinter, G. Mika, Process for the recovery of shale oil, heavy oil, kerogen, or tar from their natural sources, US 4419214, Dec. 6, 1981.
68. W.H. Dumbaugh, W.N. Lawless, J.W. Malmendier, D.R. Wexell, Extraction of oil from oil shale and tar sand, Canadian Patent, 1108081, Sept. 2001.
69. Sahni, M. Kumar, R. Knapp, Electromagnetic heating methods for heavy oil reservoirs, Society of Petroleum Engineers, SPE-62550 presented at the SPE/AAPG Western Regional Meeting held in Long Beach, California, June 19–23, 2000.
70. Cho W, Lee S-H, Ju W-S, Baek Y, Lee JK. Conversion of natural gas to hydrogen and carbon black by plasma and application of plasma carbon black. Catalysis Today. 2004;98(4):633-8.
71. Klepfer JS, Honeycutt TW, Sharivker V, Tairova G. Process and reactor for microwave cracking of plastic materials. Google Patents; 2001. US 6184427 B1.
72. Hemmings J, Pinto T, Sharivker V. Method and apparatus for microwave depolymerization of hydrocarbon feedstocks. Google Patents; 2013. US 8466332 B1.
73. Trautman M, PARSCHE FE. Radio frequency enhanced steam assisted gravity drainage method for recovery of hydrocarbons. Google Patents; 2014. US 8783347 B2.
74. Strohm JJ, Linehan JC, Roberts BQ, Mcmakin DL, Griffin JW, Franz JA. Heavy fossil hydrocarbon conversion and upgrading using radio-frequency or microwave energy. Google Patents; 2015. EP 2817392 A4.
75. Wan JKS. Microwave induced catalytic conversion of methane to ethylene and hydrogen. Google Patents; 1986. US 4574038 A.
76. Suib SL, Zhang Z. Low power density plasma excitation microwave energy induced chemical reactions. Google Patents; 1992. US 5131993 A.

77. Honeycutt T, Sharivker V, Sharivker S, Blinov V. Process for the microwave treatment of oil sands and shale oils. Google Patents; 2004. US 20040031731 A1.
78. Kirkbride CG. Use of microwaves in petroleum refinery operations. Google Patents; 1981. US 4279722 A.
79. Strausz OP, Mojelsky TW, Lown EM. 1977. The chemistry of the Alberta oil sand bitumen. Hydrocarbon Research Center, Department of Chemistry, University of Alberta, Edmonton.
80. Bicer Y, Dincer I. Development of a multigeneration system with underground coal gasification integrated to bitumen extraction applications for oil sands. Energy Conversion and Management. 2015;106:235-48.
81. Bicer Y, Dincer I. Energy and exergy analyses of an integrated underground coal gasification with SOFC fuel cell system for multigeneration including hydrogen production. International Journal of Hydrogen Energy. 2015;40(39):13323-37.
82. AHI Carbon Saver Technologies Inc. http://ahi.carbonsavertechnologies.com [accessed online November 2015]
83. Keun Su K, Jun Ho S, Jun Seok N, Won Tae J, Sang Hee H. Production of hydrogen and carbon black by methane decomposition using DC-RF hybrid thermal plasmas. Plasma Science, IEEE Transactions on. 2005;33(2):813-23.
84. CarbonSaver Overview - Nova Scotia Energy Research & Development Forum, Halifax, Nova Scotia, Canada, 2012
85. Bartels JR. A feasibility study of implementing an ammonia economy [M.S.]. Ann Arbor: Iowa State University; 2008.
86. Harvey LDD. The potential of wind energy to largely displace existing Canadian fossil fuel and nuclear electricity generation. Energy. 2013;50:93-102.
87. http://www.bloomberg.com/news/articles/2016-04-20/green-ammonia-made-with-wind-is-future-of-fertilizer-at-siemens
88. Comparison of electricity prices in major North American cities, Rates in effect April 1, 2015, Hydro Quebec, 2015, ISBN 978-2-550-73559-5 (PDF).
89. http://marketrealist.com/2016/03/weekly-ammonia-price-update-week-ending-march-4-2016/
90. http://farmfutures.com/story-weekly-fertilizer-review-0-30765
91. Abánades A, Rathnam RK, Geißler T, Heinzel A, Mehravaran K, Müller G, et al. Development of methane decarbonisation based on liquid metal technology for CO2-free production of hydrogen. International Journal of Hydrogen Energy. 2016;41(19):8159-67.
92. H2A Central Hydrogen Production Model, Version 3.1, Hydrogen Analysis Resource Center, Hydrogen & Fuel Cells Program, U.S. Department of Energy.
93. Transport Canada Economic Analysis Directorate, Estimation of Costs of Heavy Vehicle Use Per Vehicle-Kilometer In Canada, Transport Canada Economic Analysis Directorate, http://www.bv.transports.gouv.qc.ca/mono/0965385.pdf
94. Energy Transportation and Tanker Safety in Canada, by Philip John January 2015, Fraser Institute
95. Acar C, Dincer I. Comparative assessment of hydrogen production methods from renewable and non-renewable sources. International Journal of Hydrogen Energy. 2014;39(1):1-12.
96. Dincer I, Zamfirescu C. Sustainable hydrogen production options and the role of IAHE. International Journal of Hydrogen Energy. 2012;37(21):16266-86.
97. Petitpas G, Rollier JD, Darmon A, Gonzalez-Aguilar J, Metkemeijer R, Fulcheri L. A comparative study of non-thermal plasma assisted reforming technologies. International Journal of Hydrogen Energy. 2007;32(14):2848-67.